Applications of polyoxometalates in heterogenous catalysis

Piotr Putaj

N° d'ordre 38-2012 Année 2012

THESE DE L'UNIVERSITE DE LYON

délivrée par

L'UNIVERSITE CLAUDE BERNARD LYON 1

ECOLE DOCTORALE DE CHIMIE

DIPLOME DE DOCTORAT
(arrêté du 7 août 2006)

soutenue publiquement le

21/03/2012

par

M. Piotr Putaj

Applications des polyoxométalates en catalyse hétérogène

Directeur de thèse : M. Frédéric Lefebvre

Jury :

M. Stéphane Daniele (Président)
Mme Catherine Marchal-Roch
M. Régis Gauvin
M. Richard Villanneau
M. José M. Fraile
M. Frédéric Lefebvre

N° d'ordre 38-2012 Année 2012

THESE DE L'UNIVERSITE DE LYON

délivrée par

L'UNIVERSITE CLAUDE BERNARD LYON 1

ECOLE DOCTORALE DE CHIMIE

DIPLOME DE DOCTORAT
(arrêté du 7 août 2006)

soutenue publiquement le

21/03/2012

par

M. Piotr Putaj

Applications of polyoxometalates in heterogenous catalysis

Directeur de thèse : M. Frédéric Lefebvre

Jury :

M. Stéphane Daniele (Président)

Mme Catherine Marchal-Roch

M. Régis Gauvin

M. Richard Villanneau

M. José M. Fraile

M. Frédéric Lefebvre

UNIVERSITE CLAUDE BERNARD - LYON 1

Président de l'Université	**M. A. Bonmartin**
Vice-président du Conseil d'Administration	M. le Professeur G. Annat
Vice-président du Conseil des Etudes et de la Vie Universitaire	M. le Professeur D. Simon
Vice-président du Conseil Scientifique	M. le Professeur J-F. Mornex
Secrétaire Général	M. G. Gay

COMPOSANTES SANTE

Faculté de Médecine Lyon Est – Claude Bernard	Directeur : M. le Professeur J. Etienne
Faculté de Médecine et de Maïeutique Lyon Sud - Charles Mérieux	Directeur : M. le Professeur F-N. Gilly
UFR d'Odontologie	Directeur : M. le Professeur D. Bourgeois
Institut des Sciences Pharmaceutiques et Biologiques	Directeur : M. le Professeur F. Locher
Institut des Sciences et Techniques de la Réadaptation	Directeur : M. le Professeur Y. Matillon
Département de formation et Centre de Recherche en Biologie Humaine	Directeur : M. le Professeur P. Farge

COMPOSANTES ET DEPARTEMENTS DE SCIENCES ET TECHNOLOGIE

Faculté des Sciences et Technologies	Directeur : M. le Professeur F. De Marchi
Département Biologie	Directeur : M. le Professeur F. Fleury
Département Chimie Biochimie	Directeur : Mme le Professeur H. Parrot
Département GEP	Directeur : M. N. Siauve
Département Informatique	Directeur : M. le Professeur S. Akkouche
Département Mathématiques	Directeur : M. le Professeur A. Goldman
Département Mécanique	Directeur : M. le Professeur H. Ben Hadid
Département Physique	Directeur : Mme S. Fleck
Département Sciences de la Terre	Directeur : Mme le Professeur I. Daniel
UFR Sciences et Techniques des Activités Physiques et Sportives	Directeur : M. C. Collignon
Observatoire de Lyon	Directeur : M. B. Guiderdoni
Ecole Polytechnique Universitaire de Lyon 1	Directeur : M. P. Fournier
Ecole Supérieure de Chimie Physique Electronique	Directeur : M. G. Pignault
Institut Universitaire de Technologie de Lyon 1	Directeur : M. le Professeur C. Coulet
Institut de Science Financière et d'Assurances	Directeur : M. le Professeur J-C. Augros
Institut Universitaire de Formation des Maîtres	Directeur : M. R. Bernard

Dla tych, którzy byli pewni, że ten dzień jednak kiedyś nadejdzie:
dla mojej Rodziny.

"To jest miś na miarę naszych możliwości.
My tym misiem otwieramy oczy niedowiarkom!
Mówimy: to jest nasz miś, przez nas zrobiony
i to nie jest nasze ostatnie słowo!"

„Miś" reż. Stanisław Bareja

Résumé

L'objectif de ce travail de thèse était la préparation et la caractérisation des catalyseurs à base de polyoxometalates et démonstration de leur utilité dans plusieurs domaines de la catalyse hétérogène.

Plus concrètement, l'étude mécanistique de la réaction d'oxydation du méthane jusqu'au méthanol a été présentée. Sur des polyoxometalates supportes sur la silice l'activation de la liaison C-H du méthane a lieu déjà à la température ambiante et, contre toute attente, ne constitue jamais étape limitant de la réaction d'oxydation. L'adsorption du méthane enrichi en ^{13}C sur l'acide silicomolybdique supporte, suivie par RMN de l'état solide a mis en évidence la création de l'espèce surfacique du type methoxy $[SiMo_{12}O_{40}(CH_3)]^{3-}$, qui est le premier intermédiaire réactionnel de l'oxydation. Le cycle catalytique est complété, lui, par l'hydrolyse consécutive de cette espèce, pendant laquelle méthanol est formé et une molécule de l'eau recrée la structure du départ de polyoxometalate. Par ailleurs l'adsorption du méthanol-^{13}C sur des polyoxometalates cristallins et supportés sur la silice a montré la possibilité de la création de deux types des espèces methoxy, localisées sur des atomes d'oxygène terminaux ou pontants des polyanions est caractérisées par deux signaux RMN distincts – à 58 et 77 ppm, respectivement. Transformations des ces espèces methoxy se réalisent par deux voies : soit déshydratation et couplage jusqu'au éther diméthylique, soit oxydation jusqu'a l'espèce formyl, elle aussi observé par RMN du solide à 172 ppm. Les deux voies sont complémentaires et ce sont des propriétés chimiques dominantes des polyanions (l'acidité pour polyoxometalates tungstiques et proprietes redox pour polyoxometalates molybdiques) qui décident dans chaque cas laquelle sera suivie principalement.

Trois méthodes différents de la derivatisation des sels inorganiques des polyoxometalates avec grandes surfaces spécifiques sont utilisées afin d'obtenir des catalyseurs hétérogènes bien définis et multifonctionnels : par déposition de polyanions vanadomolybdiques, par l'imprégnation avec des sels des métaux nobles et par la voie COMS (chimie organométallique du surface). En greffant un complexe de platine $PtMe_2COD$ sur les sels de césium de polyoxometalates, le dégagement du méthane ou du mélange du méthane et de l'éthane a été observé et lié avec des propriétés chimiques des supports. Le mécanisme a été proposé qui explique les données expérimentales par la séquence de l'addition oxydative du proton de polyoxometalate au centre métallique, couplage C-H ou C-C et finalement l'élimination réductrice et libération d'une molécule de gaz.

Au niveau de la catalyse acide, les sels inorganiques de l'acide phosphotungstique $H_3PW_{12}O_{40}$ et silicotungstique $H_4SiW_{12}O_{40}$ ont été montrées de catalyser l'isomérisation du *n*-butane à l'isobutane de façon effectif et dans des conditions douces (225°C, pression atmosphérique). L'introduction de l'hydrogène dans le flux de gaz ainsi que l'utilisation de co-catalyseur en platine ont permis d'éliminer des effets néfastes du craquage.

Finalement, ont résulté, de la déposition du composé de cuivre $Cu(OTf)_2$ sur la surface des sels inorganiques des polyoxometalates, des catalyseurs très actifs en insertion des carbenes, générés à partir des espèces diazo tel phenyldiazoacetate de méthyl, aux liaisons C-H des éthers cycliques comme tétrahydrofurane (THF) et tétrahydropyrane (THP).

Table of contents

Abbreviations and symbols

Å	Angstrom
AcOEt	ethyl acetate
BET	Brunauer-Emmett-Teller type isotherm of adsorption
°C	Celsius degree (temperature)
CP	Cross-Polarisation
$Cu(OTf)_2$	copper(II) triflate
DBU	1,8-diazabicyclo[5.4.0]undec-7-ene
DMSO	dimethylsulfoxide
DRIFT	diffuse reflectance infrared Fourier transform
DRX	powder diffraction
ESR	electron spin resonance
Et_2O	diethyl ether
FT	Fourier transform
GC	gas chromatography
g	gram
h	hour
HPMo	phosphomolybdic acid $H_3PMo_{12}O_{40}$
HPVMo	phosphovanadomolybdic acid $H_4PVMo_{11}O_{40}$
HPV_2Mo	phosphodivanadomolybdic acid $H_5PV_2Mo_{10}O_{40}$
HPW	phosphotungstic acid $H_3PW_{12}O_{40}$
HSiMo	silicomolybdic acid $H_4SiMo_{12}O_{40}$
HSiW	silicotungstic acid $H_4SiW_{12}O_{40}$
Hz	Hertz, s^{-1}
IR	infrared
kJ	kiloJoule
LN_2	liquid nitrogen
MAS	magic angle spinning
Me	methyl
Meallyl	methallyl, $(\eta^3\text{-}C_4H_7)^-$
MeCN	acetonitrile
MeOH	methanol
min.	minute
mL	mililitre
NMR	nuclear magnetic resonance
Ph	phenyl
POM	polyoxometalate
ppm	part per million (10^{-6})
$PtMe_2(COD)$	dimethyl(1,5-cyclooctadiene) platinum(II)
$Rh_2(OAc)_4$	rhodium(II) acetate dimer
s	second
SS	solid-state
TEPO	triethylphosphine oxide
THF	tetrahydrofuran
THP	tetrahydropyran
TPD	temperature-programmed desorption

Introduction

In the most general sense the aim of this work was preparation and characterization of catalysts based on polyoxometalates and their use in various catalytic reactions in heterogenous conditions.

Chapter 1 is a literature study which introduces the chemistry of polyoxometalates, stressing the structure-reactivity relationship of these compounds. Main properties of polyanions, namely: acidity and redox properties, are briefly described and shown to be the source of their usefulness in catalysis. Examples of polyoxometalates-based catalytic systems are given.

Chapter 2 deals with the mechanistic aspects of methane-to-methanol partial oxidation reaction on silica-supported polyoxometalates and is divided into two parts.
In the first part (**Part A**) methane activation on silica-supported polyoxometalates is shown to occur even at room temperature. Reactivity of polyoxometalates towards methane is discussed in the context of their chemical properties (acidity, redox properties). It is clearly evidenced that whatever the polyoxometalate type, the first reaction stage i.e. the C-H activation is never a limiting step for the overall process. First reaction intermediate, a methoxy species $[SiMo_{12}O_{40}(CH_3)]^{3-}$ was generated on the surface of silica-supported silicomolybdic acid and characterized by means of ^{13}C SS NMR technique. Hydrolysis of this species in water leads to desorption of methanol and reconstitution of the parent polyoxometalate, thus closing the catalytic cycle.
In the second part (**Part B**) formation reactivity of methoxy species coming from ^{13}C-MeOH adsorption on bulk and silica-supported polyoxometalates is detailed and compared. Two types of methoxy species, bound to terminal and bridging oxygen atoms of the polyoxometalates are shown to give distinct ^{13}C NMR signals. Two pathways of methoxy species transformations, namely: coupling/dehydration yielding dimethyl ether and oxidation to formyl species are observed and explained to originate from the different chemical properties of tungstic and molybdic systems, respectively.

Chapter 3 describes ways of preparing and characterizing high surface area materials based on polyoxometalates that could serve as universal platforms for other species and be consecutively used as heterogenous catalysts, and is divided into two parts.
In the first part (**Part A**) acidic clusters of the Keggin type of polyoxometalates are shown to develop high specific surface areas upon partial exchange of their protons with alkaline metal cations (e.g. Cs^+). These compounds can be further derivatized by means of classical wet

impregnation with other polyoxometalates or inorganic salts of late transition metals or by means of SOMC (surface organometallic chemistry) methodology with organometallic complexes of late transition metals. The so-obtained composite materials, though showing some loss of initial surface area values, still constitute an attractive alternative to the bulk polyoxometalates in terms of applications in heterogenous catalysis.

In the second part (**Part B**) a special case of SOMC (surface organometallic chemistry) of platinum dialkyl complex on self-supported polyoxometalates is discussed in detail, in a wider context of mechanistic studies of alkanes activation on Pt(II) centers. Upon grafting of $PtMe_2COD$ on cesium salts of tungstic or molybdic clusters methane or combined methane and ethane release was noted, respectively. Observed phenomena were explained by means of oxidative addition/reductive elimination mechanism on metal centers and were shown to be controlled by the different chemical properties of the polyoxometalate supports. ^{195}Pt NMR was used to characterize the reaction products.

Chapter 4 presents an example of acidic catalysis with polyoxometalates. Different types of self-supported clusters were synthesized and characterized and evidenced to catalyze efficiently *n*-butane to isobutane skeletal isomerisation reaction at mild conditions (225 °C, atmospheric pressure). Platinum co-catalyst and addition of hydrogen to the gas flow were used to prevent desactivation by coking. Contributions of mono- and bimolecular mechanisms of isomerisation to the overall conversion and selectivity were discussed.

Chapter 5 is devoted to heterogenization of copper catalysts active in enantioselective C-H carbene insertion reactions. Copper(II) precursors deposited on various high surface area polyoxometalate materials were shown to be highly active in the insertion of carbene generated from methyl phenyldiazoacetate, into C-H bonds of cyclic ethers like tetrahydrofuran THF and tetrahydropyran THP.

Chapter 1

Polyoxometalates

State-of-the-art

Polyoxometalates (abbreviated as POMs in the following) are known since the beginning of the XIXth century as it is generally admitted that the first species of this class (the ammonium salt of phosphomolybdic acid $H_3PMo_{12}O_{40}$) was discovered by Berzelius in 1826 [1]. The first structural determination of the phosphotungstic anion $[PW_{12}O_{40}]^{3-}$ was done by Keggin in 1933 [2]. However, these compounds remained only laboratory curiosities during many years. It is only at the end of the nineteen seventies that extensive studies by many groups around the world put them in the spotlight and nowadays their applications have exploded, in catalysis [3-5] as well as in various other domains, such as analytical chemistry [6-9], biochemistry/medicinal chemistry [10-12] or development of new materials with optical [13-18] or magnetic [19-21] properties.

1.1 Polyoxometalates - systematics and structure

From a structural point of view, the polyoxometalates can be considered as aggregates, generally anionic, formed by oxo species of transition metals with one or more bridging oxygen atoms. These clusters contain at least three metal atoms, in most cases from groups 5 or 6 of the periodic table, usually in their highest oxidation states, with (heteropolyoxometalates) or without (isopolyoxometalates) heteroatoms (such as B, Al, Ge, Si, P and many more). A lot of structures have been described, the most ubiquitous being the Lindqvist $[M_6O_{19}]^{n-}$, Anderson $[XM_6O_{24}]^{n-}$, Keggin $[XM_{12}O_{40}]^{n-}$ and Wells-Dawson $[X_2M_{18}O_{62}]^{n-}$ [22] ones (where: X = heteroatom, M = metal, n = overall cluster charge) (Figure 1).

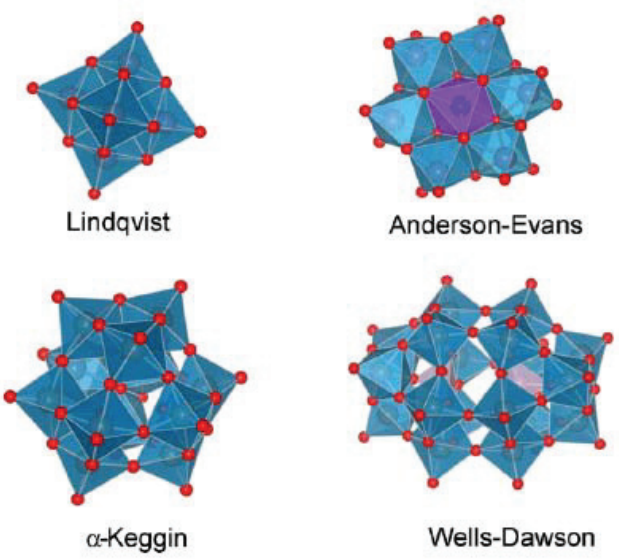

Figure 1. Various structural types of polyoxometalates. Mo or W (V, Nb, Ta) = blue polyhedra, heteroatoms = violet polyhedra, O = red balls.

A majority of heteropolycompounds are based on molybdenum or tungsten (with notable exceptions [23]) while numerous isopolycompounds containing also vanadium, niobium or tantalum have been described.

Modifications of these species can be made easily by removing M=O entities (where M=Mo or W) leading to various lacunary entities [24-26] or by replacing them with other transition [27-28] or rare earth metals [29]. New structures were also obtained by joining two (or more) units via metal ions [30] or clusters [31]. Hybrid organic-inorganic compounds are another fast developing branch of polyoxometalates research [32-34]. As a consequence, the number of compounds which can be prepared is very large and every day new structures are reported in the literature.

The Keggin-type polyoxometalates are the most widely applied because of their stability, commercial availability, low price and last but not the least, interesting chemical properties. Typically the Keggin polyoxometalate has the formula $[XM_{12}O_{40}]^{n-}$ and its structure is shown in Figure 2.

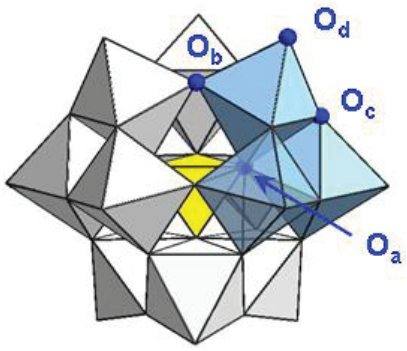

Figure 2. Keggin-type polyoxometalate. Mo or W = gray octahedra, heteroatom X = yellow tetrahedron. One of $\{M_3O_{13}\}$ triads is shown in light blue with different types of oxygen shown as blue balls. The symbols are explained in the text.

In the middle of the structure there is a heteroatom, tetrahedrally coordinated by four O_a oxygens. Four $\{M_3O_{13}\}$ triads, made of three edge–sharing octahedra, are connected to this heteroatom via the O_a oxygen atoms. The oxygen atoms common to two octahedra in the same triad are indicated as O_c whereas those common to two octahedra from different triads as O_b. Finally, the terminal oxygen atoms completing the octahedral coordination of the M atoms are called O_d.

It is clearly visible that a different possible arrangement of the four triads can lead to structural isomers. The easiest way to imagine their formation is to pick a triad and rotate it

clockwise by a 60 degrees angle around its O_a atom. This operation applied to consecutive triads yields the five possible isomers abbreviated with Greek letters and shown in Figure 3.

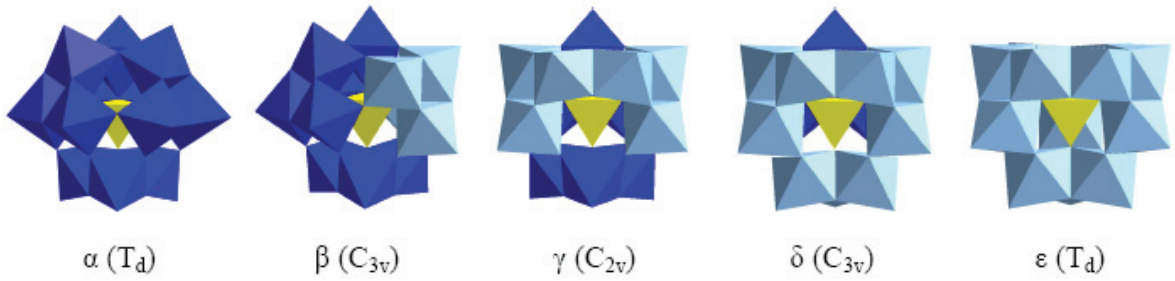

Figure 3. The five different Keggin isomers, resulting from the 60° rotation of $\{M_3O_{13}\}$ triads, and their point symmetry group (in parentheses).

In the solid state the polyoxometalates form ionic crystals with various charge compensating agents such as protons (so called acidic form of POMs), metal (K^+, Rb^+, Cs^+ Mg^{2+}, Cd^{2+}, Ni^{2+}, La^{3+}, Ce^{3+} and so on), ammonium (NH_4^+) and organic (e.g. Bu_4N^+ - tetra *n*-butylammonium) cations (creating thus salts of POMs) and crystallization water molecules (or another solvent). In the crystal structure of the purely acidic hydrated forms, the polyanions are linked through a network of hydrogen bonds with water molecules, as shown in Figure 4. The hydrated protons of POMs are then localized on the terminal oxygen atoms [35].

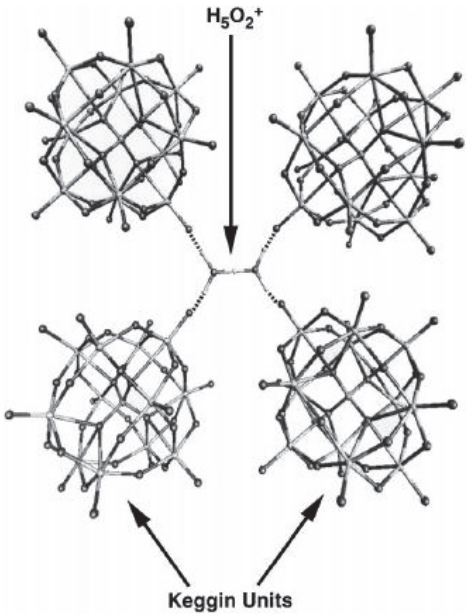

Figure 4. Interactions between polyanions in the structure of the phosphotungstic acid hydrate $H_3PW_{12}O_{40}\cdot 6H_2O$ ([35]).

The number of crystallization water molecules per polyoxometalate is variable (up to 30) and can be controlled to some extent by a thermal treatment. Thermogravimetric studies on phosphomolybdic acid $H_3PMo_{12}O_{40}$ showed two types of water molecules in the lattice: the crystallization water whose loss leads to the formation of the anhydrous POMs and, after treatment at a higher temperature, one additional release of one and half H_2O molecule per POM, resulting from the partial decomposition of the polyacid [36-37]. A $\{PMo_{12}O_{38.5}\}$ phosphomolybdic anhydride species was claimed to be formed upon this process but its existence remains controversial [38]. However, as far as the temperature is kept below 250°C (for $H_3PMo_{12}O_{40}$) or 350°C (for $H_3PW_{12}O_{40}$) the polyoxometalates are not affected and dehydration is a reversible process. Above these temperatures the decomposition occurs gradually, leading to the complete transformation into various crystalline phases of respective metal oxides.

Clearly, the thermal resistance of POMs vary strongly with the transition metal as well as the heteroatom and the cluster type [39]. For the acidic forms of POMs the following order of decreasing stability has been proposed:

$$H_3PW_{12}O_{40} > H_4SiW_{12}O_{40} > H_3PMo_{12}O_{40} > H_4SiMo_{12}O_{40}$$
$$\text{and } H_3PW_{12}O_{40} >> H_6P_2W_{18}O_{62}$$

Moreover, it has been observed that the formation of inorganic salts of POMs by proton exchange leads to a pronounced increase of their thermal stability, although only in the case of ammonium $(NH_4)^+$ and alkaline cations like Cs^+ or K^+ [40].

In a striking contrast to hydrated acidic POMs, for which the protons location on terminal oxygen atoms is unequivocally accepted, the location of protons in their anhydrous forms is a matter of ongoing controversy. While IR results are in favour of bridging oxygen atoms [41-42], solid-state NMR studies lead to opposite conclusions [43-44]. DFT calculations were shown to support both hypotheses, depending on the approach to the problem [45-47].

1.2 Polyoxometalates – properties

1.2.1 Acidity

The acidity of polyoxometalates can be considered either in solution or in the solid state. Because of their ionic nature, they are well soluble in polar solvents such as water, alcohols, ketones, acetonitrile MeCN, dimethylsulfoxide DMSO, etc. Their dissociation constants have been measured in many solvents [48-49] and the results are compiled in Table I. In water all polyoxometalates are strong acids, undergoing a complete dissociation. In organic solvents their acidity is more pronounced than that of typically used strong mineral acids.

Table I. Dissociation constants of various polyoxometalates and mineral acids measured in acetone, ethanol and acetic acid.

Compound	Acetone			Ethanol			Acetic acid
	pK_1	pK_2	pK_3	pK_1	pK_2	pK_3	pK_1
$H_3PW_{12}O_{40}$	1,6	3,0	4,0	1,6	3,0	4,1	4,8
$H_4PW_{11}VO_{40}$	1,8	3,2	4,4	-	-	-	4,7
$H_5PW_{10}V_2O_{40}$	-	-	-	-	-	-	4,8
$H_4SiW_{12}O_{40}$	2,0	3,6	5,3	2,0	4,0	6,3	5,0
$H_3PMo_{12}O_{40}$	2,0	3,6	5,3	1,8	3,4	5,1	4,7
$H_4PMo^{VI}_{11}Mo^{V}O_{40}$	2,1	3,7	5,5	1,9	3,8	5,9	-
$H_4PMo_{11}VO_{40}$	2,1	3,7	5,6	1,9	3,7	5,8	4,7
$H_4SiMo_{12}O_{40}$	2,1	3,9	5,9	-	-	-	4,8
$H_4GeW_{12}O_{40}$	-	-	-	-	-	-	4,3
$H_5GeW_{11}VO_{40}$	-	-	-	-	-	-	4,7
$H_6GeW_{10}V_2O_{40}$	-	-	-	-	-	-	4,6
$HClO_4$	-	-	-	-	-	-	4,9
HBr	-	-	-	-	-	-	5,6
H_2SO_4	-	-	-	-	-	-	7,0
HCl	4,0	-	-	-	-	-	8,4

Another approach, using the titration in presence of Hammett indicators, allowed POMs to be classified according to their decreasing acidity in acetonitrile [50]:

$$H_3PW_{12}O_{40} > H_4SiW_{12}O_{40} > H_4GeW_{12}O_{40} > H_6P_2W_{18}O_{40} > H_5BW_{12}O_{40} > H_6CoW_{12}O_{40}$$

Clearly, for a given structure, e.g. $[XW_{12}O_{40}]^{n-}$, the acidity decreases when the number of protons increases. However, it is difficult to predict relative acidities of compounds with different structures.

Numerous methods have been employed to describe the acidity of POMs in the solid state both qualitatively and quantitatively. From a general point of view, the degree of hydration of POMs was evidenced as a main factor influencing the number and strength of their acid sites [51-52]. Another conclusion of great importance for their applications in heterogenous catalysis was that deposition of POMs on various carriers (e.g. silica) results in a weakening of their acidity [53].

Adsorption of ammonia [54-55] or pyridine [56-57] monitored by IR showed the purely Brönsted nature of the acid sites of both acidic POMs and their salts – with the exception of $AlPW_{12}O_{40}$, for which the presence of Al^{3+} cations introduces some Lewis acidity [58]. Triethylphosphine oxide TEPO is another useful probe molecule for this kind of investigations. Its adsorption on various solids and the comparison of ^{31}P chemical shifts by means of solid-state NMR led to the conclusion that POMs possess stronger acid sites than classical solid state acids like sulfated silica or zeolites [51].

Quantitatively, calorimetric studies of NH_3 adsorption [59] (see Fig. 5) allowed to establish a sequence of POMs with decreasing acid strength, based on the initial values of their heat of adsorption:

$$H_3PW_{12}O_{40} > H_4SiW_{12}O_{40} > H_6P_2W_{21}O_{71} > H_6P_2W_{18}O_{62}$$

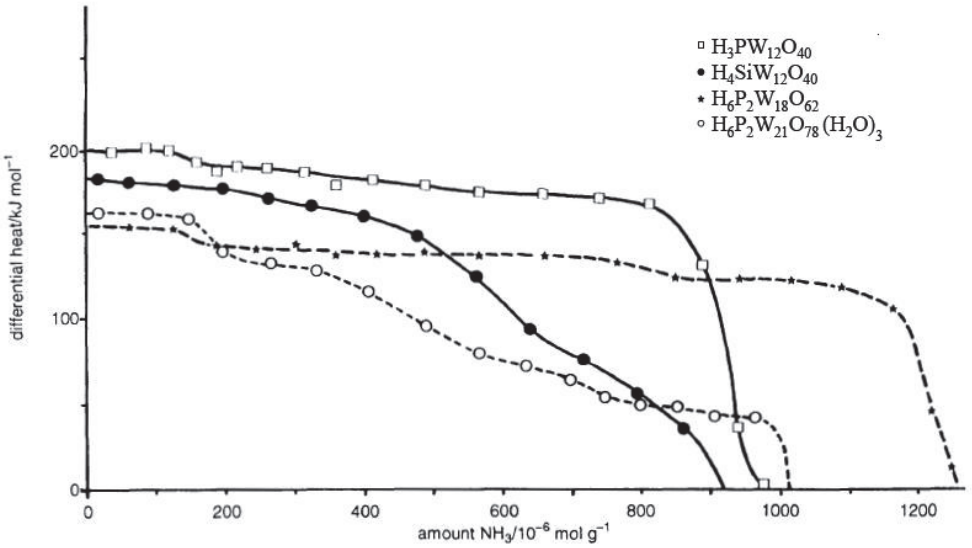

Figure 5. Differential heat of adsorption of NH_3 on various POMs ([59]).

The inverse approach, based on the temperature of desorption of previously adsorbed bases (ammonia, pyridine) gave similar results [57]:

$$H_3PW_{12}O_{40} > H_4SiW_{12}O_{40} \geq H_3PMo_{12}O_{40} > H_4SiMo_{12}O_{40}$$
$$T = 592°C \qquad 532°C \qquad 463°C \qquad 423°C$$

The already mentioned above Hammett indicator method applied to solids is simply a titration of a suspension of the desired compound (here the POM) in e.g. benzene or cyclohexane with a neutralizing agent (base, here *n*-butylamine) in presence of a species changing of colour upon completion of the acid-base reaction (the Hammett indicator). It permits to establish the number (by the amount of titrant used) and the force of acid sites (by using indicators with different H_0 values) simultaneously. A sequence of salts based on phosphotungstic acid with various metal cations were evaluated this way [52]. The results are reproduced in Table II.

Table II. Distribution of acid sites in various salts of phosphotungstic acid.

Polyoxometalate	***n*-butylamine/POM [mol/mol]**					
	$H_0 \leq 6,8$	**$H_0 \leq 5,0$**	**$H_0 \leq 3,3$**	**$H_0 \leq 1,5$**	**$H_0 \leq -3,0$**	**$H_0 \leq -5,6$**
$Ca_{3/2}PW_{12}O_{40}$	4,38	1,20	0,59	0,29	-	-
$Mg_{3/2}PW_{12}O_{40}$	4,60	1,57	0,87	0,29	-	-
$Zn_{3/2}PW_{12}O_{40}$	4,76	3,03	0,89	0,45	0,24	0,09
$AlPW_{12}O_{40}$	5,34	3,98	2,00	0,90	0,29	0,15
$Zr_{3/4}PW_{12}O_{40}$	8,96	4,71	3,33	2,65	0,74	0,44
$Na_3PW_{12}O_{40}$	0,74	0,59	0,41	0,12	-	-
$H_3PW_{12}O_{40}$	8,90	5,30	4,75	4,20	3,40	2,59

Clearly these results do not correspond with what is expected for these compounds. Indeed the polyoxometalates salts do not have any acid function so no acid sites are to be detected. Coordination of butylamine to the cations could be put forward as a reason of observed discrepancies. Moreover, for the polyacid $H_3PW_{12}O_{40}$ only the surface acid sites should be evidenced this way, the number of which is significantly lower than the one observed experimentally. The only explanation is that butylamine goes inside the crystals and reacts with all the protons leading then to a number of strong acid sites quite similar to that obtained in solution. It is also known that additional coordination of the base to the ammonium cations

can occur, as observed in the case of pyridine and pyridinium ion [60]. This too could explain the additional weak sites detected by this method.

1.2.2 Redox properties

In order to describe the redox properties of POMs various parameters were proposed like e.g. ionization potential, electronegativity or enthalpies of oxides formation. Accordingly, numerous experimental techniques were used for the investigations: measurements of reduction rate [61-66], IR [67], ESR [68] or X-ray photoelectron spectroscopy (XPS) [69-71]. Nevertheless, the results depend strongly on the reduction method [72]. In addition, some of the probe molecules used, according to their polarity, react solely on the surface of solid POMs while others are able to penetrate the bulk as well (so called "pseudo-liquid" phase, as for butylamine in the above paragraph).

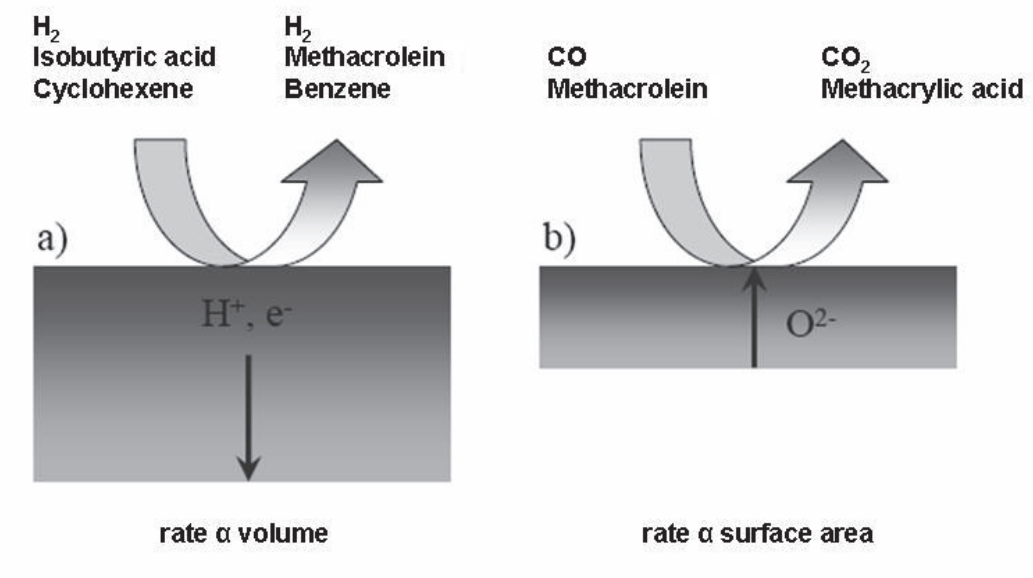

Figure 6. Schematic view of reactions of gas phase compounds with solids: a) on the surface and in the bulk ("pseudo-liquid" phase) and b) solely on the surface.

It has been established that both the composition of POMs and the nature of counteractions have an influence on the redox properties [62,71,73]. A sequence of polyoxometalates was proposed according to their decreasing capability of reduction, based on the values of their oxidation potential [74]:

$$H_3PMo_{12}O_{40} > H_4SiMo_{12}O_{40} >> H_3PW_{12}O_{40} > H_4SiW_{12}O_{40}$$

The redox properties of purely tungstic or molybdic POMs can be tuned by incorporation of other transition metals into the structure of the clusters. A classical example is the replacement of one or more {Mo=O} groups in the $(PMo_{12}O_{40})^{3-}$ Keggin structure by a {V=O} one. The resulting $(PV_xMo_{12-x}O_{40})^{(3+x)-}$ polyoxometalates are far more redox active than their precursors.

From a mechanistic point of view, the reduction of $H_3PM_{12}O_{40}$ (M = W, Mo) with hydrogen was suggested to proceed via consecutive steps [65,73,75]:

$$x\ H_{2(gas)} + PM_{12}O_{40}{}^{3-}{}_{(surface)} \rightleftharpoons 2x\ H^+{}_{(bulk)} + PM_{12}O_{40}{}^{(3+2x)-}{}_{(bulk)} \quad (1)$$

A **B**

$$2x\ H^+{}_{(bulk)} + PM_{12}O_{40}{}^{(3+2x)-}{}_{(bulk)} \rightleftharpoons PM_{12}O_{40}{}^{3-}{}_{(bulk)} + x\ H_2O_{(bulk)} \quad (2)$$

C

$$x\ H_2O_{(bulk)} \longrightarrow x\ H_2O_{(gas)} \quad (3)$$

In the first stage two surface protons are created from a polyoxometalate-assisted dissociation of a hydrogen molecule, followed by a transfer of two electrons to the POM, serving as a negative charge reservoir. These protons react with a polyoxometalate oxygen atom and a water molecule is formed, which, in the final step, is released in the gas phase. IR studies showed that only the bridging oxygen atoms O_b and O_c are involved in these transformations [76-77]. Fast H_2-D_2 equilibria were observed both in gaseous and solid phases, indicating that charge carriers diffusion into the bulk of POMs is more rapid than the rate of reduction of clusters (in other words the reduction becomes the rate determining step for overall process) [73,78]. The slow reduction is reversible, accompanied by a faster reoxidation, especially between species **B** and **A**. The rate of reoxidation in the second step decreases when the process occurs deeper in the bulk [75].

It has been observed that reduction with hydrogen of the mixed-addenda clusters $[PV_xMo_{12-x}O_{40}]^{(3+x)-}$ is slower than that of their precursor $[PMo_{12}O_{40}]^{3-}$ [39]. This phenomenon is not clearly understood. In addition, the extraction of the vanadyl ion VO^{2+} from the clusters which takes place at high temperature, complicates the interpretation of the experimental data.

1.3 Polyoxometalates - catalytic applications

The usefulness of POMs in catalysis is a direct consequence of their properties. Two main domains of applications are therefore acid and redox processes, with tungstic clusters being more commonly used in the former case and molybdic and vanadomolybdic ones in the latter. In addition, their thermal stability, facility of synthesis and modification and low environmental impact serve to explain a plethora of catalytic reactions employing polyoxometalates described in the literature and commercialized. Significantly though, while POMs-based homogenous catalysis seems to flourish, there are only scarce examples of applications of pure solid heteropolyoxometalates in heterogenous catalysis. This is due, as it has been mentioned already, to their very low specific surface area (only a few m^2/g). In most cases, reactions of polar molecules were reported, as they can react not only on the surface of the crystals but also in the first layers of the bulk, thus overcoming this issue (the "pseudo-liquid phase").

Various approaches were proposed to solve the problem of low surface areas of polyoxometalates: i) they can be deposited by impregnation on various carriers such as silica, alumina or carbon. However, supporting POMs leads to a weakening of the purely Brönsted acid sites [53,79-81]; ii) the oxide support (mainly silica) is first modified by anchoring amine groups, for example by reaction with $NH_2RSi(OEt)_3$. Reaction with the heteropolyacid leads then to protonation of the amine and formation of well-dispersed polyoxometalates on the support but most of the acidity is lost; iii) the polyoxometalates can be introduced to the support during its preparation, for example during the condensation of $Si(OEt)_4$. A lot of studies reported the use of this strategy [82] which can lead to systems more active than the homogenous ones, mainly due to the increase of the local concentration of POMs [83]; iv) the precipitation of partially saturated Cs^+, K^+, $(NH_4)^+$ or Rb^+ salts of polyoxometalates results in materials with very high surface areas (more than 100 m^2/g) and where the unreacted acidic clusters are deposited on the surface, and stabilized by interactions with the cations [84].

Some examples of catalytic systems based on POMs are presented below.

1.3.1 Acid catalysis

1.3.1.1 Skeletal isomerization of alkanes

The skeletal isomerization of low carbon *n*-paraffins to *iso*-paraffins is of great importance for the petroleum industry as it allows the preparation of fuel mixtures of improved performance as low-octane-number compounds are replaced by high-octane-number ones. As a consequence, the use of lead-containing fuel additives could be suppressed almost completely, resulting in economical and environmental benefits.

High activity and selectivity of Pt-doped cesium salts of $PW_{12}O_{40}^{3-}$ in butane-isobutane reaction were reported in presence of H_2 [85-87]. The activity was correlated with the surface acidity (i.e. the number of protons per unit of mass). The overall performance of $Cs_{2.5}H_{0.5}PW_{12}O_{40}$ at 300°C, the best catalyst in the series, was higher than that of sulfated zirconia (in terms of conversion), zeolites (in terms of selectivity to isobutane) and even silica-supported $H_3PW_{12}O_{40}$ (in both conversion and selectivity). From a mechanistic point of view the reaction was evidenced to proceed via two competing pathways, mono- and bimolecular (see Figure 7), their respective contributions varying strongly with the temperature [88-89].
Isomerization of *n*-pentane and *n*-hexane was also performed with this catalytic system and led to promising results [90-92].

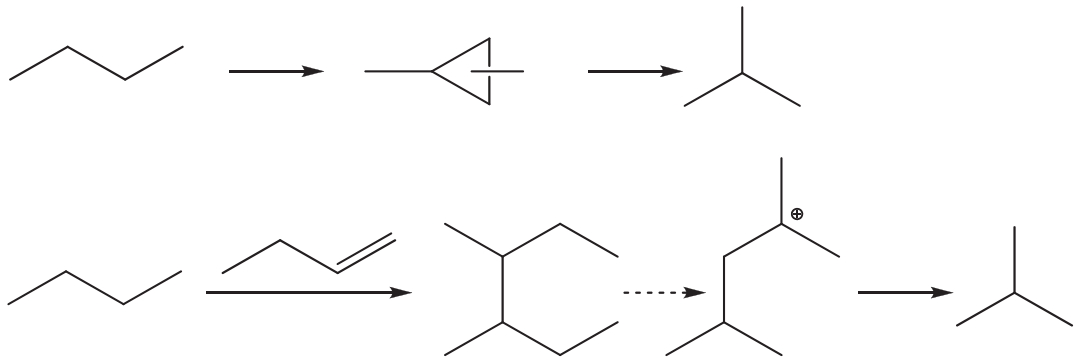

Figure 7. Proposed mechanism for the skeletal isomerization of *n*-butane [88].

1.3.1.2 Isomerization of olefins - Double bond shift

The cesium salts of phosphotungstic acid were reported to be active in the 1-butene → 2-butene isomerization at 75°C under atmospheric pressure (see Table III), a reaction that requires significantly weaker acid sites than the alkanes skeletal isomerization. The better performance of $Cs_2HPW_{12}O_{40}$ was attributed to its highest specific surface area [93].

Table III. Performance of POMs catalysts in 1-butene double bond shift reaction [93].

Catalyst	Reaction rate [10^{-6} mol/(g·s)]	Total conversion (%)	*Cis/trans* ratio
$H_3PW_{12}O_{40}$	4,8	10,0	1
$CsH_2PW_{12}O_{40}$	18,0	4,0	0,33
$Cs_2HPW_{12}O_{40}$	61,0	9,0	0,5
$Cs_{2.5}H_{0.5}PW_{12}O_{40}$	0,2	3,0	1,2
$Cs_3PW_{12}O_{40}$	0,0	0,0	-
SO_4^{2-}/ZrO_2	0,8	0,4	1

Catalyst pre-treatment at 200°C; total gas flow rate = 33 ml min^{-1}; 5% vol. 1-butene in He

1.3.1.3 Alkylation of olefins

The alkylation of olefins with branched alkanes allows the preparation of high-octane-number compounds and so is of key importance for the petroleum industry. Typically, isobutane is coupled with butenes to yield isooctane.

The Mobil Oil company has patented a catalyst made of phosphotungstic acid deposited on mesoporous MCM-41 (75 % wt.), which is able to catalyze this reaction with 87 % conversion of olefine, at 75-200°C under a pressure between 1 and 140 bars [94]. When supported on classical silica, a sample with 40% wt. of polyacid showed the best performance at 33°C and 25 bars [95]. Its cesium and ammonium salts with a varying degree of saturation were also studied and the corresponding results are listed in Table IV [96]:

Table IV. Performance of POMs catalysts in 2-butene alkylation [96].

Catalyst	Conversion of 2-butene (%)	Yield of trimethylpentane (%)	Ratio trimethylpentane/ dimethylhexane
$H_3PW_{12}O_{40}$	56.9	35.4	4.5
$(NH_4)_2HW_{12}O_{40}$	45.3	34.4	3.7
$Cs_2HPW_{12}O_{40}$	73.1	38.5	2.8
$Cs_{2.5}H_{0.5}PW_{12}O_{40}$	85.7	41.1	3.5

1.3.2 Redox catalysis

1.3.2.1 Oxidation of alkanes and alkenes

Short chain carboxylic acids (acetic acid, acrylic acid, methacrylic acid, …) and their esters are important industrial chemicals. These versatile monomers undergo polymerization, sometimes with other functional monomers as co-polymers, to produce various important polymers which have many commercial applications, such as super absorbents, detergent, textiles, paper additives, adhesives, plastics and coating materials.

Propane was shown to be catalytically oxidized to acrylic acid with molecular oxygen over molybdic POMs that were pre-treated with pyridine. A selectivity of 24 % to acrylic acid at a 12 % conversion of propane could be achieved at 360°C. Tungstic POMs were inactive in this reaction [97-99]. Partially reduced niobium- and pyridine-exchanged salts of phosphomolybdic ($NbPMo_{12}Pyr$) and phosphovanadomolybdic acids ($NbPVMo_{11}Pyr$) were also tested and at 380°C a 10.5 % yield of acrylic acid could be obtained with a propane conversion of 21 % [100-101].

Some results of bifunctional (noble metal + POM) systems active in the same process [102] are given in Table V.

Table V. Selective oxidation of propane over $M_{0.08}^{N+}Cs_{2.5}H_{(0.5-0.08N)}PMo_{12}O_{40}$ [102].

M^{N+}	Conversion (%)	Selectivity (%)					
		Acrylic acid	Acrolein	Propylene	Acetic acid	CO	CO_2
Rh^{3+}	17	8	1	6	7	28	50
Fe^{3+}	13	18	2	9	11	50	10
Ni^{2+}	12	17	2	8	10	54	10
no doping	12	8	1	6	8	62	15
Co^{2+}	8	16	3	13	11	49	10
Cu^{2+}	8	9	3	10	4	55	19
Mn^{2+}	6	19	3	15	10	46	7

Catalyst = 1.0 g; total flow rate = 30 ml min^{-1}; $C_3H_8/O_2/N_2$=30/40/30; T = 360°C

The oxidation of *iso*-butane over $Cs_xH_{3-x}PMo_{12}O_{40}$ compounds has been investigated and the yield of methacrylic acid was shown to reach a maximum value for a Cs^+ content of 2.5. Further modifications of catalysts by V^{5+} and Ni^{2+} substitution of Mo^{6+} and H^+ respectively, allowed to increase the yield of methacrylic acid to 9.0 % at 340°C [66,103].

Another bifunctional system was proposed for the direct oxidation of ethylene to acetic acid under mild conditions (~200°C, 5 bars) [104], and proved to be an interesting alternative to the industrial two step procedure (see Table VI).

Table VI. Catalysts performance in oxidation of ethylene to acetic acid [104].

Catalyst	Yield	Selectivity (%)		
	$[g \cdot g_{POM}^{-1} \cdot h^{-1}]$	Acetic acid	Acetaldehyde	CO_2
Pd - $H_4SiW_{12}O_{40}$	93.1	78.5	5.5	14.2
Pd - $H_3PW_{12}O_{40}$	83.3	78.0	5.0	16.0
Pd - $H_4SiMo_6W_6O_{40}$	91.2	77.6	4.4	17.5
Pd - $H_3PMo_6W_6O_{40}$	75.1	76.5	4.1	19.2
Pd - $H_3PMo_{12}O_{40}$	68.5	77.5	4.6	17.8
Pd - $H_5PV_2Mo_{10}O_{40}$	94.0	61.4	19.4	17.6
Pd	-	0.0	0.0	0.0
$H_3PW_{12}O_{40}$	0.0	0.0	0.0	0.0

Gas flow composition: ($C_2H_4/O_2/H_2O/N_2$) = 50/7/30/13.

1.3.2.2 Oxidative dehydrogenation of alkanes

The oxidative dehydrogenation of simple alkanes to olefins proceeds often in competition with their oxidation and the polyoxometalate catalysts can be tuned to better carry out one of these processes.

SiO_2-supported molybdic POMs convert ethane to both ethylene and acetaldehyde at temperatures 450 - 570°C in presence of N_2O [105-106]. The potassium and ammonium salts of $PMo_{12}O_{40}^{3-}$ modified with antimony were less active than the antimony-free compound. The conversion of ethane ranged from 1 to 7 %, while the selectivities to ethylene were between 34 and 56 % [107]. Over SiO_2-supported $HPMoV_x$ catalysts, selectivity towards ethylene was about 70 % at temperatures ranging from 300 to 360°C, while the deposition of the same catalysts on TiO_2 led to a higher acetic acid yield [108].

Partial reduction of niobium- and pyridine-exchanged salts of phosphomolybdic ($NbPMo_{12}Pyr$) and phosphovanadomolybdic POMs ($NbPVMo_{11}Pyr$) at 420°C formed solids that could catalyze the oxidative dehydrogenation of ethane to ethylene and acetic acid in high yields at atmospheric pressure and moderate temperature, under reducing conditions [109].

$Cs_{2.5}Cu_{0.08}H_{1.34}PVMo_{11}O_{40}$ was used in the oxidative dehydrogenation of propane at 380°C. 35 % propane conversion and 27 % propylene selectivity (9.5 % yield) were reached [110]. The cesium salts of molybdic polyoxometalates $Cs_xH_{3-x}PMo_{12}O_{40}$ are also active in this process without any other transition metal added and the best yield of propylene (9.3 %) was achieved over $Cs_{2.56}H_{0.44}PMo_{12}O_{40}$ at 380°C [111]. A stable propylene yield of 20 % was obtained at 450°C over a novel kind of nanocomposites formed by NiO and $Cs_{2.5}H_{0.5}PMo_{12}O_{40}$ (NiO-POM) with particle sizes in the range 5-10 nm. This result is the highest one reported under mild temperature [112]. This system showed also superior catalytic performance for the oxidative dehydrogenation of isobutane. Over 70 % NiO-POM nanocomposites, the selectivities to isobutene were 79 % and 71 % at isobutane conversions of 15 % and 21 % at 450 and 500°C, respectively.

1.3.2.3 Partial methane oxidation

World's known gas resources can rival the petrol ones (see Figure 8) [113-114]. With methane being easily accessible as the main component of natural gas and by-product of oil refining and chemical processing, the balance is slowly shifting from simple energy acquisition by burning in favour of its valorization (methane-based chemistry). Among all possibilities (see Figure 9), its partial oxidation to methanol and/or formaldehyde is attracting increasing attention of the scientists, as both constitute useful precursors in the chemical industry.

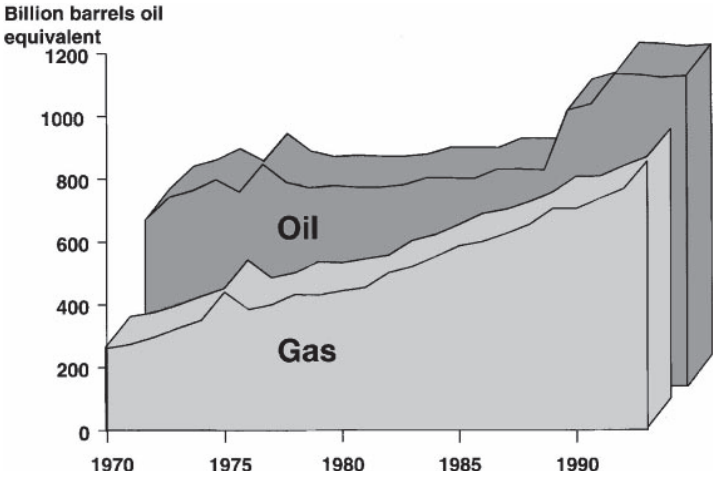

Figure 8. Confirmed world gas and oil resources [113].

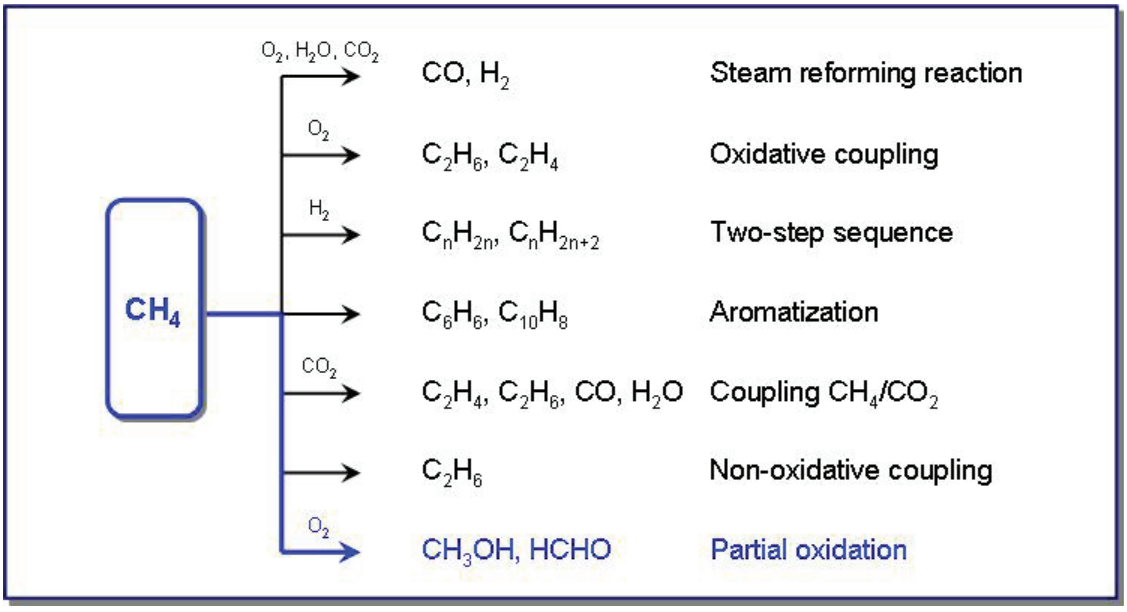

Figure 9. Overview of possible methane transformation routes.

Unfortunately, methane is also notorious for its chemical inertness, justified by its symmetry (no polar electron distribution to undergo a chemical attack) and high C-H primary bond stability (440 kJ/mol). Worse still, once activated, it is rare to obtain the partial oxidation products as they are more reactive than the substrate itself and the reaction proceeds rapidly leading to a CO_2 release.

Some of the heterogenous catalytic methane oxidation systems investigated in the course of years are presented in Table VII. One notes drastic reaction conditions (elevated temperatures, pressure) as well as mildly satisfying performance.

Table VII. Heterogenous catalytic systems for partial methane oxidation.

Catalyst	**T [°C]**	**Oxidizing agent (p)**	**Conversion (%)**	**Selectivity (%)**		**TOF [mol/(kg_{cat}·h)**	**Ref.**
				CH_3OH	HCHO		
SiO_2	620	O_2	4,8	0	24	0,2	[115]
MoO_3/SiO_2	650	O_2	5,3	0	32	3,8	[116]
W/SiO_2	650	O_2	6,9	0	11,9	0,9	[117]
V_2O_5/SiO_2	650	O_2	13,5	0	35	25,3	[118]
Fe/SiO_2	600	O_2	-	traces	~45	9,7	[119]
Mo/SBA-15	680	O_2	8,1	0	15,5	6,0	[120]
VO_x/MCM-41	625	O_2	5,4	0,2	22	46,1	[121]
$FePO_4/SiO_2$	600	O_2	~10	traces	12	9,5	[122]
$MgBOP/SiO_2$	500	O_2	8,1	0	22	2,9	[123]
$MoSnP/SiO_2$	675	O_2	7,2	traces	64,8	13,3	[124]
Sr/La_2O_3-MoO_3/SiO_2	630	Air	6,7	0	4,1	6,2	[125]
Sr/La_2O_3-V_2O_5/SiO_2	625	Air+H_2O	13,1	0,9	7,4	31,4	[126]
Cu-Fe/ZnO	750	O_2	2,5	0	10	2,5	[127]
Zr-P-O	700	O_2	2,0	0	32	0,3	[128]
Cr or Fe V-P-O	600	O_2	~0,1	0	~5	0,02-0,06	[129]
MgO	750	O_2	0,7	0	60	9	[130]
$TiO_2 + CH_2Cl_2$	650	O_2	7,5	0	33	6	[131]
Fe/sodalite	435	O_2 (50 bar)	5,8	25	-	5,8	[132]
Ga_2O_3/MoO_3	455	O_2 (15 bar)	3	22	-	2,2	[133]

Generally, redox properties are claimed to be responsible for the catalysts performance in oxidation reactions [134] although the acid-base strength was suggested to play a crucial role in the C-H activation initial step [135]. Polyoxometalates, combining both these features, could then be good candidates for methane partial oxidation. Indeed, there are many examples in the literature of such POMs-based systems, with or without addition of co-catalysts (noble metals) and studied in homogenous as well as in heterogenous conditions.

1.3.2.3.a) Homogenous methane oxidation systems based on POMs

Vanadium-containing POMs were evidenced to oxidize methane in trifluoroacetic acid CF_3COOH, in presence of $K_2S_2O_8$ as the oxidizing agent, under high pressure [136-137]. Methyl trifluoroacetate was the main product. The best performance was obtained with $H_5PV_2W_{10}O_{40}$ whereas molybdic clusters were less active. The mechanism suggested by the authors is depicted in Figure 10.

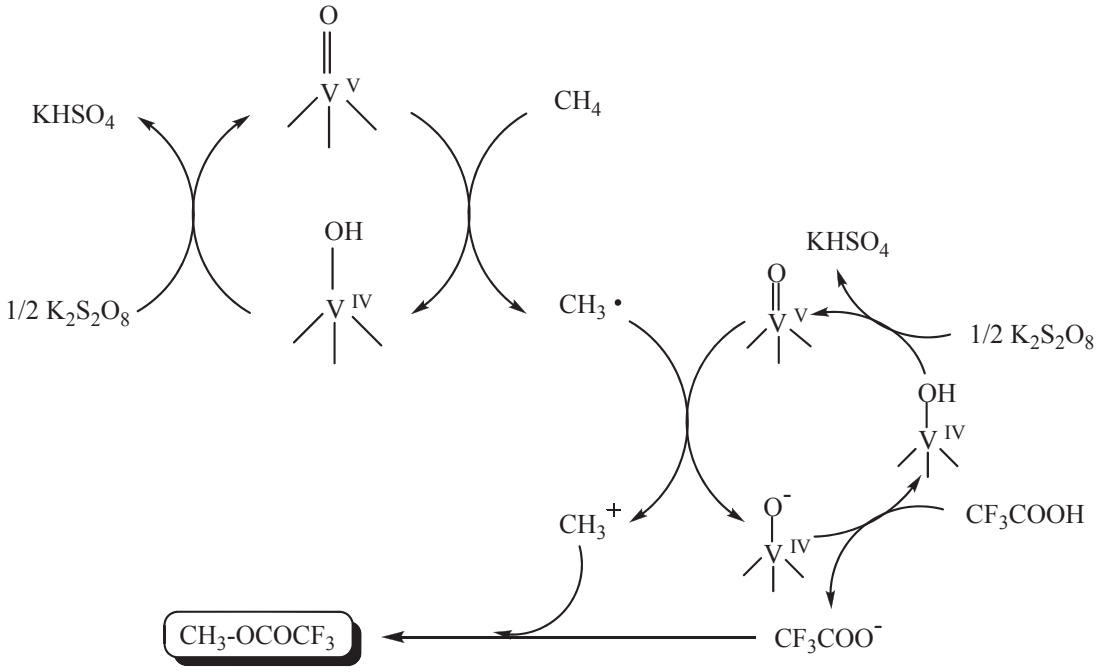

Figure 10. Proposed mechanism for methane oxidation by POMs in CF_3COOH [137].

One-step oxygenation of methane with hydrogen peroxide in presence of $H_4PVMo_{11}O_{40}$ in $(CF_3CO)_2O$ as solvent at 80°C and 50 bars was reported [138-139]. After 24 h reaction, a 33 % conversion of CH_4 could be achieved, with a yield of methyl formate of 2.4 % (the main reaction product was CO_2). Kinetic studies elucidated the key points of the mechanism: (i)

decomposition of $H_4PVMo_{11}O_{40}$ to form $VO(O_2)^+$ and $PMo_{11}O_{39}^{7-}$; (ii) $VO(O_2)^+$ as catalytically active species for the reaction and (iii) oxidation occurring via a radical-chain mechanism with methane activation as the rate determining step [140-141]:

$$CH_4 \rightarrow CH_3OH \text{ or } CF_3COOCH_3 \rightarrow HCOOH \rightarrow CO_2.$$

The di-iron-substituted silicotungstate $[\gamma\text{-}SiW_{10}\{Fe(OH_2)\}_2O_{38}]^{6-}$ (see Fig. 11) was synthesized so as to mimic the active site of the methane monooxygenase enzyme found in the methanotrophic bacteria and able to catalyze methane oxidation under mild conditions with a great efficiency. The inorganic congener was found to be also quite active, oxidizing methane to methanol in presence of hydrogen peroxide as oxidizer at 30°C [142]. Moreover, by changing the counteractions from organic $(Bu_4N)^+$ to K^+, the reaction could be successfully transferred to an aqueous environment [143].

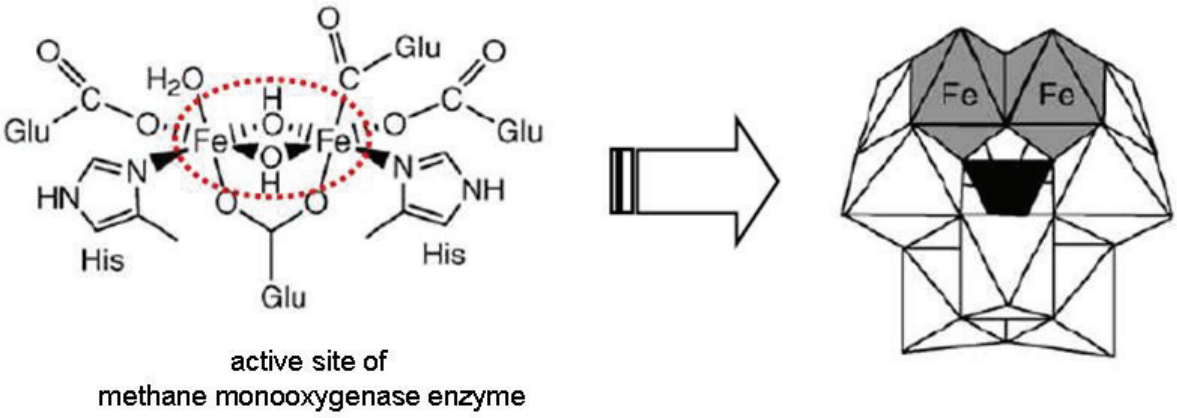

Figure 11. Analogy between the active site of the methane oxidizing enzyme and the iron-substituted POM [142].

1.3.2.3.b) Heterogenous methane oxidation systems based on POMs

In a pioneering work on the gas phase methane oxidation on supported polyoxometalates various molybdic clusters were found to be efficient catalysts at elevated temperatures (500 °C and higher) with N_2O as oxidizing agent, whereas tungstic ones were inactive [144-145]. On silica-supported silicomolybdic acid a partial methane oxidation to formaldehyde under water vapour was observed at high temperature [146]. These operating conditions corresponded to the decomposition temperature of the polyoxometalate which was then in equilibrium (due to the presence of water) with another species. As a result, formation of active oxygen atoms

which could oxidize methane was claimed. Finally, polyoxometalates were also used as precursors to highly dispersed mixed metal oxides [147-148], that showed activities in methane oxidation with O_2 at atmospheric pressure higher than oxides obtained from classical impregnation [149].

Cesium salts of polyoxometalates functionalized with Pd were successfully employed in oxidation with a O_2-H_2 mixture [150-151]. In that case the activity was probably related to the *in situ* generation of H_2O_2 on the Pd particles.

When vanadomolybdic POM supported on silica was coupled with a Periana-type Pt(II) complex (see Figure 12), methanol, formaldehyde and ethanal were detected as products of reaction carried out under mild conditions (50°C, 30 bars of CH_4 and 2 bars of O_2) [152]. Unfortunately, this promising system has not been reproduced.

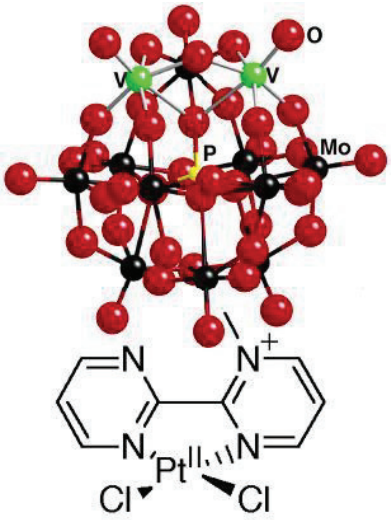

products, μmol				
CH_3OH	HCHO	CH_3CHO	acid (μmol)	TON
3	1	13	none	6
30	12	48	H_2SO_4 (150)	31
24	19	49	$H_5PV_2Mo_{10}O_{40}$ (60)	32
46	9	41	$H_5PV_2Mo_{10}O_{40}$ (30)	33

Figure 12. Neumann catalyst combining a vanadomolybdic POM and a Pt(II) complex and its performance in partial methane oxidation [152].

1.4 References

(1) Berzelius, J. J. *Poggendorffs Ann. Phys. Chem.* **1826**, *6*, 369.

(2) Keggin, J. F. *Nature* **1933**, *132*, 351.

(3) Okuhara, T.; Mizuno, N.; Misono, M. *App. Catal. A* **2001**, *222*, 63.

(4) Hill, C. L. *J. Mol. Catal. A-Chem.* **2007**, *262*, 2.

(5) Zakzeski, J.; Bruijnincx, P. C. A.; Jongerius, A. L.; Weckhuysen, B. M. *Chem. Rev.* **2010**, *110*, 3552.

(6) Vishnikin, A. B. *J. Mol. Liq.* **2005**, *118*, 51.

(7) Lee, J.; Kim, J.; Choi, W. *Environ. Sci. Technol.* **2007**, *41*, 5433.

(8) Yavari, R.; Ahmadi, S. J.; Huang, Y. D.; Khanchi, A. R.; Bagheri, G.; He, J. M. *Talanta* **2009**, *77*, 1179.

(9) Haghighi, B.; Hamidi, H.; Gorton, L. *Electrochim. Acta* **2010**, *55*, 4750.

(10) Ban, N.; Freeborn, B.; Nissen, P.; Penczek, P.; Grassucci, R. A.; Sweet, R.; Frank, J.; Moore, P. B.; Steitz, T. A. *Cell* **1998**, *93*, 1105.

(11) Ban, N.; Nissen, P.; Hansen, J.; Capel, M.; Moore, P. B.; Steitz, T. A. *Nature* **1999**, *400*, 841.

(12) Judd, D. A.; Nettles, J. H.; Nevins, N.; Snyder, J. P.; Liotta, D. C.; Tang, J.; Ermolieff, J.; Schinazi, R. F.; Hill, C. L. *J. Am. Chem. Soc.* **2001**, *123*, 886.

(13) Binnemans, K. *Chem. Rev.* **2009**, *109*, 4283.

(14) Granadeiro, C. M.; Ferreira, R. A. S.; Soares-Santos, P. C. R.; Carlos, L. D.; Nogueira, H. I. S. *Eur. J. Inorg. Chem.* **2009**, 5088.

(15) Zhang, T. R.; Liu, S. Q.; Kurth, D. G.; Faul, C. F. J. *Adv. Funct. Mater.* **2009**, *19*, 642.

(16) Granadeiro, C. M.; Ferreira, R. A. S.; Soares-Santos, P. C. R.; Carlos, L. D.; Trindade, T.; Nogueira, H. I. S. *J. Mater. Chem.* **2010**, *20*, 3313.

(17) Shen, Y.; Peng, J.; Chen, C. Y.; Chen, D.; Zhang, H. Q.; Meng, C. L. *Z. Naturforsch. B-Chem. Sci.* **2010**, *65*, 603.

(18) Wang, Z. L.; Zhang, R. L.; Ma, Y.; Peng, A. D.; Fu, H. B.; Yao, J. N. *J. Mater. Chem.* **2010**, *20*, 271.

(19) Luo, Z.; Kogerler, P.; Cao, R.; Hill, C. L. *Inorg. Chem.* **2009**, *48*, 7812.

(20) Yamase, T.; Abe, H.; Ishikawa, E.; Nojiri, H.; Ohshima, Y. *Inorg. Chem.* **2009**, *48*, 138.

(21) Kogerler, P.; Tsukerblat, B.; Muller, A. *Dalton Trans.* **2010**, *39*, 21.

(22) Briand, L. E.; Baronetti, G. T.; Thomas, H. J. *App. Catal. A* **2003**, *256*, 37.

(23) Newton, G. N.; Yamashita, S.; Hasumi, K.; Matsuno, J.; Yoshida, N.; Nihei, M.; Shiga, T.; Nakano, M.; Nojiri, H.; Wernsdorfer, W.; Oshio, H. *Angew. Chem.-Int. Ed.* **2011**, *50*, 5715.

(24) Pettersson, L.; Andersson, I.; Ohman, L. O. *Inorg. Chem.* **1986**, *25*, 4726.

(25) Laronze, N.; Marrot, J.; Herve, G. *Inorg. Chem.* **2003**, *42*, 5857.

(26) Combs-Walker, L. A.; Hill, C. L. *Inorg. Chem.* **1991**, *30*, 4016.

(27) Putaj, P.; Lefebvre, F. *Coord. Chem. Rev.* **2011**, *255*, 1642.

(28) Nomiya, K.; Sakai, Y.; Matsunaga, S. *Eur. J. Inorg. Chem.* **2011**, 179.

(29) Bassil, B. S.; Kortz, U. *Z. Anorg. Allg. Chem.* **2010**, *636*, 2222.

(30) Bi, L. H.; Li, B.; Wu, L. X.; Bao, Y. Y. *Inorg. Chim. Acta* **2009**, *362*, 3309.

(31) Zhang, W.; Liu, S. X.; Zhang, C. D.; Tan, R. K.; Ma, F. J.; Li, S. J.; Zhang, Y. Y. *Eur. J. Inorg. Chem.* **2010**, 3473.

(32) Dolbecq, A.; Dumas, E.; Mayer, C. R.; Mialane, P. *Chem. Rev.* **2010**, *110*, 6009.

(33) Berardi, S.; Carraro, M.; Sartorel, A.; Modugno, G.; Bonchio, M. *Isr. J. Chem.* **2011**, *51*, 259.

(34) Thorimbert, S.; Hasenknopf, B.; Lacote, E. *Isr. J. Chem.* **2011**, *51*, 275.

(35) Brown, G. M.; Noespirlet, M. R.; Busing, W. R.; Levy, H. A. *Acta Crystallogr. B-Struct. Sci.* **1977**, *33*, 1038.

(36) Rocchicciolideltcheff, C.; Fournier, M.; Franck, R.; Thouvenot, R. *Inorg. Chem.* **1983**, *22*, 207.

(37) Fournier, M.; Feumijantou, C.; Rabia, C.; Herve, G.; Launay, S. *J. Mater. Chem.* **1992**, *2*, 971.

(38) Marosi, L.; Platero, E. E.; Cifre, J.; Arean, C. O. *J. Mater. Chem.* **2000**, *10*, 1949.

(39) Mizuno, N.; Misono, M. *Chem. Rev.* **1998**, *98*, 199.

(40) Eguchi, K.; Yamazoe, N.; Seiyama, T. *Nippon Kagaku Kaishi* **1981**, 336.

(41) Rocchicciolideltcheff, C.; Fournier, M. *J. Chem. Soc.-Faraday Trans.* **1991**, *87*, 3913.

(42) Bielanski, A.; Datka, J.; Gil, B.; Malecka-Lubanska, A.; Micek-Ilnicka, A. *Catal. Lett.* **1999**, *57*, 61.

(43) Kozhevnikov, I. V.; Sinnema, A.; Jansen, R. J. J.; Vanbekkum, H. *Catal. Lett.* **1994**, *27*, 187.

(44) Kozhevnikov, I. V.; Sinnema, A.; Vanbekkum, H. *Catal. Lett.* **1995**, *34*, 213.

(45) Ganapathy, S.; Fournier, M.; Paul, J. F.; Delevoye, L.; Guelton, M.; Amoureux, J. P. *J. Am. Chem. Soc.* **2002**, *124*, 7821.

(46) Janik, M. J.; Davis, R. J.; Neurock, M. *J. Phys. Chem. B* **2004**, *108*, 12292.

(47) Janik, M. J.; Davis, R. J.; Neurock, M. *J. Am. Chem. Soc.* **2005**, *127*, 5238.

(48) Ivakin, A. A.; Kurbatova, L. D.; Kapustina, L. A. *Zh. Neorg. Kh.* **1978**, *23*, 2545.

(49) Kulikov, S. M.; Kozhevnikov, I. V. *Bulletin of the Academy of Sciences of the USSR Division of Chemical Science* **1981**, *30*, 348.

(50) Drago, R. S.; Dias, J. A.; Maier, T. O. *J. Am. Chem. Soc.* **1997**, *119*, 7702.

(51) Osegovic, J. P.; Drago, R. S. *J. Phys. Chem. B* **2000**, *104*, 147.

(52) Hayashi, H.; Moffat, J. B. *J. Catal.* **1982**, *77*, 473.

(53) Kapustin, G. I.; Brueva, T. R.; Klyachko, A. L.; Timofeeva, M. N.; Kulikov, S. M.; Kozhevnikov, I. V. *Kinet. Catal.* **1990**, *31*, 896.

(54) Highfield, J. G.; Moffat, J. B. *J. Catal.* **1984**, *88*, 177.

(55) Seo, G.; Lim, J. W.; Kim, J. T. *J. Catal.* **1988**, *114*, 469.

(56) Highfield, J. G.; Moffat, J. B. *J. Catal.* **1984**, *89*, 185.

(57) Hodnett, B. K.; Moffat, J. B. *J. Catal.* **1984**, *88*, 253.

(58) Cheng, W. C.; Luthra, N. P. *J. Catal.* **1988**, *109*, 163.

(59) Lefebvre, F.; Liucai, F. X.; Auroux, A. *J. Mater. Chem.* **1994**, *4*, 125.

(60) Hashimoto, M.; Misono, M. *Acta Crystallogr. C-Cryst. Struct. Commun.* **1994**, *50*, 231.

(61) Kim, H. C.; Moon, S. H.; Lee, W. Y. *Chem. Lett.* **1991**, 447.

(62) Ai, M. *Appl. Catal.* **1982**, *4*, 245.

(63) Hodnett, B. K.; Moffat, J. B. *J. Catal.* **1985**, *91*, 93.

(64) Yoshida, S.; Nilyama, H.; Echigoya, E. *J. Phys. Chem.* **1982**, *86*, 3150.

(65) Katamura, K.; Nakamura, T.; Sakata, K.; Misono, M.; Yoneda, Y. *Chem. Lett.* **1981**, 89.

(66) Mizuno, N.; Tateishi, M.; Iwamoto, M. *J. Catal.* **1996**, *163*, 87.

(67) Eguchi, K.; Toyozawa, Y.; Yamazoe, N.; Seiyama, T. *J. Catal.* **1983**, *83*, 32.

(68) Otake, M.; Komiyama, Y.; Otaki, T. *J. Phys. Chem.* **1973**, *77*, 2896.

(69) Centi, G.; Nieto, J. L.; Iapalucci, C.; Bruckman, K.; Serwicka, E. M. *Appl. Catal.* **1989**, *46*, 197.

(70) Konishi, Y.; Sakata, K.; Misono, M.; Yoneda, Y. *J. Catal.* **1982**, *77*, 169.

(71) Akimoto, M.; Shima, K.; Ikeda, H.; Echigoya, E. *J. Catal.* **1984**, *86*, 173.

(72) Okuhara, T.; Mizuno, N.; Misono, M. In *Adv. Catal. Vol 41*; Eley, D. D., Haag, W. O., Gates, B., Eds. 1996; Vol. 41, p 113.

(73) Mizuno, N.; Misono, M. *J. Phys. Chem.* **1989**, *93*, 3334.

(74) Souchay, P. In *Polyanions et polycations*; Gauthier-Villars, Ed. 1963.

(75) Komaya, T.; Misono, M. *Chem. Lett.* **1983**, 1177.

(76) Tsuneki, H.; Niiyama, H.; Echigoya, E. *Chem. Lett.* **1978**, 645.

(77) Tsuneki, H.; Niiyama, H.; Echigoya, E. *Chem. Lett.* **1978**, 1183.

(78) Mizuno, N.; Watanabe, T.; Misono, M. *J. Phys. Chem.* **1990**, *94*, 890.

(79) Lefebvre, F. *J. Chem. Soc.-Chem. Comm.* **1992**, 756.

(80) Thomas, A.; Dablemont, C.; Basset, J. M.; Lefebvre, F. *C. R. Chim.* **2005**, *8*, 1969.

(81) Grinenval, E.; Rozanska, X.; Baudouin, A.; Berrier, E.; Delbecq, F.; Sautet, P.; Basset, J. M.; Lefebvre, F. *J. Phys. Chem. C* **2010**, *114*, 19024.

(82) Dufaud, V.; Lefebvre, F. *Materials* **2010**, *3*, 682.

(83) Dufaud, V.; Lefebvre, F.; Niccolai, G. P.; Aouine, M. *J. Mater. Chem.* **2009**, *19*, 1142.

(84) Okuhara, T.; Watanabe, H.; Nishimura, T.; Inumaru, K.; Misono, M. *Chem. Mat.* **2000**, *12*, 2230.

(85) Na, K.; Okuhara, T.; Misono, M. *Chem. Lett.* **1993**, 1141.

(86) Na, K. T.; Okuhara, T.; Misono, M. *J. Chem. Soc.-Chem. Comm.* **1993**, 1422.

(87) Na, K.; Okuhara, T.; Misono, M. *J. Catal.* **1997**, *170*, 96.

(88) Suzuki, T.; Okuhara, T. *Chem. Lett.* **2000**, 470.

(89) Ma, Z. N.; Hua, W. M.; Ren, Y.; He, H. Y.; Gao, Z. *Appl. Catal. A* **2003**, *256*, 243.

(90) Liu, Y. Y.; Koyano, G.; Na, K.; Misono, M. *Appl. Catal. A* **1998**, *166*, L263.

(91) Liu, Y. Y.; Na, K.; Misono, M. *J. Mol. Catal. A-Chem.* **1999**, *141*, 145.

(92) Travers, C.; Essayem, N.; Delage, M.; Quelen, S. *Catal. Today* **2001**, *65*, 355.

(93) Bardin, B. B.; Davis, R. J. *Top. Catal.* **1998**, *6*, 77.

(94) Kresge, C. T.; Marler, D. O.; Rav, G. S.; Rose, B. H. 1994; Vol. US5324881.

(95) Blasco, T.; Corma, A.; Martinez, A.; Martinez-Escolano, P. *J. Catal.* **1998**, *177*, 306.

(96) Tundo, P.; Perosa, A.; Zecchini, F.; Ed., W.-I., Ed. 2007.

(97) Ueda, W.; Suzuki, Y. *Chem. Lett.* **1995**, 541.

(98) Li, W.; Oshihara, K.; Ueda, W. *App. Catal. A* **1999**, *182*, 357.

(99) Vitry, D.; Dubois, J. L.; Ueda, W. *J. Mol. Catal. A-Chem.* **2004**, *220*, 67.

(100) Dillon, C. J.; Holles, J. H.; Davis, R. J.; Labinger, J. A.; Davis, M. E. *J. Catal.* **2003**, *218*, 54.

(101) Holles, J. H.; Dillon, C. J.; Labinger, J. A.; Davis, M. E. *J. Catal.* **2003**, *218*, 42.

(102) Mizuno, N.; Suh, D. J.; Han, W.; Kudo, T. *J. Mol. Catal. A-Chem.* **1996**, *114*, 309.

(103) Mizuno, N.; Yahiro, H. *J. Phys. Chem. B* **1998**, *102*, 437.

(104) Sano, K.; Uchida, H.; Wakabayashi, S. *Catalysis Surveys from Japan* **1999**, *3*, 55.

(105) Hong, S. S.; Moffat, J. B. *Appl. Catal. A* **1994**, *109*, 117.

(106) Moffat, J. B. *Appl. Catal. A* **1996**, *146*, 65.

(107) Albonetti, S.; Cavani, F.; Trifiro, F.; Koutyrev, M. *Catal. Lett.* **1995**, *30*, 253.

(108) Sopa, A.; Waclaw-Held, A.; Grossy, M.; Pijanka, J.; Nowinska, K. *Appl. Catal. A* **2005**, *285*, 119.

(109) Davis, M. E.; Dillon, C. J.; Holles, J. H.; Labinger, J. *Angew. Chem.-Inter. Ed.* **2002**, *41*, 858.

(110) Min, J. S.; Mizuno, N. *Catal. Today* **2001**, *71*, 89.

(111) Sun, M.; Zhang, J. Z.; Cao, C. J.; Zhang, Q. H.; Wang, Y.; Wan, H. L. *App. Catal. A* **2008**, *349*, 212.

(112) Zhang, Q. H.; Cao, C. J.; Xu, T.; Sun, M.; Zhang, J. H.; Wang, Y.; Wan, H. L. *Chem. Commun.* **2009**, 2376.

(113) Lunsford, J. H. *Catal. Today* **2000**, *63*, 165.

(114) Alvarez-Galvan, M. C.; Mota, N.; Ojeda, M.; Rojas, S.; Navarro, R. M.; Fierro, J. L. G. *Catal. Today* **2011**, *171*, 15.

(115) Kastanas, G. N.; Tsigdinos, G. A.; Schwank, J. *Appl. Catal.* **1988**, *44*, 33.

(116) Spencer, N. D. *J. Catal.* **1988**, *109*, 187.

(117) de Lucas, A.; Valverde, J. L.; Canizares, P.; Rodriguez, L. *Appl. Catal. A* **1999**, *184*, 143.

(118) Parmaliana, A.; Frusteri, F.; Mezzapica, A.; Scurrell, M. S.; Giordano, N. *J. Chem. Soc.-Chem. Comm.* **1993**, 751.

(119) Kobayashi, T.; Nakagawa, K.; Tabata, K.; Haruta, M. *J. Chem. Soc.-Chem. Comm.* **1994**, 1609.

(120) Dai, L. X.; Teng, Y. H.; Tabata, K.; Suzuki, E.; Tatsumi, T. *Chem. Lett.* **2000**, 794.

(121) Berndt, H.; Martin, A.; Bruckner, A.; Schreier, E.; Muller, D.; Kosslick, H.; Wolf, G. U.; Lucke, B. *J. Catal.* **2000**, *191*, 384.

(122) Alptekin, G. O.; Herring, A. M.; Williamson, D. L.; Ohno, T. R.; McCormick, R. L. *J. Catal.* **1999**, *181*, 104.

(123) Otsuka, K.; Hatano, M. *Chem. Lett.* **1992**, 2397.

(124) Weng, T.; Wolf, E. E. *App. Catal. A* **1993**, *96*, 383.

(125) Sun, Q.; Dicosimo, J. I.; Herman, R. G.; Klier, K.; Bhasin, M. M. *Catal. Lett.* **1992**, *15*, 371.

(126) Shi, C. L.; Sun, Q.; Hu, H. C.; Herman, R. G.; Klier, K.; Wachs, I. E. *Chem. Commun.* **1996**, 663.

(127) Sojka, Z.; Herman, R. G.; Klier, K. *J. Chem. Soc.-Chem. Commun.* **1991**, 185.

(128) Sinev, M. Y.; Setiadi, S.; Otsuka, K. *Mendeleev Commun.* **1993**, 10.

(129) McCormick, R. L.; Alptekin, G. O.; Herring, A. M.; Ohno, T. R.; Dec, S. F. *J. Catal.* **1997**, *172*, 160.

(130) Hargreaves, J. S. J.; Hutchings, G. J.; Joyner, R. W. *Nature* **1990**, *348*, 428.

(131) Baldwin, T. R.; Burch, R.; Squire, G. D.; Tsang, S. C. *Appl. Catal.* **1991**, *75*, 153.

(132) Lyons, J. E.; Ellis, P. E.; Durante, V. A. *ACTIVE IRON OXO CENTERS FOR THE SELECTIVE CATALYTIC-OXIDATION OF ALKANES*, 1991; Vol. 67.

(133) Hargreaves, J. S. J.; Hutchings, G. J.; Joyner, R. W.; Taylor, S. H. *Chem. Commun.* **1996**, 523.

(134) Grasselli, R. K. *Top. Catal.* **2002**, *21*, 79.

(135) Moro-oka, Y. *Appl. Catal. A* **1999**, *181*, 323.

(136) Kitamura, T.; Piao, D. G.; Taniguchi, Y.; Fujiwara, Y. In *Natural Gas Conversion V*; Parmaliana, A., Sanfilippo, D., Frusteri, F., Vaccari, A., Arena, F., Eds. 1998; Vol. 119, p 301.

(137) Piao, D.; Inoue, K.; Shibasaki, H.; Taniguchi, Y.; Kitamura, T.; Fujiwara, Y. *J. Organomet. Chem.* **1999**, *574*, 116.

(138) Seki, Y.; Mizuno, N.; Misono, M. *Appl. Catal. A* **1997**, *158*, L47.

(139) Seki, Y.; Mizuno, N.; Misono, M. *Chem. Lett.* **1998**, 1195.

(140) Seki, Y.; Min, J. S.; Misono, M.; Mizuno, N. *J. Phys. Chem. B* **2000**, *104*, 5940.

(141) Seki, Y.; Mizuno, N.; Misono, M. *Appl. Catal. A* **2000**, *194*, 13.

(142) Mizuno, N.; Kiyoto, I.; Nozaki, C.; Misono, M. *J. Catal.* **1999**, *181*, 171.

(143) Mizuno, N.; Seki, Y.; Nishiyama, Y.; Kiyoto, I.; Misono, M. *J. Catal.* **1999**, *184*, 550.

(144) Kasztelan, S.; Moffat, J. B. *J.Catal.* **1987**, *106*, 512.

(145) Ahmed, S.; Moffat, J. B. *J.Phys. Chem.* **1989**, *93*, 2542.

(146) Sugino, T.; Kido, A.; Azuma, N.; Ueno, A.; Udagawa, Y. *J. Catal.* **2000**, *190*, 118.

(147) Pei, S. P.; Yue, B.; Qian, L. P.; Yan, S. R.; Cheng, J. F.; Zhou, Y.; Xie, S. H.; He, H. Y. *Appl. Catal. A* **2007**, *329*, 148.

(148) Benlounes, O.; Mansouri, S.; Rabia, C.; Hocine, S. *J. Nat. Gas Chem.* **2008**, *17*, 309.

(149) Spencer, N. D.; Pereira, C. J. *J. Catal.* **1989**, *116*, 399.

(150) Mizuno, N.; Ishige, H.; Seki, Y.; Misono, M.; Suh, D. J.; Han, W.; Kudo, T. *Chem. Commun.* **1997**, 1295.

(151) Min, J. S.; Ishige, H.; Misono, M.; Mizuno, N. *J. Catal.* **2001**, *198*, 116.

(152) Bar-Nahum, I.; Khenkin, A. M.; Neumann, R. *J. Am. Chem. Soc.* **2004**, *126*, 10236.

Chapter 2

Part A

Methane activation and a new catalytic cycle for the methane to methanol reaction

* This part has been submitted as a research article and is reproduced here accordingly.

ALKANE TRANSFORMATION ON POLYOXOMETALATES: PART 1. METHANE ACTIVATION AND A NEW CATALYTIC CYCLE FOR THE METHANE TO METHANOL REACTION

Piotr PUTAJ, Eva GRINENVAL, Frédéric LEFEBVRE*

Université de Lyon ICL, C2P2 UMR 5265 (CNRS – CPE – Université Lyon 1) LCOMS – CPE Lyon, 43 Boulevard du 11 Novembre 1918 F-69616, Villeurbanne, France
E-mail : lefebvre@cpe.fr

Abstract

Methane is activated at moderate temperature on polyoxometalates, leading to the evolution of hydrogen and the formation of a methoxy species which has been characterized by solid-state ^{13}C CP-MAS NMR. In the case of a molybdic polyoxometalate the methyl group is linked to an edge-shared oxygen atom of the polyoxometalate. Treatment of this methoxy species with water leads to the restoration of the starting polyoxometalate and evolution of methanol.

Keywords

methane, oxidation, polyoxometalates, mechanism

2.A.1 Introduction

Interest of the scientists in the direct methane conversion does not seem to falter as the 21st century world faces the perspective of dwindling petrol supplies [1, 2]. However, an economically feasible methane valorization system by its partial oxidation to methanol or formaldehyde, though tempting, remains still rather an elusive perspective. Indeed, methane is notorious for its chemical inertness, justified by its symmetry and the highest C-H primary

bond stability (440 kJ.mol^{-1}). Unfortunately, once activated, it is rare to obtain the partial oxidation products as they are more reactive than the substrate itself and the reaction proceeds rapidly leading to a CO_2 release. Generally, redox properties are claimed to be responsible for the catalysts performance in oxidation reactions [3] although the acid-base strength was suggested to play a crucial role in the C-H activation initial step [4]. As the methane "neutral" chemical character makes it easily adaptable to activator's properties, various C-H dissociation paths were evidenced [5-7]. If the task was not complicated enough, another trend should also be taken into account when developing catalytic oxidation systems - while chemistry becomes more and more environmentally aware, combinations of noble metal compounds and highly toxic reaction media [8-10] are bound to give way to "greener" and cheaper alternatives. Polyoxometalates seem a reasonable choice with this respect.

The polyoxometalates constitute a well-known class of compounds, based on transition metals (Mo, W, V and to a lesser degree Ta and Nb) and oxygen, and could be perceived as discreet analogues of metal oxide surfaces [11]. They are widely used in homogenous and heterogenous catalysis, due to their pronounced and tunable acidic and redox properties. As they are easily soluble in polar solvents they can be used in a lot of homogeneous reactions involving polar molecules. On the other hand, there are only very limited examples of applications of pure solid heteropolyoxometalates in heterogenous catalysis, due to their very low specific surface area (only a few m^2.g^{-1}). These applications are limited mostly to polar molecules which can react not only on the surface of the crystals but also in the first layers of the bulk, thus overcoming this issue (the "pseudo-liquid phase").

Various approaches were proposed to solve the problem of low surface areas of polyoxometalates: (i) they can be deposited by impregnation on various carriers such as silica, alumina or carbon. However physico-chemical studies showed that this method can lead to a weakening of the purely Brönsted acid sites [12-15]; (ii) the oxide support (mainly silica) is first modified by anchoring amine groups, for example by reaction with $NH_2RSi(OEt)_3$. Reaction with the heteropolyacid leads to protonation of the amine and formation of well-dispersed polyoxometalates on the support but most of the acidity is lost; (iii) the polyoxometalates can be dispersed inside the support during its preparation, for example during the condensation of $Si(OEt)_4$ moieties. A lot of studies reported the use of this strategy [16] which can lead to systems more active than the homogeneous ones, mainly due to the increase of the local concentration of the reagents near the polyoxometalates [17]; (iv) the polyoxometalate can be dispersed on a Cs^+, K^+, NH_4^+ or Rb^+ salt of $[PM_{12}O_{40}]^{3-}$ [18]. Indeed these insoluble salts have a very high surface area (more than 100 m^2.g^{-1}) and the acid can be

deposited on their surface and stabilized by interactions with the cations. This results in solids with formulas such as $A_xH_{3-x}PM_{12}O_{40}$ with A = Cs, K, NH_4, Rb and M = Mo, W.

The light alkanes oxidation requires both acidic and redox features of the catalytic system, explaining why polyoxometalates have been extensively studied over the years. As a result, numerous gas or liquid phase catalytic systems were described. A pioneering work on the gas phase methane oxidation on supported polyoxometalates was reported by Moffat et al. [19, 20]. Various molybdic polyoxometalates were found to be efficient for the partial methane oxidation with N_2O at elevated temperatures (500°C and higher), whereas tungstic ones were inactive. Cesium salts of polyoxometalates functionalized with Pd were successfully used by Mizuno et al. in the oxidation of alkanes with a O_2-H_2 mixture [21, 22]. In that case the activity was probably related to the *in situ* generation of H_2O_2 on the Pd particles. On silica-supported silicomolybdic acid a partial methane oxidation to formaldehyde under water vapour was observed at high temperature [23]. These operating conditions corresponded to the decomposition temperature of the polyoxometalate which was then in equilibrium (due to the presence of water) with other species. This resulted in the formation of active oxygen atoms which could oxidize methane. Finally, Pei et al. [24] and Benlounes et al. [25] used polyoxometalates as precursors of highly dispersed mixed metal oxides, that showed higher activities in methane oxidation with O_2 at atmospheric pressure than oxides obtained from classical impregnation [26]. This reaction has also been studied in the liquid phase on other alkanes and a recent review describes the state-of the-art of liquid phase oxidation of hydrocarbons using vanadium-based polyoxometalates [27].

Despite all these efforts only fragmentary pieces of information are available about the light alkanes oxidation reaction mechanism (or mechanisms, for that matter) on polyoxometalates, therefore formulations of the catalytic systems are still mostly empirical. The aim of this series of papers is to study in details the alkane oxidation on polyoxometalates in order to clearly define consecutive stages of the process and to determine their limiting (or not) character for this reaction. We choose to work on polyoxometalates supported on silica but the conclusions drawn here can be extended to the other types of catalysts. In a wider perspective such investigations can lead to more rational design of efficient catalytic systems thus bridging the gap between theory and applications. In this first paper we describe more specifically a new catalytic cycle for methane partial oxidation which does not involve molecular oxygen.

2.A.2 Experimental part

Materials. Silicomolybdic acid $H_4SiMo_{12}O_{40}.xH_2O$ (99+ %, Strem), silicotungstic acid $H_4SiW_{12}O_{40}.xH_2O$ (99.9+ %, Aldrich), phosphomolybdic acid $H_3PMo_{12}O_{40}.xH_2O$ (99+ %, Aldrich) and phosphotungstic acid $H_3PW_{12}O_{40}.xH_2O$ (99+ %, Aldrich) were used as received. $H_4PVMo_{11}O_{40}$ and $H_5PV_2Mo_{10}O_{40}$ were synthesized from MoO_3 (99 %, Acros), V_2O_5 (99.6 %, Acros) and phosphoric acid H_3PO_4 (85 wt.%, Aldrich) according to Berndt et al. [28] and characterized by IR, elemental analyses and ^{31}P solution NMR. For simplicity the polyoxometalates will be denoted in the following as HSiMo, HSiW, HPMo, HPW, HPVMo and HPV_2Mo, for $H_4SiMo_{12}O_{40}$, $H_4SiW_{12}O_{40}$, $H_3PMo_{12}O_{40}$, $H_3PW_{12}O_{40}$, $H_4PVMo_{11}O_{40}$ and $H_5PV_2Mo_{10}O_{40}$ respectively. Silica (flame Aerosil® from Degussa, 200 $m^2.g^{-1}$) was compacted and sieved before use. Methane-^{13}C (99.5 % atom ^{13}C, Aldrich) was used without further purification. If not stated otherwise, all samples were kept under dry inert atmosphere in the glovebox. All manipulations were performed under vacuum or Ar atmosphere using standard Schlenk techniques.

Sample preparation. A mixture of heteropolyacid dissolved in water (10 mL) and silica was stirred vigorously until evaporation of all the solvent at RT. The powder (containing 60 % wt. of polyoxometalate) was collected and ground in the mortar. This material was then treated under high vacuum (10^{-5} Torr) for 2 hours at 200 °C to dehydrate the polyoxometalate and afterwards heated for another 2 hours at 200 °C under dry O_2 to reoxidize any clusters that might have been reduced upon previous manipulations (after this treatment the color of the samples returned to the initial one).

Temperature-programmed reaction experiments. The sample (250 mg of solid) was loaded in a continuous tubular reactor and heated at a rate of 50 °C/h from 40 to 500 °C under methane flow (5 mL/min.) or methane with air (CH_4:O_2 = 2:3; global gas flow 5 mL/min.). The temperature was carefully recorded as a function of time and the composition of the evolved gases was determined online by gaseous chromatography.

Alkane adsorption. Typically, the dehydrated and reoxidized POM sample (300 mg) was introduced in a glass reactor of known volume, equipped with an IR cell (CaF_2 windows) and evacuated until high vacuum (10^{-5} Torr) was reached. 200 Torr of methane or propane was then introduced in the reactor and the sample was heated for 12 hours at a given temperature. After cooling down, the residual gases were evacuated and the reactor filled

again with 200 Torr of dry oxygen. The sample was then burnt at 500 °C for 3 hours and the evolved CO_2 quantified by means of IR spectroscopy (Nicolet 5700-FT spectrometer in transmission mode with a resolution of 1 cm^{-1}, typical number of scans: 32). Control experiments (burning of the supported polyoxometalate in O_2 at 500 °C, without alkane exposure and treatment of silica alone by methane) were also performed.

$^{13}CH_4$ adsorption. Similarly, the dehydrated and reoxidized POM sample was put in a glass reactor and evacuated until high vacuum (10^{-5} Torr) was reached. 500 Torr of ^{13}C-enriched methane was introduced to the reactor and the sample was heated during 2 hours at 200 °C (for MAS NMR experiments) or during 12 hours (for desorption of surface species).

NMR experiments. In all cases the zirconia rotors were filled with the samples in a glovebox and tightly closed. The ^{13}C solid state MAS NMR experiments were performed on a Bruker Avance 500 spectrometer equipped with a standard 4 mm double-bearing probehead. The rotation frequency was set to 10 kHz. A typical cross polarization sequence was used**,** with 4 ms contact time and a recycle delay of 1 to 4 s to allow the complete relaxation of the ^{1}H nuclei. All measured chemical shifts are given with respect to TMS as an external reference. The solution NMR spectra were recorded on a Bruker AM-300 spectrometer.

ESR experiments. The ESR spectra were recorded on a Bruker Elexsys e500 X-band (9.4 GHz) spectrometer with a high sensitivity cavity at 110 K. The magnetic field was measured with a gaussmeter.

2.A.3 Results and discussion

2.A.3.1 Methane activation on polyoxometalates. The first step of methane oxidation is the activation of the C-H bond, which is often considered as very difficult. We decided to initially focus our attention on this stage and performed a series of experiments by heating the supported polyoxometalates under methane flow and analyzing the output gases. We studied both tungstic heteropolyacids (used for acid catalysis) and molybdic ones (used in redox reactions).

In addition to methane, only hydrogen and carbon dioxide were observed in the output gases (water could not be analyzed). Their amounts as a function of the temperature and of the polyoxometalate are plotted in Figure 1.

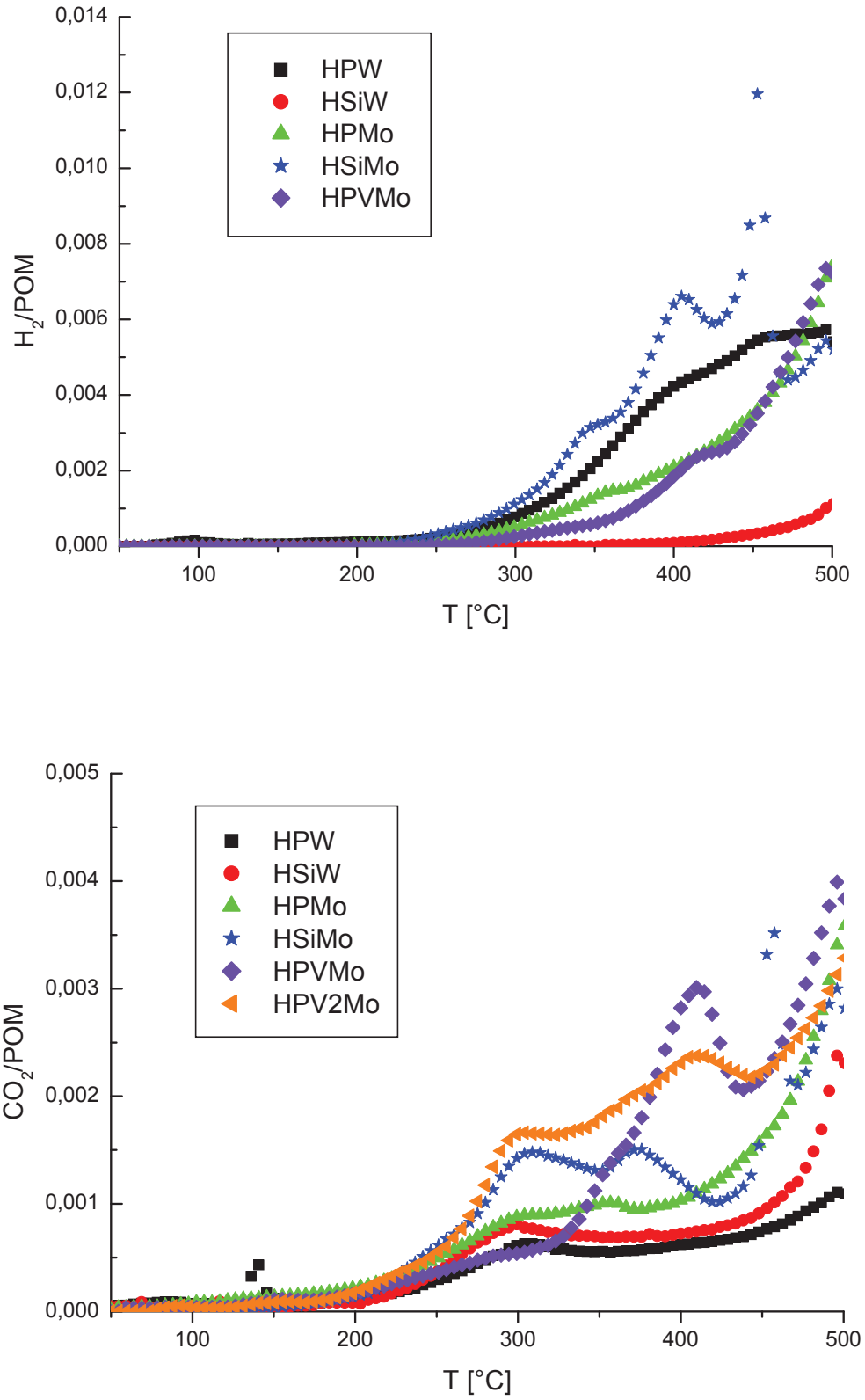

Figure 1: H_2 (top) and CO_2 (down) release during the reaction of flowing CH_4 with various silica-supported polyoxometalates at increased temperatures.

These data show some interesting features: (i) whatever the polyoxometalate only the product of full oxidation is detected, methanol and formaldehyde are not observed; (ii) as whatever the polyoxometalate CO_2 is observed, both tungstic and molybdic heteropolyacids can activate methane; (iii) CO_2 begins to appear at temperatures as low as 200 °C; (iv) the evolution of hydrogen follows quite the same curves than CO_2.

Quantification of the amount of carbon dioxide evolved during the heating from room temperature to 500 °C gives ca. 0.1 CO_2 per tungstic polyacid, ca. 1.0 per molybdic one and ca. 2.0 per vanadomolybdic one. These values are in agreement with what is known for the oxidation of higher alkanes, for which introduction of vanadium leads to an enhancement of the catalytic activity.

The key point of these experiments is the evolution of hydrogen in parallel to that of CO_2. Indeed methane activation could, *a priori*, proceed via different ways:

- Acid reaction with the protons of the polyoxometalate. This reaction is usually proposed for alkane activation by acid catalysts, such as zeolites.

$$CH_4 + H^+ \rightarrow [CH_3^+] + H_2\uparrow$$

- Redox reaction with the polyoxometalate. We have observed this reaction when reacting silanes with molybdic or vanadomolybdic heteropolyacids [29, 30].

$$[POM] + CH_4 \rightarrow [POM]^{2-}[CH_3^+][H^+]$$

- Homolytic cleavage of the C-H bond. This mechanism has never been observed on polyoxometalates.

$$CH_4 \rightarrow CH_3^{\bullet} + H^{\bullet}$$

The evolution of hydrogen shows unambiguously that the acidic pathway is the preferred one although the redox one cannot be definitively excluded.

The CO_2 release in these anaerobic conditions shows a strong methane conversion dependence on the polyanion type, with molybdic and vanadomolybdic clusters being the most active. Since methane is the only gas present, the oxygen atoms of the CO_2 molecules must come from polyanions undergoing a partial decomposition under the reaction conditions. The complete transformation of methane into carbon dioxide on a surface of polyoxometalates requires replacing four H atoms with two O atoms and should proceed via a sequence of consecutive oxidation steps and reaction intermediates. Quite understandably then easily reducible Mo-based clusters exhibit higher activities than tungstic ones when no other source of oxygen is present. The reactions occurring in that case are then: (i) activation of methane by the polyoxometalate, followed by (ii) oxidation of the "activated methane species" by the oxygen atoms of the polyoxometalate.

When O_2 is added to methane in the gas flow, the situation changes significantly. Methane burns much more effectively. The cumulative values of CO_2 released per polyoxometalate in the temperature range 40-500 °C increase by a factor of 20 in case of molybdic compounds and up to 600 times for tungstic ones (see Figure 2).

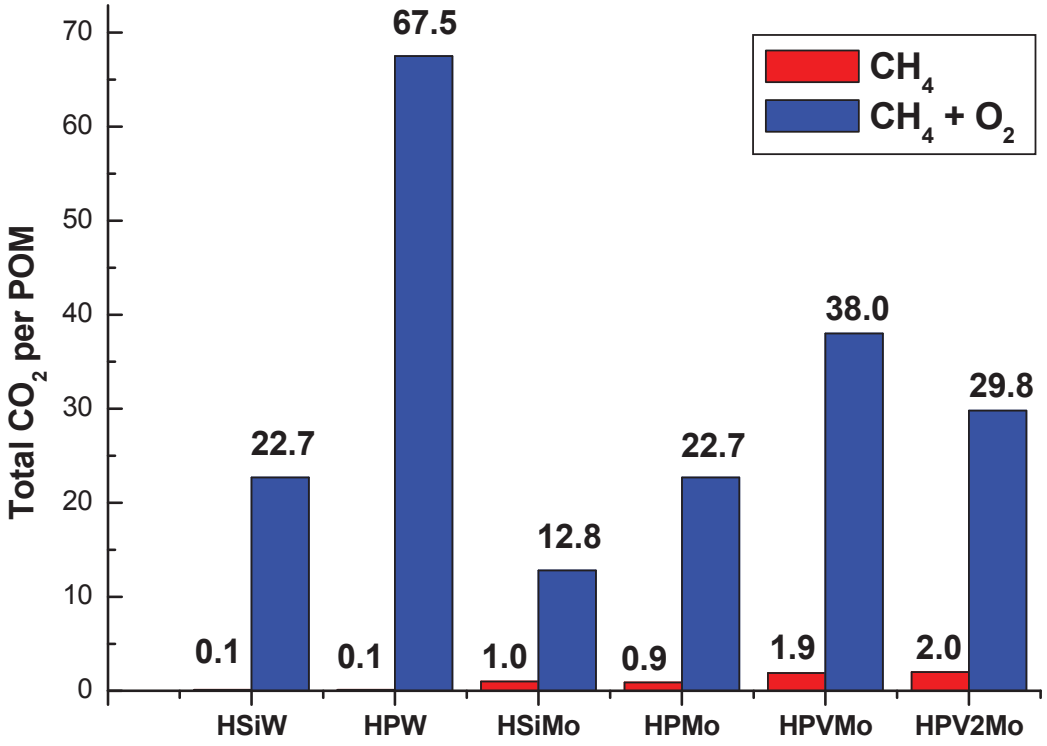

Figure 2: Total quantity of CO_2 released during reaction of CH_4 with various silica-supported polyoxometalates in absence (red vertical bars) and presence (blue bars) of O_2 over the 40-500 °C temperature range.

These data show unambiguously that in presence of oxygen the reaction becomes catalytic, with an additional step to the above mechanism, the reoxidation of the polyoxometalate. Clearly the reoxidation is not the limiting step in the case of the tungstic compounds for which the CO_2 rate was the lowest in absence of oxygen and is the highest in its presence. In that case the limiting step is then the activation of the C-H bond of methane or the oxidation of the "activated methane" species.

Clearly, for molybdic and vanadomolybdic polyacids the reoxidation of the polyoxometalate is a limiting step, showing then a great difference with the tungstic

compounds. This is not surprising as these compounds are easily reduced. Their reoxidation is then more difficult than that of tungstic polyanions. An unexpected consequence of this observation is that for molybdic polyacids the methane activation is not the limiting step of the reaction. In order to confirm this assumption, we studied the adsorption of CH_4 on $HSiMo/SiO_2$ at different temperatures. For this purpose methane was first contacted with the polyoxometalate during 12 hours at a given temperature. The gaseous phase was then removed at room temperature and dry oxygen added to the reaction vessel. Heating at 500 °C resulted in a complete transformation of all sorbed species into CO_2 (and H_2O) which was analyzed by means of IR, allowing a quantification of the amount of methane which had been activated. The results are shown on Figure 3 together with those obtained for propane, instead of methane.

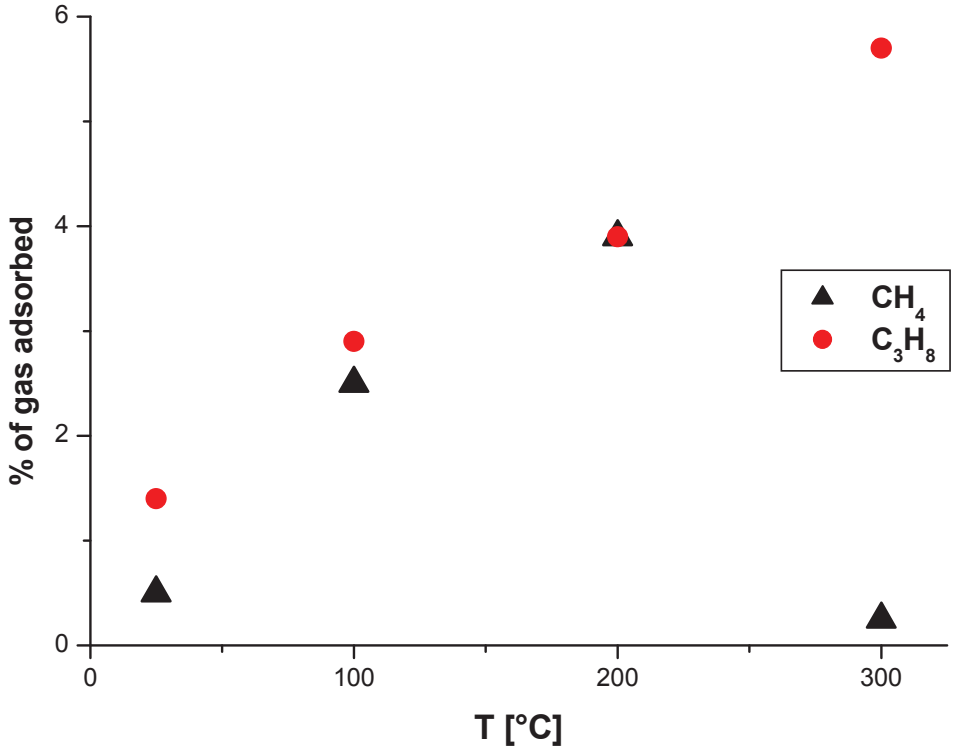

Figure 3: Percentage of methane (black triangles) and propane (red circles) adsorbed on $H_4SiMo_{12}O_{40}/SiO_2$ at various temperatures.

Clearly, the methane activation on the polyoxometalate occurs already at room temperature and the amount of activated alkane increases rapidly with temperature. The drastic decrease after activation at 300 °C is probably related to the fact that at this temperature CO_2 evolves

during the activation step (see Figure 1). At low temperatures propane is activated more easily than methane (e.g. at room temperature by a factor of 3), in agreement with the lower C-H bond energy of this compound ($\Delta H°_{C\text{-}H}$ = 439 kJ/mol for CH_3-H and 413 kJ/mol for $(CH_3)_2C$-H). However, at higher temperatures this difference becomes smaller and the two molecules are activated quite at the same yield. In contrast to methane, the amount of sorbed propane continues to increase at 300 °C. The propane and higher alkanes cracking on polyoxometalates followed by formation of unsaturated aromatic products is a well-known phenomenon, responsible for the loss of catalytic activity in e.g. *n*-butane or *n*-pentane skeletal isomerisation processes [31]. We can tentatively put forward propane cracking as an explanation for the observed discrepancies and stress a fundamental difference between chemistry of methane and its higher homologues in this respect.

Upon treatment with alkanes, all molybdenum-containing samples turned from yellowish to dark green suggesting a Mo(VI) reduction. Mo(V) species are well known to be paramagnetic. A control sample of $HSiMo/SiO_2$ was therefore reduced under H_2 at 150 °C and analyzed by ESR together with the same sample heated under methane at 200 °C (Figure 4).

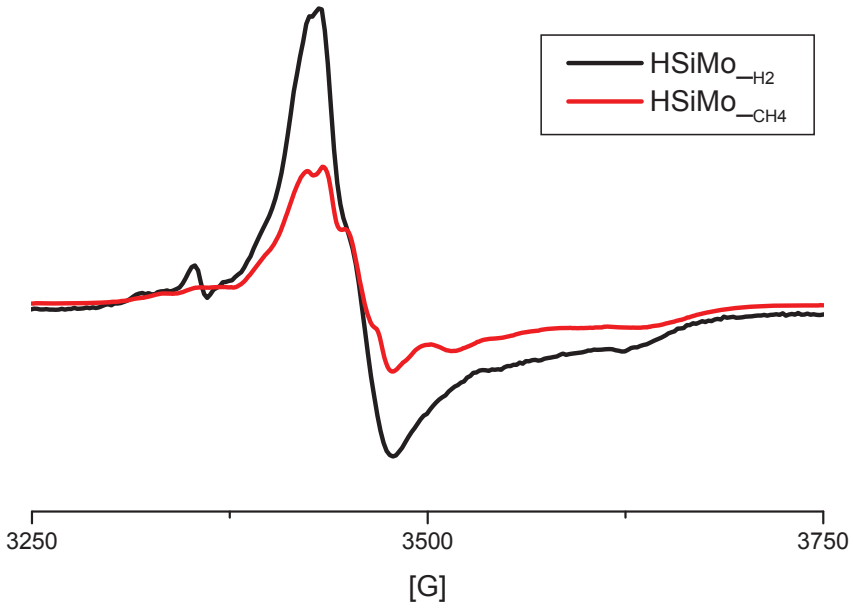

Figure 4: ESR spectra of: a) $HSiMo/SiO_2$ reduced with H_2 at 150 °C and b) $HSiMo/SiO_2$ after reaction with CH_4 at 200 °C.

The spectrum obtained after the reduction under hydrogen is quite comparable to those reported in the literature [32] and corresponds to a Mo(V) species. The spectrum obtained after reaction of $HSiMo/SiO_2$ with CH_4 at 200 °C can also be attributed to a Mo(V) species. However the hyperfine structure is different from that observed after reduction under hydrogen and could be due to a slightly different environment around molybdenum(V), or as in [32] to a different concentration of Mo(V) species. The presence of Mo(V) can be explained by: (i) a reaction mechanism involving an acid reaction of CH_4 with the protons of the polyacid and a further reduction of the polyacid by the evolved hydrogen or (ii) a direct two-electrons reduction of the polyacid by CH_4 (called redox reaction above). The second pathway can be excluded as neutral salts of molybdic polyoxometalates (such as $K_3PMo_{12}O_{40}$) do not activate methane at moderate temperature. Moreover, the two electrons reduced polyoxometalate formed via the redox reaction should not be paramagnetic, the two electrons being coupled [33] in such derivatives.

As a consequence of this conclusion and as tungstic heteropolyacids are at least as acidic than molybdic ones, we can conclude that whatever the heteropolyacid the limiting step is not the methane C-H activation. In presence of oxygen and in the case of molybdic compounds it is the reoxidation of the polyoxometalate while for tungstic ones it is the oxidation of the polyoxometalate-methyl group species. These remarks will also be valid for the other alkanes as their C-H activation is easier than for methane.

2.A.3.2 Methane activation on silicomolybdic acid: a new catalytic cycle. In order to better understand what happened on the polyoxometalate surface, we performed the reaction of $HSiMo/SiO_2$ with $^{13}CH_4$ and studied the resulting solid by ^{13}C CP-MAS NMR. After activation at 200 °C the NMR spectrum shows unambiguously a relatively broad signal at 77 ppm (Figure 5). This chemical shift is uncommon for the methoxy species which should be expected for a Me^+ cation interacting with a polyoxometalate. For example, methoxy species are observed at around 55-60 ppm on zeolites [34-36]. Methoxy species were also synthesized on $H_3PW_{12}O_{40}$ by reacting the solid with vapors of methanol at room temperature [37, 38]. These species were characterized by solid-state ^{13}C NMR and led to a signal at ca. 55-60 ppm, as on zeolites. The direct methylation of organic salts of $[PMo_{12}O_{40}]^{3-}$ and $[PW_{12}O_{40}]^{3-}$ by $(CH_3)_3OBF_4$ in 1,2-dichloroethane was also reported by Knoth [39]. While the tungstic heteropolyoxometalate did not lead to a clean reaction, the trimethyloxonium salt being the main product, the molybdic compound led to the formation of the methylated compound $[PMo_{12}O_{40}(CH_3)]^{2-}$ which was characterized by single crystal X-ray crystallography. In this

compound the methyl group is not located on a terminal oxygen atom but on an edge-shared one. Unfortunately, no ^{13}C NMR data were available for this species. So we synthesized it and recorded its ^{13}C NMR spectrum. However, due to the high amount of organic cations, no clear information could be deduced from this study. All attempts to replace the organic cation by an inorganic one failed. We decided then to synthesize the ^{13}C enriched compound by performing an exchange reaction with $^{13}CH_3OH$. Indeed, it is well known that the oxygen atoms of $[PMo_{12}O_{40}]^{3-}$ can be easily exchanged in water at room temperature [40, 41]. It seemed then logical that such an exchange reaction should also occur, even partially, with methanol:

$$[PMo_{12}O_{40}(CH_3)]^{2-} + {}^{13}CH_3OH \rightarrow [PMo_{12}O_{40}({}^{13}CH_3)]^{2-} + CH_3OH$$

For this purpose 0.2 g of the Knoth salt were solubilized in 2 ml CH_3CN in presence of 0.1 ml of $^{13}CH_3OH$ and the solution was kept at room temperature overnight. A partial exchange occurred as evidenced by ^{13}C NMR. However the ^{13}C solution NMR spectrum of the ^{13}C partially exchanged salt did not show any signal in the 55 – 60 ppm range which could be ascribed to a methoxy species but a peak was observed at 74.5 ppm. Such a value is not so surprising for a methyl group linked to a triply coordinated oxygen atom, as, for example, the trimethyloxonium salt gives a signal at ca. 80 ppm both in superacid solution and on the surface of acidic zeolites [38]. The great analogy between this peak and that observed after methane activation allows us to propose that the species formed after methane activation on $H_4SiMo_{12}O_{40}$ is a methyl group linked to an edge-shared bridging atom of the polyoxometalate. A simultaneous formation of Mo-O-CH_3 species on terminal oxygen atoms cannot be excluded but if they are formed they are not stable and decompose at the reaction temperature (200 °C).

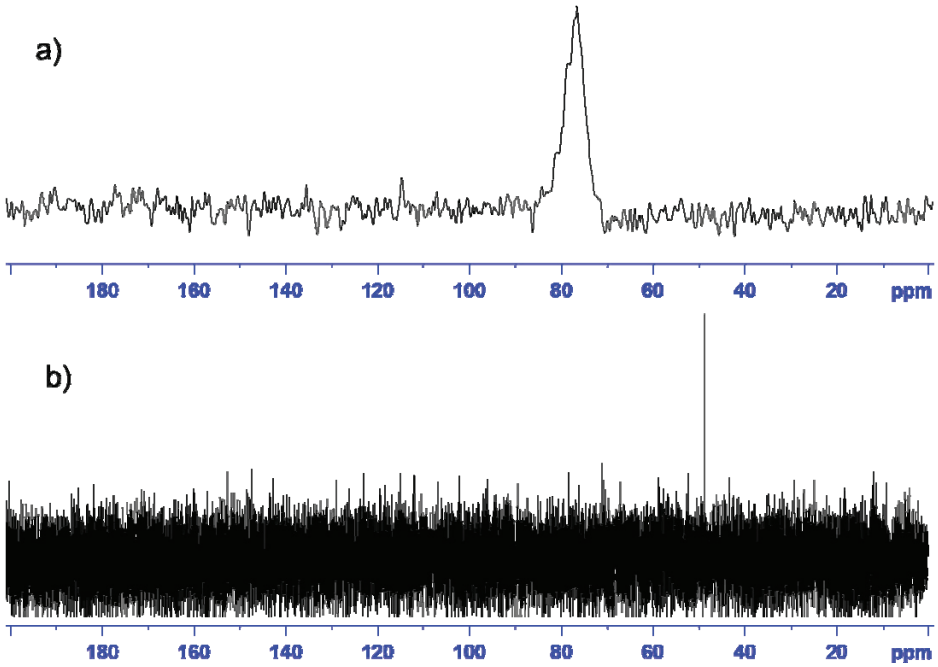

Figure 5: (a) ^{13}C CP MAS NMR spectra of the reaction product of ^{13}C-CH_4 with $HSiMo/SiO_2$ at 200 °C, (b) ^{13}C solution NMR spectrum after reaction of sample (a) with D_2O at room temperature.

When looking at the equation describing the exchange between unlabeled and labeled methanol on the polyoxometalate it seems logical to think that labeled methanol could be replaced by water. In that case methanol should evolve and the starting polyoxometalate be restored:

Figure 5b shows the ^{13}C NMR spectrum obtained after contacting the $HSiMo/SiO_2$ sample treated with methane with D_2O at 60 °C. The signal at 49 ppm of methanol is clearly seen showing that the concept is valid. The catalytic cycle could then be written as:

$$H_4[SiMo_{12}O_{40}] + CH_4 \rightarrow H_3[SiMo_{12}O_{40}(CH_3)] + H_2$$
$$H_3[SiMo_{12}O_{40}(CH_3)] + H_2O \rightarrow H_4[SiMo_{12}O_{40}] + CH_3OH$$

The limiting step is probably the second one as the NMR signal is not very intense. This can be understood easily, for example by molecular modeling: the methyl group will protect the oxygen atom from the reagents (methanol or water), leading then to a small reaction rate.

2.A.4 Conclusions

We have shown that methane can be activated under mild conditions on both tungstic and molybdic heteropolyacids. The reaction passes through an attack of the C-H bond by a proton of the polyacid and evolution of hydrogen. The resulting methyl-polyoxometalate species is then oxidized to CO_2 by the oxygen atoms of the polyoxometalate. For tungstic polyacids this step is the limiting one while for molybdic (or vanadomolybdic) polyoxometalates the limiting step is the reoxidation of the polyanion by oxygen.

The methyl polyoxometalate species has been characterized by solid-state ^{13}C CP-MAS NMR for a molybdenum polyoxometalate. In that case the methyl group is attached to an edge-shared oxygen atom of the polyoxometalate. By reaction with water the starting polyoxometalate is restored while methanol evolves. The reaction can then be written as:

$$CH_4 + H_2O \rightarrow CH_3OH + H_2$$

The limiting step is probably the reaction with water, due to a protecting effect of the methyl group. This could be overcome by a treatment with water at higher temperatures but in these conditions the methyl group is not stable and undertakes a further oxidation to a formyl species as it will be seen in the next paper of this series. Another key problem before application of this reaction is that an optimization of the reaction parameters will be necessary. Indeed only the anhydrous heteropolyacid has a sufficient acid strength for activating methane and water will decrease this acidity, requiring then a right choice of the ratio between the two reagents. The problem of the methyl exchange could probably be solved by using substituted polyoxometalates for which the M-O-M' bridge will be less stable while that of the evolved hydrogen (which can reduce the polyoxometalate) could be solved by introduction of a small amount of oxygen combined to a platinum catalyst allowing the $H_2 + O_2$ reaction to proceed at low temperature or by use of a membrane reactor.

Acknowledgments

Financial support for presented work was provided by the 7th European framework research program FP7/2007-2013, subvention no. 215193.

2.A.5 References

[1] J. H. Lunsford, Catal. Today 63 (2000) 165-174.

[2] M. C. Alvarez-Galvan, N. Mota, M. Ojeda, S. Rojas, R. M. Navarro, J. L. G. Fierro, Catal. Today, 171 (2011) 15-23.

[3] R. K. Grasselli, Topics Catal., 21 (2002) 79-88.

[4] Y. Moro-oka, Applied Catal. A-Gen., 181 (1999) 323-329.

[5] M. V. Luzgin, A. A. Gabrienko, V. A. Rogov, A. V. Toktarev, V. N. Parmon, A. G. Stepanov, J. Phys. Chem. C, 114 (2010) 21555-21561.

[6] E. V. Starokon, M. V. Parfenov, L. V. Pirutko, S. I. Abornev, G. I. Panov, J. Phys. Chem. C, 115 (2011) 2155-2161.

[7] K. Kwapien, M. Sierka, J. Dobler, J. Sauer, ChemCatChem, 2 (2010) 819-826.

[8] R. A. Periana, D. J. Taube, E. R. Evitt, D. G. Loffler, P. R. Wentrcek, G. Voss, T. Masuda, Science, 259 (1993) 340-343.

[9] R. A. Periana, D. J. Taube, S. Gamble, H. Taube, T. Satoh, H. Fujii, Science, 280 (1998) 560-564.

[10] C. J. Jones, D. Taube, V. R. Ziatdinov, R. A. Periana, R. J. Nielsen, J. Oxgaard, W. A. Goddard, Angew. Chem.-Int. Ed., 43 (2004) 4626-4629.

[11] C. L. Hill; (Ed.), Chem. Rev., 98 (1998) 1-390 (whole issue).

[12] G. I. Kapustin, T. R. Brueva, A. L. Klyachko, M. N. Timofeeva, S. M. Kulikov, I. V. Kozhevnikov, Kinet. Catal., 31 (1990) 896-898.

[13] F. Lefebvre, J. Chem. Soc. Chem. Commun., (1992) 756-757.

[14] E. Grinenval, X. Rozanska, A. Baudouin, E. Berrier, F. Delbecq, P. Sautet, J. M. Basset, F. Lefebvre, J. Phys. Chem. C, 114 (2010) 19024-19034.

[15] A. Thomas, C. Dablemont, J. M. Basset, F. Lefebvre, C. R. Chim., 8 (2005) 1969-1974.

[16] V. Dufaud, F. Lefebvre, Materials, 3 (2010) 682-703.

[17] V. Dufaud, F. Lefebvre, G. P. Niccolai, M. Aouine, J. Mater. Chem., 19 (2009) 1142-1150.

[18] T. Okuhara, H. Watanabe, T. Nishimura, K. Inumaru, M. Misono, Chem. Mater., 12 (2000) 2230-2238.

[19] S. Kasztelan, J. B. Moffat, J. Catal., 106 (1987) 512-524.

[20] S. Ahmed, J. B. Moffat, J. Phys. Chem., 93 (1989) 2542-2548.

[21] N. Mizuno, H. Ishige, Y. Seki, M. Misono, D. J. Suh, W. Han, T. Kudo, Chem. Commun., (1997) 1295-1296.

[22] J. S. Min, H. Ishige, M. Misono, N. Mizuno, J. Catal., 198 (2001) 116-121.

[23] T. Sugino, A. Kido, N. Azuma, A. Ueno, Y. Udagawa, J. Catal., 190 (2000) 118-127.

[24] S. P. Pei, B. Yue, L. P. Qian, S. R. Yan, J. F. Cheng, Y. Zhou, S. H. Xie, H. Y. He, Applied Catal. A-Gen., 329 (2007) 148-155.

[25] O. Benlounes, S. Mansouri, C. Rabia, S. Hocine, J. Natural Gas Chem., 17 (2008) 309-312.

[26] N. D. Spencer, C. J. Pereira, J. Catal., 116 (1989) 399-406.

[27] N. Mizuno, K. Kamata, Coord. Chem. Rev., 255 (2011) 2358-2370.

[28] S. Berndt, D. Herein, F. Zemlin, E. Beckmann, G. Weinberg, J. Schütze, G. Mestl, R. Schlögl, Ber. Phys. Chem., 102 (1998) 763-774.

[29] E. Grinenval, J. M. Basset, F. Lefebvre, Inorg. Chem., 49 (2010) 8749-8755.

[30] E. Grinenval, J. M. Basset, F. Lefebvre, Inorg. Chim. Acta, 370 (2011) 297-303.

[31] K. Na, T. Okuhara, M. Misono, J. Chem. Soc. - Faraday Trans., 91 (1995) 367-373.

[32] M. Otake, Y. Komiyama, T. Otaki, J. Phys. Chem., 77 (1973) 2896-2903.

[33]. C. de Graaf, R. Caballol, S. Romo, J. M. Poblet, Theor. Chem. Acc., 123 (2009) 3-10.

[34]. V. Bosacek, J. Phys. Chem., 97 (1993) 10732-10737.

[35] D. K. Murray, J. W. Chang, J. F. Haw, J. Am. Chem. Soc., 115 (1993) 4732-4741.

[36] W. Wang, M. Seiler, M. Hunger, J. Phys. Chem. B, 105 (2001) 12553-12558.

[37] H. L. Zhang, A. M. Zheng, H. G. Yu, S. H. Li, X. Lu, F. Deng, J. Phys. Chem. C, 112 (2008) 15765-15770.

[38] M. V. Luzgin, M. S. Kazantsev, W. Wang, A. G. Stepanov, J. Phys. Chem. C, 113 (2009) 19639-19644.

[39] W. H. Knoth, R. L. Harlow, J. Am. Chem. Soc., 103 (1981) 4265-4266.

[40] I. V. Kozhevnikov, A. Sinnema, H. van Bekkum, Catal. Lett., 34 (1995) 213-221.

[41] I. V. Kozhevnikov, A. Sinnema, H. van Bekkum, M. Fournier, *Catal. Lett.*, 41 (1996) 153-157.

Chapter 2

Part B

Reactivity of methoxy species on the surface of polyoxometalates

* This part will be submitted as a research article and is reproduced here accordingly.

ALKANE TRANSFORMATION ON POLYOXOMETALATES: PART 2. SURFACE METHOXY SPECIES REACTIVITY

Piotr PUTAJ, Frédéric LEFEBVRE*

Université de Lyon ICL, C2P2 UMR 5265 (CNRS – CPE – Université Lyon 1) LCOMS – CPE Lyon, 43 Boulevard du 11 Novembre 1918 F-69616, Villeurbanne, France
E-mail : lefebvre@cpe.fr

Abstract

Methanol adsorption on bulk- and silica-deposited Keggin-type polyoxometalates yields the surface methoxy species. Presence of two distinct entities is evidenced by means of ^{13}C SS NMR. Their consecutive evolution follows two pathways: 1) coupling by dehydration and 2) oxidation, which originate from different properties of tungstic and molybdic carrier polyoxometalates. The study of the reactivity of the methoxy species on the surface of $H_4SiMo_{12}O_{40}/SiO_2$ completes the picture of the multiple-step oxidation mechanism of methane on polyoxometalates.

Keywords

methoxy, polyoxometalates, oxidation, formyl

2.B.1 Introduction

Mechanistic studies on alkoxy species, considered to be important intermediates in a plethora of reactions on the surface of solid state catalysts, such as e.g. alkylations [1], isomerisations [2], carbonylations [3] or oxidations [4] are thriving. Among all these processes, partial methane oxidation to methanol constitutes the greatest challenge of chemistry in the XXIst century. We have shown recently a new catalytic cycle of methane to methanol reaction, promoted by silica-supported polyoxometalates [5]. Gaseous methane reacts with the polyoxometalate yielding a surface methoxy species, which then can be hydrolysed to

methanol. In order to apply this system on a wider scale it is of utmost importance to fully understand the reactivity of these entities.

Whereas generation of methoxy species on a large scale from methane is laborious and not feasible economically, the adsorption of methanol on the surface of solids has been proven an attractive alternative [6]. The formation and evolution of these intermediates can be then readily monitored by means of ^{13}C SS NMR. This way, methoxy species have been formed and characterized so far on the surface of zeolites by Bosacek et al. [7-9] and Murray et al. [10-11], silicoaluminophosphate H-SAPO-34 [12-13] and polyoxometalates themselves [14-15]. However, in the case of polyoxometalates, the given interpretations of experimental data are still far from being unanimously accepted.

The polyoxometalates are a class of compounds, based on transition metals (Mo, W, V and to a lesser degree Ta and Nb) and oxygen, and could be perceived as discreet analogues of metal oxide surfaces [16]. The Keggin-type clusters are among the most widely studied and applied, because of their stability, commercial availability, low price and last but not the least, interesting chemical properties. Typically, the Keggin polyoxometalate has the formula $[XM_{12}O_{40}]^{n-}$ and its structure is shown in Figure 1. In the middle of the structure there is a heteroatom X, tetrahedrally coordinated by four O_a oxygens. Four $\{M_3O_{13}\}$ triads, made of three edge–sharing octahedra, are connected to this heteroatom via the O_a oxygen atoms. The oxygen atoms common to two octahedra in the same triad are indicated as O_b whereas those common to two octahedra from different triads as O_c Finally, the terminal oxygen atoms completing the octahedral coordination of the M atoms are called O_d.

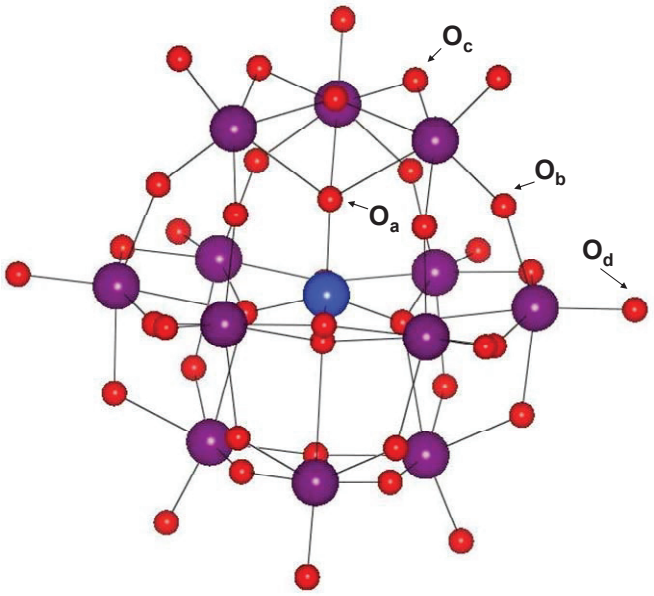

Figure 1. Keggin-type polyoxometalate. Mo or W = violet balls, heteroatom X = blue ball, O = red balls. The symbols are explained in the text.

The aim of this paper is therefore to study in detail the methanol adsorption on bulk and silica-supported polyoxometalates by means of ^{13}C SS NMR in order to clearly define the so-obtained chemical species, elucidate the consecutive stages of their evolution and complete the mechanistic picture of methane oxidation cycle on polyanionic clusters.

2.B.2 Experimental part

Materials. Silicomolybdic acid $H_4SiMo_{12}O_{40}.xH_2O$ (99+ %, Strem) and silicotungstic acid $H_4SiW_{12}O_{40}.xH_2O$ (99.9+ %, Aldrich) were used as received. For the simplicity POMs will be denoted in the text as: HSiMo and HSiW, for $H_4SiMo_{12}O_{40}$ and $H_4SiW_{12}O_{40}$, respectively.
Silica (flame Aerosil® from Degussa, 200 m^2/g) was compacted and sieved.
Methanol-^{13}C (99 % atom ^{13}C, Aldrich) and formaldehyde-^{13}C (20 % solution in H_2O, 99 % atom ^{13}C, Aldrich) were used without further purification.
If not stated otherwise, all samples were kept under dry, inert atmosphere in the glovebox. All manipulations were performed under vacuum or Ar atmosphere using standard Schlenk techniques.

Sample preparation. A mixture of heteropolyacid dissolved in water (10 mL) and silica (compacted and sieved flame silica Aerosil® from Degussa, 200 m^2/g) was stirred vigorously until solvent evaporated to dryness at RT. The powder (containing 60 % wt. of POM) was collected and ground in the mortar. This material was then treated under high vacuum (10^{-5} Torr) for 2 hours at 200 °C to dehydrate polyoxometalates and afterwards heated for another 2 hours at 200 °C under dry O_2 to reoxidize any clusters that might have been reduced upon previous manipulations.
This sample will be referred to in the following as: POM/SiO_2.

^{13}C-CH_3OH and ^{13}C-HCHO adsorption. The dehydrated and reoxidized POM sample was put in a glass reactor and evacuated until high vacuum (10^{-5} Torr) was reached. After cooling down to liquid nitrogen temperature, the sample was briefly exposed to vapours of ^{13}C- enriched methanol/formaldehyde and then allowed to warm up to room temperature over

a period of one hour. The sample was then evacuated for one hour on a high vacuum line at 60 °C.

NMR experiments. In all cases zirconia rotors were filled with the samples in a glovebox and tightly closed. The ^{13}C solid state MAS NMR experiments were performed on a Bruker Avance 500 spectrometer equipped with a standard 4 mm double-bearing probehead. The rotation frequency was set to 10 kHz. A typical cross polarization sequence was used**,** with 4 ms contact time and a recycle delay of 1 to 4 s to allow the complete relaxation of the ^{1}H nuclei. All measured chemical shifts are given with respect to TMS as an external reference. After initial measurements the rotors with samples were opened under Ar and heated at 120 °C for 1 hour, cooled down, tightly closed once again and remeasured.

2.B.3 Results and discussion

When it comes to the generation of methoxy species on polyoxometalates from methanol, so far only bulk anhydrous $H_3PW_{12}O_{40}$ was studied in detail [14-15]. It was shown in [14] that after methanol adsorption followed by prolonged standing at room temperature two peaks were detected in the ^{13}C SS NMR spectrum, at 55 and 59 ppm. They were consecutively attributed to methyl groups linked to two types of oxygen atoms: terminal O_d and bridging O_c, respectively. Later on, however, the peak at 55 ppm was argued to originate from the methanol molecules physisorbed on the surface of POMs [15], especially as its consumption was observed to be thermally-stimulated. Thus, either formation of only one type of surface methoxy species at 59 ppm (CH_3-O_c) was said to take place or different methoxy species linked to different oxygen atoms of polyoxometalates were supposed to give similar NMR signal shifts. At the same time thermal treatment induced dehydration of methanol to dimethyl ether and further reaction of DME molecules with methoxy species and appearance of new bands in the spectrum, localised between 77-82 ppm. They were proposed to come from the formation of a trimethyloxonium ion [17-18], in different spatial arrangements versus the polyoxometalate cluster. It is important to note here the nature of this species – the oxygen atom triply coordinated by methyl groups.

On the other hand, our recent study of the methane activation on silica-supported polyoxometalates has shown that during the process an intermediate species is created on the surface of the solid (see discussion in [5]). This entity was unequivocally characterized by

means of ^{13}C SS NMR and to give rise to a signal at 77 ppm. Similar NMR data was found for a discreet compound obtained some time ago by Knoth [19], which is in fact a methylated Keggin-type polyoxometalate: $[PMo_{12}O_{40}(CH_3)]^{2-}$. In its structure a methyl group is anchored on the doubly-coordinated (bridging) oxygen atom. This observation led us to assume that our species is in fact a congener of Knoth's one. In the light of new experimental data a revised picture is therefore needed of the phenomena that involve simple organic species on the surface of the polyoxometalates.

As we have intended to compare the behaviour of bulk and silica-supported polyoxometalates we decided to work with silicotungstic $H_4SiW_{12}O_{40}$ and silicomolybdic $H_4SiMo_{12}O_{40}$ acids rather than their phosphorus-containing analogues. This choice comes from the necessity to preserve the acid function of the polyoxometalates once they are deposited on the carrier and interactions with silica are known to result in consumption of three protons of the polyanionic cluster [20-21].

First of all, we performed the methanol adsorption on bulk and silica-supported clusters of the same type. Anhydrous $H_4SiW_{12}O_{40}$ and $H_4SiW_{12}O_{40}/SiO_2$ were exposed to ^{13}C-CH_3OH vapors and after evacuation at 60 °C on a high-vacuum line, samples were collected and their ^{13}C SS NMR spectra were recorded (see Fig. 2 a) and b), respectively).

Behaviour of bulk $H_4SiW_{12}O_{40}$ (Fig. 2 a) is in agreement with already published data for bulk $H_3PW_{12}O_{40}$ [14-15]. Anyhow, no major differences were to be expected as both tungstic polyoxometalates exhibit comparable acid strengths. In attributing the peaks between 52-54 ppm to methanol physisorbed on polyoxometalate we follow the line of reasoning of [15]. Methoxy species are identified at 58 ppm and some dehydration of methanol leads to formation of dimethyl ether visible at 62 ppm. The presence of minor bands between 77-80 ppm is also noted. Similarly, spectrum of methanol on $HSiW/SiO_2$ after evacuation at 60 °C (Fig. 2 b) is dominated by a peak at 54 ppm with a shoulder extending down to 48 ppm. Obviously, both come from physisorbed alcohol molecules, respectively on polyoxometalate and silica (see inset of Fig. 2 showing spectrum of methanol adsorbed on silica, for comparison). Some dimethyl ether can be detected as well at its respective position together with bands between 77-80 ppm. In striking contrast with a bulk polyoxometalate, however, spectrum of supported clusters does not show peak at 58 ppm, originating from surface methoxy species. We tend to think that the reason for this is their much faster evolution on well-dispersed clusters. Further heating at 120 °C of the sample b) is required to stimulate chemical reactions of methanol on a larger scale (spectrum shown in Fig. 2 c) – physisorbed alcohol is consumed and products peaks gain in intensity.

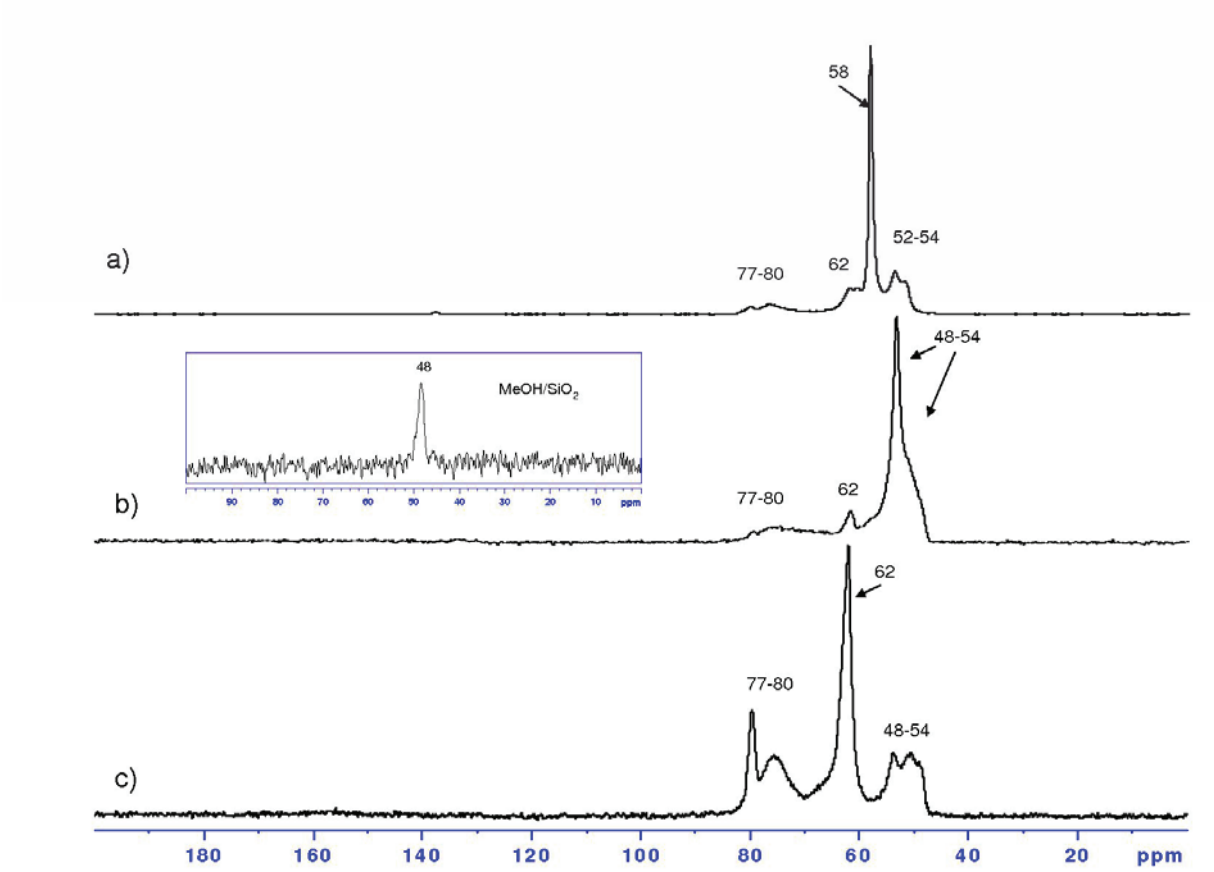

Figure 2. ^{13}C SS NMR spectra of: a) product of ^{13}C-MeOH adsorption on bulk HSiW after evacuation at 60 °C, b) product of ^{13}C-MeOH adsorption on HSiW/SiO_2 after evacuation at 60 °C, and c) sample b) after heating at 120 °C. Spectrum of ^{13}C-MeOH adsorbed on SiO_2 is shown in the inset.

Now, heating at 120 °C stimulates also the prominent rise of the 77-80 ppm region, which consists of at least two different bands. We would like to propose here a new view of the observed phenomena. The attribution of the peak at 58 ppm to the methoxy species is valid, however the nature of this entity has not been specified correctly. In our opinion, the methyl group of this species is attached not to the bridging O_c (or O_b for that matter) oxygen atom but rather to the terminal one O_d. The other type of methoxy species – identical with the one obtained by us upon methane adsorption on silica-supported silicomolybdic acid – is more difficult to produce and it appears in the 77-80 ppm region after heating. So as to the presence of trimethyloxonium ion observed between 77-82 ppm by Luzgin et al. [15] - there is no reason to think that one of the two species is the right one and the other not. Both can well co-exist on the surface of POMs. From the chemical point of view both are composed of a methyl group linked to doubly-coordinated oxygen atom (see Figure 3) and as such are

expected to give similar NMR signal shifts in the 80 ppm region.

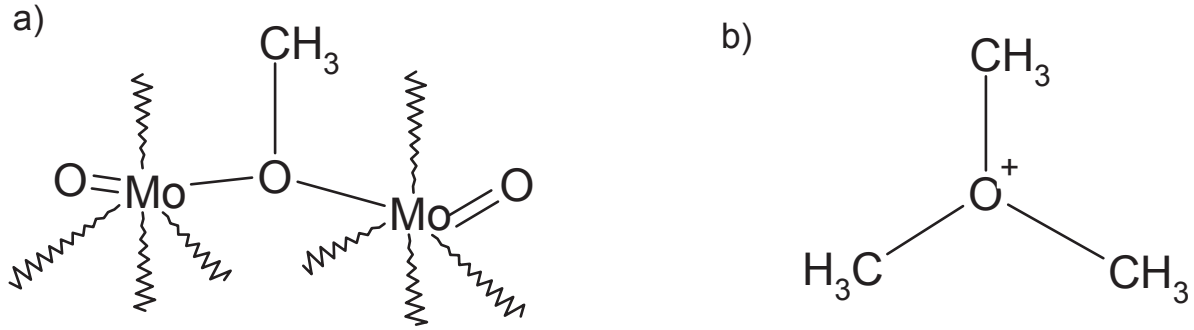

Figure 3. Schematic view of the: a) Methoxy species linked to a bridging oxygen atom of the molybdic polyoxometalate and b) trimethyloxonium ion.

The most fascinating results, though, come from the ^{13}C-methanol adsorption experiments on $HSiW/SiO_2$ and $HSiMo/SiO_2$ (see Fig. 4 a) and b), respectively). Significant differences between tungstic and molybdic polyoxometalates, considering their acidic and redox properties, find their reflection in methoxy species chemistry. While on tungstic clusters their evolution proceeds via dimethyl ether to trimethyloxonium ions (Fig. 4 a), on molybdic ones step-by-step oxidation leads to formation of carbonyl (strictly speaking - formyl) group, giving rise to a bumpy peak at around 172 ppm (Fig. 4 b) and after polymerization – to paraformaldehyde localized in the 75-83 ppm region. Confirmation of these attributions comes from the comparison with the spectra of ^{13}C-labeled formaldehyde adsorbed on $HSiMo/SiO_2$ (see Fig. 4 c) and pure paraformaldehyde, shown in the inset.

It has already been argued that both types of polyoxometalates, i.e. tungstic and molybdic ones, exhibit both kinds of properties, i.e. acidic and redox, albeit to the various degree. The methoxy species evolution should be perceived as a mixture of both available pathways. Although on $HSiMo/SiO_2$ oxidative way seems preferable, 62 ppm peak of dimethyl ether is also clearly distinguishable in the spectrum in Fig. 4 b) and there is no reason to exclude the presence of trimethyloxonium ions in the large band between 75-85 ppm. Symmetrically, it has been shown that methoxy species generated on bulk $H_3PW_{12}O_{40}$ can be photochemically oxidized to formaldehyde [14].

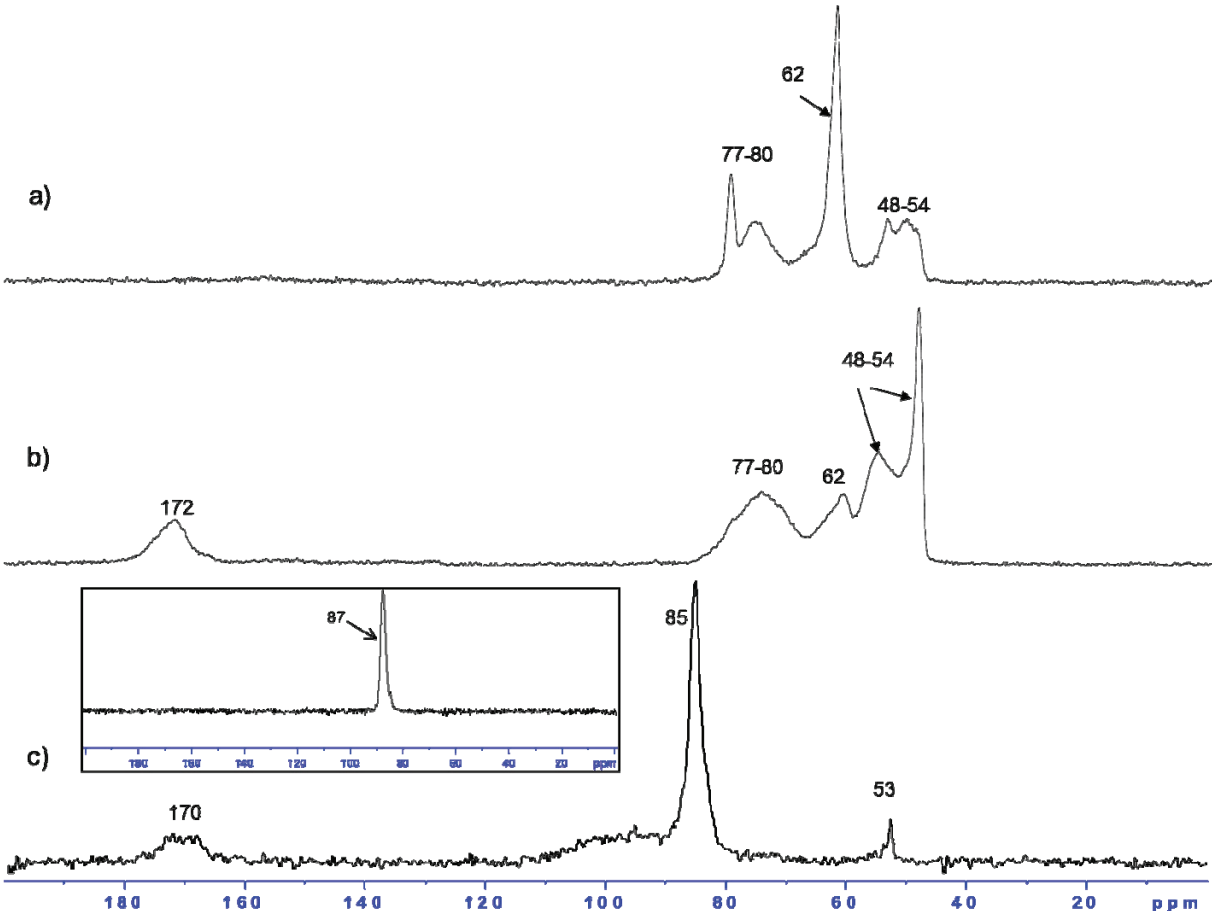

Figure 4. ^{13}C SS NMR spectra of: a) product of ^{13}C-MeOH adsorption on $HSiW/SiO_2$ after treatment at 120 °C, b) product of ^{13}C-MeOH adsorption on $HSiMo/SiO_2$ after evacuation at 60 °C and c) product of ^{13}C-HCHO adsorption on $HSiMo/SiO_2$ after evacuation at 60 °C. Spectrum of pure paraformaldehyde is shown in the inset.

According to all gathered data, the overall $CH_4 \rightarrow CO_2$ transformation on the surface of silica-supported $H_4SiMo_{12}O_{40}$ in absence of oxygen could be illustrated in a simplified way by Eq. 1:

$$H_4SiMo^{VI}_{12}O_{40} + CH_4 \rightarrow (CH_3O)H_3SiMo^{VI}_{12}O_{39} + H_2\uparrow \rightarrow (HCOO)H_5SiMo^{VI}_{8}Mo^{V}_{4}O_{38} \rightarrow H_6SiMo^{VI}_{6}Mo^{V}_{6}O_{38} + CO_2\uparrow \qquad \text{(Eq. 1)}$$

After an initial C-H activation step, resulting in H_2 release, surface methoxy species are created. While carbon atom leaves its protons behind, polyoxometalate is slowly drained from its oxygens and reduced. Methoxy groups then give way to formyl entities and finally CO_2 is made. Desorption experiments show that cleavage and isolation of intermediate species is possible [5]. There are still questions that remain unanswered, e.g. whether reduction of

Mo(VI) is one- or more-electron process is not clear. At this point we are turning our attention towards DFT calculations.

2.B.4 Conclusions

Methanol is an extremely useful precursor of surface methoxy species, allowing detailed study of their chemistry on various supports with SS NMR. In view of the recent new experimental data, reattribution of the various organic species generated from methanol on the surface of polyoxometalates was proposed, pointing towards existence of two types of methoxy entities. Differences between tungstic and molybdic POMs result in two parallel pathways of methoxy species evolution: "acidic" (already described in the literature) and "redox", reported herein.

Acknowledgments

Financial support for presented work was provided by the 7th European framework research program FP7/2007-2013, subvention no. 215193.

2.B.5 References

(1) Ivanova, II; Pomakhina, E. B.; Rebrov, A. I.; Hunger, M.; Kolyagin, Y. G.; Weitkamp, J. *J. Catal.* **2001**, *203*, 375.

(2) Li, X. B.; Nagaoka, K.; Simon, L. J.; Olindo, R.; Lercher, J. A.; Hofmann, A.; Sauer, J. *J. Am. Chem. Soc.* **2005**, *127*, 16159.

(3) Fujimoto, K.; Shikada, T.; Omata, K.; Tominaga, H. *Chem. Lett.* **1984**, 2047.

(4) Pilkenton, S.; Hwang, S. J.; Raftery, D. *J. Phys. Chem. B* **1999**, *103*, 11152.

(5) Putaj, P.; Grinenval, E.; Lefebvre, F. *J. Catal.*, *submitted*.

(6) Derouane, E. G.; Gilson, J. P.; Nagy, J. B. *Zeolites* **1982**, *2*, 42.

(7) Bosacek, V. *J. Phys. Chem.* **1993**, *97*, 10732.

(8) Bosacek, V.; Ernst, H.; Freude, D.; Mildner, T. *Zeolites* **1997**, *18*, 196.

(9) Bosacek, V.; Klik, R.; Genoni, F.; Spano, G.; Rivetti, F.; Figueras, F. *Magn. Reson. Chem.* **1999**, *37*, S135.

(10) Murray, D. K.; Chang, J. W.; Haw, J. F. *J. Am. Chem. Soc.* **1993**, *115*, 4732.

(11) Murray, D. K.; Howard, T.; Goguen, P. W.; Krawietz, T. R.; Haw, J. F. *J. Am.*

Chem. Soc. **1994**, *116*, 6354.

(12) Wang, W.; Seiler, M.; Hunger, M. *J. Phys. Chem. B* **2001**, *105*, 12553.

(13) Wang, W.; Buchholz, A.; Seiler, M.; Hunger, M. *J. Am. Chem. Soc.* **2003**, *125*, 15260.

(14) Zhang, H. L.; Zheng, A. M.; Yu, H. G.; Li, S. H.; Lu, X.; Deng, F. *J. Phys. Chem. C* **2008**, *112*, 15765.

(15) Luzgin, M. V.; Kazantsev, M. S.; Wang, W.; Stepanov, A. G. *J. Phys. Chem. C* **2009**, *113*, 19639.

(16) Hill, C. L.; (ed.) *Chem. Rev.* **1998**, *98*, 1.

(17) Hellring, S. D.; Schmitt, K. D.; Chang, C. D. *J. Chem. Soc.-Chem. Commun.* **1987**, 1320.

(18) Munson, E. J.; Haw, J. F. *J. Am. Chem. Soc.* **1991**, *113*, 6303.

(19) Knoth, W. H.; Harlow, R. L. *J. Am. Chem. Soc.* **1981**, *103*, 4265.

(20) Thomas, A.; Dablemont, C.; Basset, J. M.; Lefebvre, F. *C. R. Chim.* **2005**, *8*, 1969.

(21) Legagneux, N.; Basset, J. M.; Thomas, A.; Lefebvre, F.; Goguet, A.; Sa, J.; Hardacre, C. *Dalton Trans.* **2009**, 2235.

Chapter 3

Part A

Functionalization of cesium salts of polyoxometalates

3.A.1 Introduction

One of the great challenges of heterogenous catalysis is finding ways to overcome low specific surface areas of bulk catalysts, limiting their contact time with reagents and thus drastically diminishing their activity. Over the years various *supports* were therefore proposed – more or less chemically inert materials, suitable for deposition of catalytic species. Nowadays their design, synthetic paths, characterization methods and investigating their affinity towards particular catalysts comprise a scientific field of its own - a very much of a thriving one indeed [1-5].

Polyoxometalate-based catalysis (i.e. in most cases Keggin-type-polyoxometalate-based catalysis as this family of clusters is the best known and has been the most extensively studied so far) is no exception here [6] and two main solutions were proposed to the above-mentioned issue: deposition of clusters on, so to say, classical supports (such as silica [7], alumina [8], zirconia [8], active carbon [9] etc.) as well as more exotic ones (single wall carbon nanotubes come to mind at once [10-11]) or developing high specific surface areas of polyoxometalates themselves by exchanging their acidic protons with inorganic cations (like e.g. K^+, Cs^+, $(NH_4)^+$ etc.). Chemically speaking, it is nothing more than the creation of inorganic *salts* of POMs in aqueous solutions .

These materials possess wide range of properties predisposing them for heterogenous catalysis. First of all, in contrast to their acidic forms, they are water insoluble, precipitating instantaneously from mother liquor as extremely fine (in fact microcrystalline) powders. As such, their specific surface areas increase 100-fold in comparison with parent clusters. By adjusting stoechiometry of cation exchange it is possible to obtain partially neutralized materials, with remaining protons guaranteeing preservation of activity in acidic catalysis. At this point it is worth stressing the fact that what one tends to think about as not fully saturated salt of POMs is in fact a *composite* material made of crystalline aggregates of *fully saturated* polyanions decorated on the external surface and inside micropores with *fully protonated* ones. It is only a matter of convenience to abbreviate them by their *average* cationic compositions. It follows therefore that this *self-supported* polyoxometalate materials can act as carriers *and* catalysts at the same time. Such simplification of molecular environment of catalysts fits well into single-site approach to heterogenous catalytic systems, facilitating reaction mechanism studies. Finally, thermal stability is greatly enhanced in such compounds,

making them more robust. Material properties are directly influenced by cation type and by now comprehensive knowledge on the subject has been gathered [12-16].

Salts of POMs, similarly to any other support, can be further derivatized by deposition of various chemical species, serving as co-catalysts, on them – examples include introducing other polyoxometalates, inorganic salts of transition metals, or – as will be shown in this work for the first time – also organometallic complexes of d block transition metals. One cannot help but notice that in direct contrast to classical supports, salts of POMs are expected to be much less neutral towards deposited species, resulting in unprecedented chemical phenomena, that could be a point of interest on its own.

3.A.2 Experimental part

Materials. Phosphomolybdic acid $H_3PMo_{12}O_{40}.xH_2O$ (99+%, Aldrich), phosphotungstic acid $H_3PW_{12}O_{40}.xH_2O$ (99+%, Aldrich) and cesium carbonate Cs_2CO_3 (99%, Aldrich) were used as received.

$H_4PVMo_{11}O_{40}$, $H_5PV_2Mo_{10}O_{40}$ and $H_6PV_3Mo_9O_{40}$ were synthesized from MoO_3 (99%, Acros), V_2O_5 (99.6%, Acros) and phosphoric acid H_3PO_4 (85%, Aldrich) according to Berndt et al. [17] and characterized by IR, elemental analyses and ^{31}P solution NMR.

$RuCl_3$ (hydrate, 40-43% Ru, 99.9%-Ru, STREM), $RhCl_3$ (hydrate, 38-41% Rh, STREM), K_2PdCl_4 (98%, Aldrich) and K_2PtCl_6 (98%, Aldrich) were used as received.

$PtMe_2COD$(99%, STREM), $Ru(Meallyl)_2COD$ (97%+, STREM) and $Pd_2(Meallyl)_2Cl_2$ (98%+, STREM) were used as received.

Solvents (*n*-pentane, CH_2Cl_2) were purified according to published procedures, stored under argon and degassed prior to use.

Syntheses of supports. Cesium salts of phosphomolybdic/phosphotungstic acid given with a general formula: $Cs_xH_{3-x}PM_{12}O_{40}$; M=Mo, W were synthesized as follows - to an aqueous solution of a polyoxometalate ($H_3PM_{12}O_{40}$) solid Cs_2CO_3 (90% of a value calculated from reaction's stoechiometry) was added under vigorous stirring, resulting in effervescence and immediate precipitation of a microcrystalline salt. Stirring continued until complete evaporation of the solvent at room temperature. Powder was collected without washing and ground in the mortar.

For $Cs_xH_{3-x}(PMo_{12}O_{40}+PW_{12}O_{40})$ mixed compounds, aqueous solutions of $H_3PMo_{12}O_{40}$ and

$H_3PW_{12}O_{40}$ were mixed before precipitation with Cs_2CO_3.
For composite compounds: vanadomolybdic POM deposited on molybdic or tungstic POM - at first precipitation of a carrier POM had been performed as described above and after half an hour of stirring at room temperature, an appropriate amount of corresponding vanadomolybdic cluster was added to the reaction mixture. Resulting powder was gathered after the evaporation of the solvent, without any washing. Starting from a known value of the surface area of the carrier POMs and not taking into account the contribution from their micropores, quantity of each vanadomolybdic acid was calculated so as to create the monolayer coverage. Each Keggin unit was assumed to possess a surface area of 1.9 nm^2 [18].
For composite compounds: salt of transition metal deposited on molybdic or tungstic POM - at first precipitation of a carrier POM had been performed as described above and after half an hour of stirring at room temperature, an appropriate amount of corresponding salt (loading of metal: 3% wt.) was added to the reaction mixture. Resulting powder was gathered after the evaporation of the solvent, without any washing.

Proton quantification/Grafting of organometallic complexes. Carrier POMs were treated under high vacuum (10^{-5} Torr) for 2 hours at 200°C to dehydrate polyoxometalates and afterwards heated for another 2 hours at 200°C under the atmosphere of dry O_2 to reoxidize any clusters that might have been reduced upon previous manipulations. In a typical procedure a carrier and a stirring bar were put in a Schlenk with a septum. Schlenk was evacuated until high vacuum (10^{-5} Torr) was reached. A known quantity of reference gas (2ml of C_3H_8) was added then through septum. 10-fold excess of MeMgBr (3M solution in Et_2O) or 0.1 g of an organometallic complex was dissolved in 5 ml of dry solvent (CH_2Cl_2 or *n*-pentane) under Ar. Liquid mixture was transferred to the reaction vessel with a syringe, again via septum. After 24 hours of stirring at RT all volatile compounds were condensed in another vessel of known volume and allowed to equilibrate overnight. Gas phase was then analyzed by means of a Hewlett-Packard 5890 series II gas chromatograph equipped with a flame ionization detector and a KCl/Al_2O_3 on fused silica column (50 m x 0.32 mm).
Solids were washed three times with small portions (10 mL) of an appropriate solvent, dried under vacuum and transferred to the glovebox.

Physicochemical characterization techniques. All compounds were sealed in glass tubes under vacuum and sent to CNRS Central Analysis Department of Solaize in order to establish their elemental compositions.

The surface area of the samples was measured by BET method with an N_2 adsorption system (Micromeritics ASAP-2000) after the pretreatment under vacuum at 200°C for 2 h.
X-ray diffraction patterns were recorded with an X-ray Bruker D8 Advance diffractometer using CuK_α radiation.
Infrared spectra were recorded on a Nicolet 5700-FT spectrometer in transmission mode. Diffuse reflectance Fourier-transformed infrared (DRIFT) spectra were recorded on a Nicolet 6700-FT spectrometer by using a cell equipped with CaF2 windows. Typically, 32 scans were accumulated for each spectrum (resolution 1 cm^{-1}).

NMR experiments. In all cases zirconia rotors were filled with the samples (sometimes in a glovebox) and tightly closed. The ^{13}C solid state MAS NMR experiments were performed on a Bruker Avance 500 spectrometer equipped with a standard 4 mm double-bearing probehead. The rotation frequency was set to 10 kHz. A typical cross polarization sequence was used**,** with 4 ms contact time and a recycle delay of 1 to 4 s to allow the complete relaxation of the ^1H nuclei. All measured chemical shifts are given with respect to TMS as an external reference. ^1H, ^{31}P and ^{137}Cs SS MAS NMR experiments were performed on a Bruker DSX-300 spectrometer equipped with a standard 4 mm double-bearing probehead. The rotation frequency was set to 10 kHz. ^{51}V SS MAS NMR experiments were performed on a Bruker Avance 300 spectrometer with no rotation applied. ^1H chemical shifts are given with respect to H_2O as an external reference. ^{31}P chemical shifts are given with respect to 85% H_3PO_4 in water as an external reference. ^{137}Cs chemical shifts are given with respect to an aqueous solution of CsCl.

3.A.3 Results and discussion

3.A.3.1 Synthesis and characterization of supports. Literature perusal suggested using Cs^+ salts of polyoxometalates as the most suitable for our applications. In the first step, three series of salts of Keggin-type POMs with variable cesium content were synthesized by a straightforward precipitation from their aqueous solutions (details in the Experimental part). $H_3PW_{12}O_{40}$ and $H_3PMo_{12}O_{40}$ classical compounds were chosen, due to their stability, commercial availability and complementary properties: tungstic clusters exhibit pronounced acidic and molybdic ones – redox properties. An attempt to co-precipitate salts from mixtures of both compounds has been undertaken as well.

In order to find the best candidates to serve as supports for other co-catalysts, preliminary characterization of so-prepared samples has been performed by means of elemental composition analyses and results are presented in Tables I, II and III. The most important information that can be extracted at this stage is the quantity of cesium introduced to each system and as a consequence – number of remaining protons which are distributed over the surface of the samples.

Table I. Elemental composition of the samples.

sample code	nominal composition	calculated values				experimental values			
		%W	%Mo	%Cs	%P	%W	%Mo	%Cs	%P
1	$Cs_2HPW_{12}O_{40}$	70.18	-	8.46	0.99	63.47	-	3.89	1.07
2	$Cs_{2.5}H_{0.5}PW_{12}O_{40}$	68.74	-	10.35	0.97	61.49	-	6.39	1.02
3	$Cs_3PW_{12}O_{40}$	67.36	-	12.17	0.95	61.53	-	8.62	1.01
4	$Cs_2HPMo_{12}O_{40}$	-	55.12	12.72	1.48	-	52.30	9.53	1.16
5	$Cs_{2.5}H_{0.5}PMo_{12}O_{40}$	-	53.43	15.42	1.44	-	51.20	13.90	1.33
6	$Cs_3PMo_{12}O_{40}$	-	51.85	17.96	1.40	-	49.61	12.87	0.96
7	$Cs_2H(PW_{12}O_{40}+PMo_{12}O_{40})$	42.17	22.00	10.16	1.18	37.04	20.00	3.17	1.23
8	$Cs_{2.5}H_{0.5}(PW_{12}O_{40}+PMo_{12}O_{40})$	41.13	21.46	12.39	1.16	36.60	19.95	4.08	1.22
9	$Cs_3(PW_{12}O_{40}+PMo_{12}O_{40})$	40.15	20.95	14.51	1.13	36.65	19.47	6.37	1.18

Table II. Elemental ratios of samples.

sample code	nominal composition	calculated values					experimental values				
		W/Cs	W/P	Mo/Cs	Mo/P	W/Mo	W/Cs	W/P	Mo/Cs	Mo/P	W/Mo
1	$Cs_2HPW_{12}O_{40}$	6.0	12.0	-	-	-	11.8	10.0	-	-	-
2	$Cs_{2.5}H_{0.5}PW_{12}O_{40}$	5.0	12.0	-	-	-	7.0	10.2	-	-	-
3	$Cs_3PW_{12}O_{40}$	4.0	12.0	-	-	-	5.2	10.3	-	-	-
4	$Cs_2HPMo_{12}O_{40}$	-	-	6.0	12.0	-	-	-	7.6	14.6	-
5	$Cs_{2.5}H_{0.5}PMo_{12}O_{40}$	-	-	5.0	12.0	-	-	-	5.1	12.4	-
6	$Cs_3PMo_{12}O_{40}$	-	-	4.0	12.0	-	-	-	5.3	16.7	-
7	$Cs_2H(PW_{12}O_{40}+PMo_{12}O_{40})$	3.0	6.0	3.0	6.0	1.0	8.5	5.1	8.7	5.3	1.0
8	$Cs_{2.5}H_{0.5}(PW_{12}O_{40}+PMo_{12}O_{40})$	2.5	6.0	2.5	6.0	1.0	6.5	5.1	6.8	5.3	1.0
9	$Cs_3(PW_{12}O_{40}+PMo_{12}O_{40})$	2.0	6.0	2.0	6.0	1.0	4.2	5.2	4.2	5.3	1.0

Elemental ratios calculated from the general formula: $A/B = (\%A/M_A)/(\%B/M_B)$, where M_A and M_B are molar masses of elements A and B, respectively.

Table III. Nominal vs. experimentally established compositions of the samples.

sample code	nominal composition	established composition
1	$Cs_2HPW_{12}O_{40}$	$CsH_2PW_{12}O_{40}$
2	$Cs_{2.5}H_{0.5}PW_{12}O_{40}$	$Cs_{1.7}H_{1.3}PW_{12}O_{40}$
3	$Cs_3PW_{12}O_{40}$	$Cs_{2.3}H_{0.7}PW_{12}O_{40}$
4	$Cs_2HPMo_{12}O_{40}$	$Cs_{1.6}H_{1.4}PMo_{12}O_{40}$
5	$Cs_{2.5}H_{0.5}PMo_{12}O_{40}$	$Cs_{2.4}H_{0.6}PMo_{12}O_{40}$
6	$Cs_3PMo_{12}O_{40}$	$Cs_{2.3}H_{0.7}PMo_{12}O_{40}$
7	$Cs_2H(½PW_{12}O_{40} + ½PMo_{12}O_{40})$	$Cs_{1.4}H_{1.6}(PW_{12}O_{40}+PMo_{12}O_{40})$
8	$Cs_{2.5}H_{0.5}(½PW_{12}O_{40} + ½PMo_{12}O_{40})$	$Cs_{1.8}H_{1.2}(PW_{12}O_{40}+PMo_{12}O_{40})$
9	$Cs_3(½PW_{12}O_{40} + ½PMo_{12}O_{40})$	$Cs_{2.9}H_{0.1}(PW_{12}O_{40}+PMo_{12}O_{40})$

Both bulk POMs and a precipitating agent Cs_2CO_3 are extremely hygroscopic. Moreover, POMs contain also a lot of crystallization water molecules in their crystal lattices [19]. In order to compensate for this fact an 10% excess of each polyanion was used during each precipitation rather than an exact quantity calculated from reaction's stoechiometry. Results of elemental analyses presented in Tables I, II and III show however, that this approach was somehow too crude and large differences are noted between calculated and experimental values for obtained solids. One needs to take into consideration also the 5% margin of error for all experimental data.

Another method needs therefore to be employed to corroborate (or contradict) elemental analyses results. E.g. protons of the support can be reacted with a simple organometallic compound leading to formation of alkanes, which then could be quantified. This way, the amount of the evolved gaseous product corresponds directly to the number of protons present in the sample. To this end, 0.25 g of each sample was treated with 10-fold excess of MeMgBr dissolved in CH_2Cl_2 at RT (details in the Experimental part). After the reaction completion the evolved gases were condensed in another vessel and quantified by means of GC. As seen in Table IV, on one of the examined compounds, the chemical composition established via this method confirms elemental analyses results.

Table IV. Proton quantification results.

sample code	nominal composition	nominal n H^+ [*10^{-3} mol]	evolved n CH_4 [*10^{-3} mol]	established n H^+ [*10^{-3} mol]	established composition
2	$Cs_2H_1PW_{12}O_{40}$	0.080	0.127	0.127	$Cs_{1.6}H_{1.4}PW_{12}O_{40}$

Samples morphologies were elucidated via analysis their N_2 adsorption-desorption isotherms. Surface area values obtained from BET method are given in Table V accompanied by the increments from the presence of micropores (understood as pores exhibiting diameters between 7-20 Å) and ultramicropores (less than 7 Å) combined together [20].

Table V. Surface area of the samples with contribution from the (ultra)micropores.

sample code	established composition	total surface area [m^2/g]	(ultra)micropores (< 20Å) [m^2/g]
1	$CsH_2PW_{12}O_{40}$	60	54
2	$Cs_{1.7}H_{1.3}PW_{12}O_{40}$	97	72
3	$Cs_{2.3}H_{0.7}PW_{12}O_{40}$	126	61
4	$Cs_{1.6}H_{1.4}PMo_{12}O_{40}$	33	30
5	$Cs_{2.4}H_{0.6}PMo_{12}O_{40}$	140	77
6	$Cs_{2.3}H_{0.7}PMo_{12}O_{40}$	155	94
7	$Cs_{1.4}H_{1.6}(½PW_{12}O_{40} + ½PMo_{12}O_{40})$	60	55
8	$Cs_{1.8}H_{1.2}(½PW_{12}O_{40} + ½PMo_{12}O_{40})$	117	78
9	$Cs_{2.9}H_{0.1}(½PW_{12}O_{40} + ½PMo_{12}O_{40})$	140	103

Typically observed N_2 adsorption isotherms are presented in Figure 1, while pore sizes distribution curves derived from the desorption branches by BJH method [21] are shown in Figure 2.

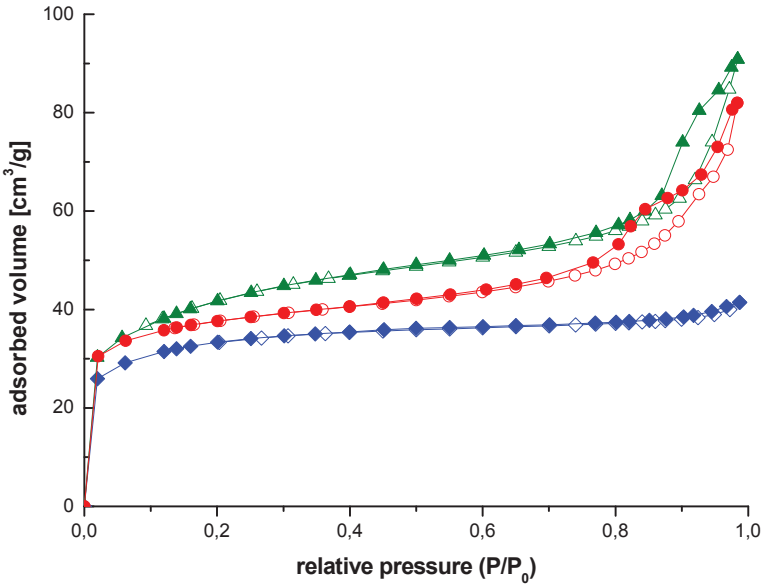

Figure 1. Adsorption-desorption isotherms of N_2 at 77 K for: $Cs_{1.7}H_{1.3}PW_{12}O_{40}$ (♦, ◊); $Cs_{2.4}H_{0.6}PMo_{12}O_{40}$ (▲, Δ) and $Cs_{1.8}H_{1.2}(PW_{12}O_{40}+PMo_{12}O_{40})$ (●, ○). Open symbols, adsorption branch, solid symbols, desorption branch.

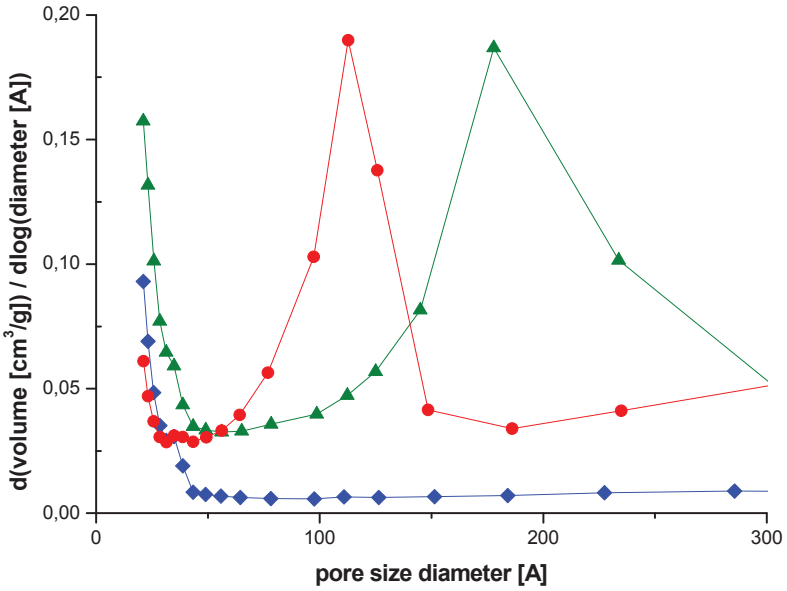

Figure 2. Pore size distribution curves derived from BJH method for: $Cs_{1.7}H_{1.3}PW_{12}O_{40}$ (♦); $Cs_{2.4}H_{0.6}PMo_{12}O_{40}$ (▲) and $Cs_{1.8}H_{1.2}(PW_{12}O_{40}+PMo_{12}O_{40})$ (●).

Samples: $Cs_{2.4}H_{0.6}PMo_{12}O_{40}$ and $Cs_{1.8}H_{1.2}(PW_{12}O_{40}+PMo_{12}O_{40})$ exhibit isotherms of Type IV, typical for mesoporous materials, with a hysteresis loop due to the vaporization of nitrogen condensed in the mesopores. Another interesting feature is the steep increase in the adsorption at low-pressure ranges ($P/P_0 < 0.1$), suggesting also presence of micropores in these samples. On the other hand, the curve of $Cs_{1.7}H_{1.3}PW_{12}O_{40}$ sample is of type I, characteristic of purely microporous materials [22]. Pore size distribution curves derived from BJH method [21] for $Cs_{2.4}H_{0.6}PMo_{12}O_{40}$ and $Cs_{1.8}H_{1.2}(PW_{12}O_{40}+PMo_{12}O_{40})$ contain information about the structure of their mesopores [22]. From peaks positions the diameters of the necks of mesopores of the samples can be estimated roughly as 105 and 175 Å, respectively. Much broader peak in the latter case suggests less uniform distribution of pore sizes in $Cs_{2.4}H_{0.6}PMo_{12}O_{40}$ material.

During typical synthetic procedure of cesium salts of polyoxometalates pH value of the mother liquor rises significantly. Although a recent study has shown that Keggin structure can be preserved in solution up to pH = 8 [23], the possibility of presence of products of partial decomposition of the clusters in the synthesized samples needs to be verified. To this purpose ^{31}P solid state NMR technique was employed. Figure 3 presents typical spectra obtained for series of supports based on tungstic and molybdic polyoxometalates, respectively.

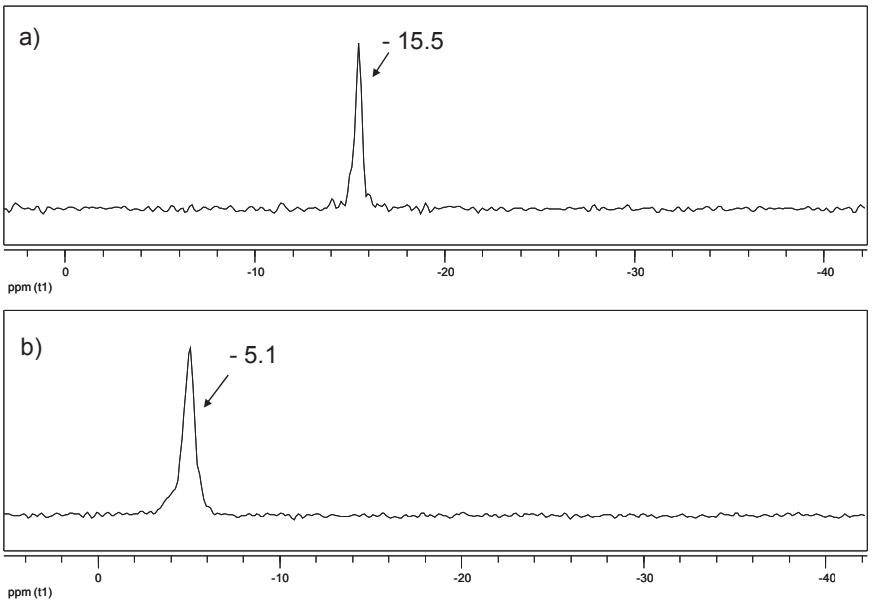

Figure 3. ^{31}P SS NMR spectra of: a) $Cs_{2.3}H_{0.7}PW_{12}O_{40}$ and b) $Cs_{2.3}H_{0.7}PMo_{12}O_{40}$.

Spectra of both samples consist of a single peak situated at -15.5 and -5.1 ppm respectively for: $Cs_{2.3}H_{0.7}PW_{12}O_{40}$ and $Cs_{2.3}H_{0.7}PMo_{12}O_{40}$. These peaks are characteristic for complete Keggin-type clusters based on tungsten – in the former, or molybdenum – in the latter case. In occurrence, there was no decomposition of parent polyoxometalates during the syntheses.

^{133}Cs SS NMR spectra of Cs^{+} cations introduced into the polyoxometalate lattices presented in Fig. 4, show signal shifts of -43.4 ppm for $Cs_{2.3}H_{0.7}PW_{12}O_{40}$ and -51.8 ppm for $Cs_{2.3}H_{0.7}PMo_{12}O_{40}$. They are a good illustration of high local-environment-related sensitivity of this nucleus, which originates from combined small quadrupole moment and a large chemical shift range (ca. 400 ppm) [24].

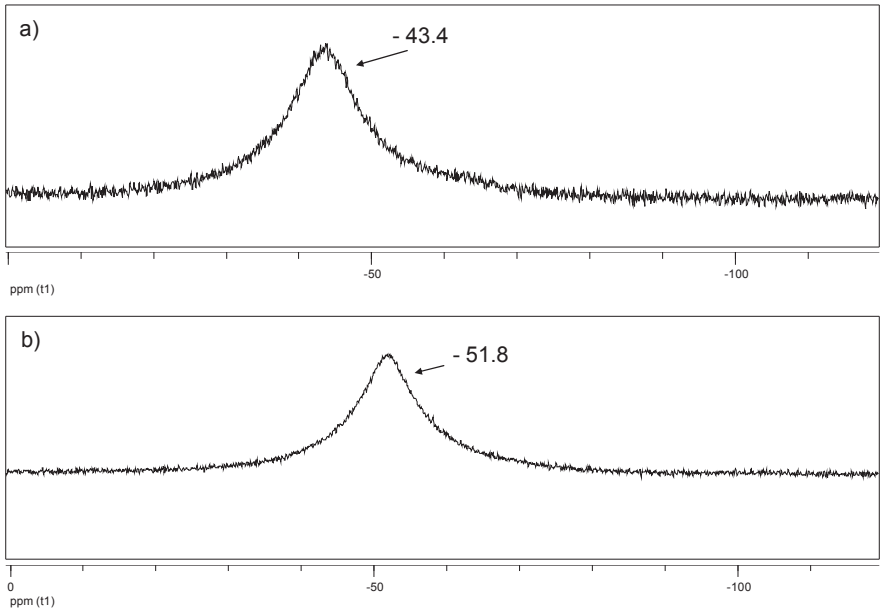

Figure 4. ^{133}Cs SS NMR spectra of: a) $Cs_{2.3}H_{0.7}PW_{12}O_{40}$ and b) $Cs_{2.3}H_{0.7}PMo_{12}O_{40}$.

Finally, characterization by means of powder diffraction technique (DRX) showed unequivocally presence of only one crystalline phase in all investigated samples. That is to say that purely acidic Keggin clusters are evenly distributed over the whole surface of granular $Cs_3PW_{12}O_{40}$ salt, according to the model [14]. Moreover, as clearly visible in Figure 5, diffraction lines are distinctly broadened, suggesting pronounced microcrystallinity of obtained compounds (as described by Debye-Scherrer's law [25]).

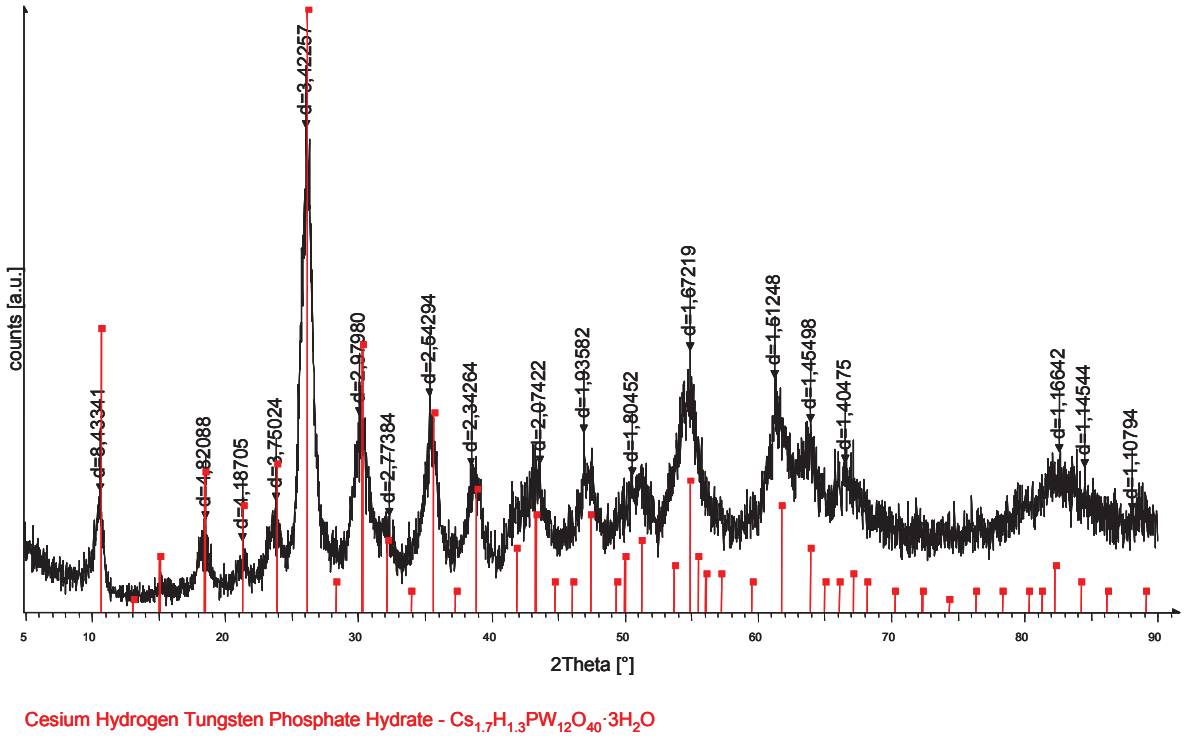

Figure 5. Powder diffraction pattern of $Cs_{1.7}H_{1.3}PW_{12}O_{40}$ sample, showing fingerprint diffraction lines together with their calculated interplanar distances values.

To sum up this part, three series of cesium salts of different types of polyoxometalates, with variable alkaline cation content, were obtained and characterized in order to be further derivatized and used as heterogenous catalysts. The supports exhibit high surface areas, micro- or combined micro- and mesoporosities and consist of acidic Keggin-type polyoxometalates evenly dispersed over the granular particles of their corresponding cesium salts. Moreover, as shown by the results of proton quantification by means of reaction with an organometallic complex, despite of the supports morphologies all the surface protons are accessible for other chemical species (at least of a size comparable with MeMgBr) – an important observation in the context of their prospective catalytic applications.

3.A.3.2 Deposition of vanadium-containing POMs. One envisageable way of functionalization of so-obtained salts of POMs is by deposition of other POMs on their surface. Particularly desirable would be dispersion of Keggin-type mixed vanadomolybdic clusters, namely: $H_4PVMo_{11}O_{40}$, $H_5PV_2Mo_{10}O_{40}$ and $H_6PV_3Mo_9O_{40}$. These compounds are known to exhibit excellent performance as catalysts in numerous oxidation reactions (both in

homogenous and heterogenous conditions) [26] but do not develop high specific surface area values upon exchange of their protons with alkaline metal cations.

As a result of preliminary characterization of all the supports, samples: $Cs_{2.3}H_{0.7}PW_{12}O_{40}$ and $Cs_{2.3}H_{0.7}PMo_{12}O_{40}$ were chosen to serve as carriers for vanadium-containing POMs. The main reasons for this were their high specific surface area values as well as moderate level of microporosity (50-60%). The quantity of each vanadomolybdic cluster that has been introduced to the system was adjusted in order to create a monolayer on the external surface and inside the mesopores of the support (corresponds to 15 % wt.). Table VI presents the results of elemental analyses, evaluating quantities of vanadium present in each sample.

Table VI. Elemental composition of the samples.

sample code	**nominal composition**	**calculated %V**	**experimental %V**
10	$H_4PVMo_{11}O_{40}$ / $Cs_{2.3}H_{0.7}PW_{12}O_{40}$	0.43	0.39
11	$H_5PV_2Mo_{10}O_{40}$ / $Cs_{2.3}H_{0.7}PW_{12}O_{40}$	0.88	0.79
12	$H_6PV_3Mo_9O_{40}$ / $Cs_{2.3}H_{0.7}PW_{12}O_{40}$	1.36	1.13
13	$H_4PVMo_{11}O_{40}$ / $Cs_{2.3}H_{0.7}PMo_{12}O_{40}$	0.45	0.26
14	$H_5PV_2Mo_{10}O_{40}$ / $Cs_{2.3}H_{0.7}PMo_{12}O_{40}$	0.91	0.66
15	$H_6PV_3Mo_9O_{40}$ / $Cs_{2.3}H_{0.7}PMo_{12}O_{40}$	1.41	1.00

In general, the introduced quantities of vanadium are lower than the predicted values (which is understandable taking into account the hygroscopicity of vanadomolybdic POMs). Another problem encountered here is posed by the sheer limits of analytical techniques used (low concentration of vanadium in the samples, homogenization issues etc.).

Results of analysis of N_2 adsorption-desorption isotherms of prepared samples were compiled in Table VII. Total surface area values obtained from BET method (third column) are lower than for parent compounds (average decrease of about 40%). Introduction of vanadomolybdic clusters (15 % wt.) with low specific surface areas of about 5 m^2/g accounts only partially for the overall loss of surface area. Some pore entrance blocking must have therefore occurred as well (see loss of the surface of micropores in column 4). Still, the numbers remain much higher than for bulk POMs and are promising for catalytic applications.

Table VII. Surface area of the samples with contribution from the (ultra)micropores.

sample code	composition	total surface area [m^2/g]	micropores (< 20Å) [m^2/g]
3	$Cs_{2.3}H_{0.7}PW_{12}O_{40}$	126	61
10	$H_4PVMo_{11}O_{40}$ / $Cs_{2.3}H_{0.7}PW_{12}O_{40}$	75	67
11	$H_5PV_2Mo_{10}O_{40}$ / $Cs_{2.3}H_{0.7}PW_{12}O_{40}$	58	51
12	$H_6PV_3Mo_9O_{40}$ / $Cs_{2.3}H_{0.7}PW_{12}O_{40}$	88	48
6	$Cs_{2.3}H_{0.7}PMo_{12}O_{40}$	155	94
13	$H_4PVMo_{11}O_{40}$ / $Cs_{2.3}H_{0.7}PMo_{12}O_{40}$	114	72
14	$H_5PV_2Mo_{10}O_{40}$ / $Cs_{2.3}H_{0.7}PMo_{12}O_{40}$	110	74
15	$H_6PV_3Mo_9O_{40}$ / $Cs_{2.3}H_{0.7}PMo_{12}O_{40}$	69	49

By means of powder diffraction technique (DRX) it has been established that vanadomolybdic POMs are evenly distributed over the surface of their carriers as presence of no other crystalline phase (besides the carrier) was detected (see e.g. Fig. 6).

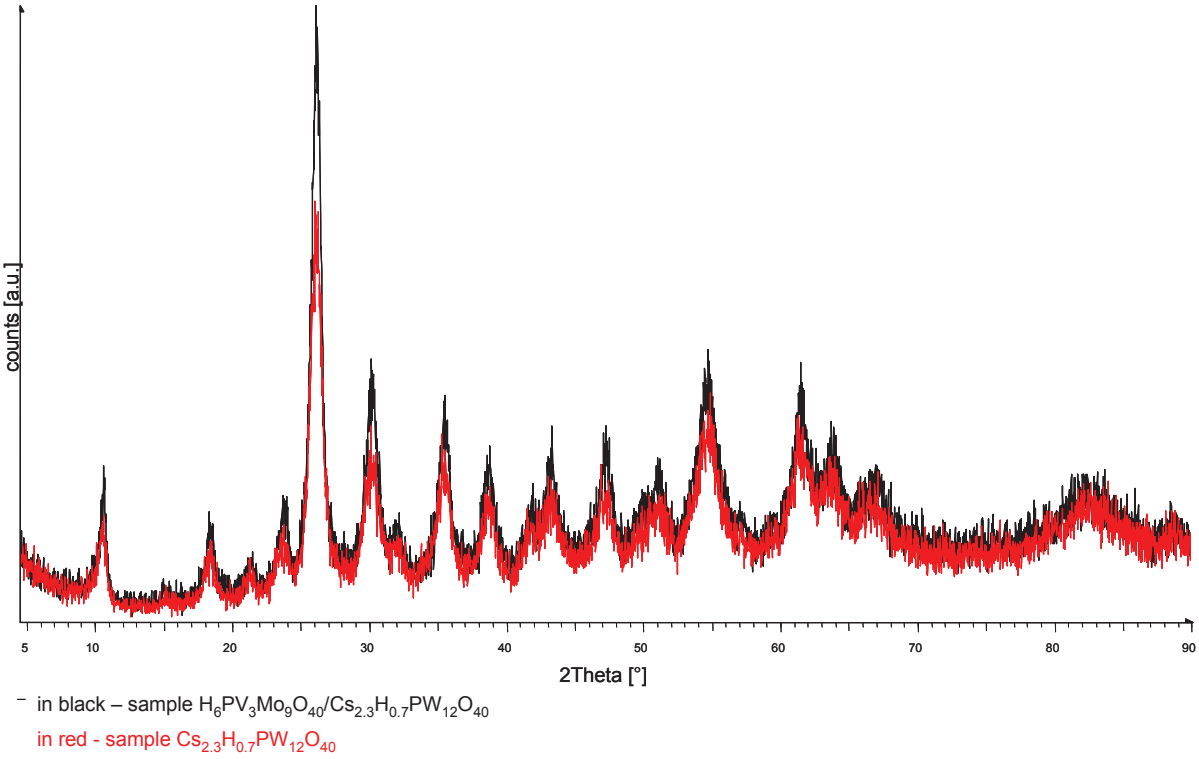

Figure 6. Superimposed powder diffraction patterns of $Cs_{2.3}H_{0.7}PW_{12}O_{40}$ (red) and $H_6PV_3Mo_9O_{40}$ / $Cs_{2.3}H_{0.7}PW_{12}O_{40}$ (black) samples.

^{31}P SS NMR spectra of vanadomolybdic clusters supported on $Cs_{2.3}H_{0.7}PW_{12}O_{40}$ are shown in Fig. 7 (general view) and 8 (magnification).

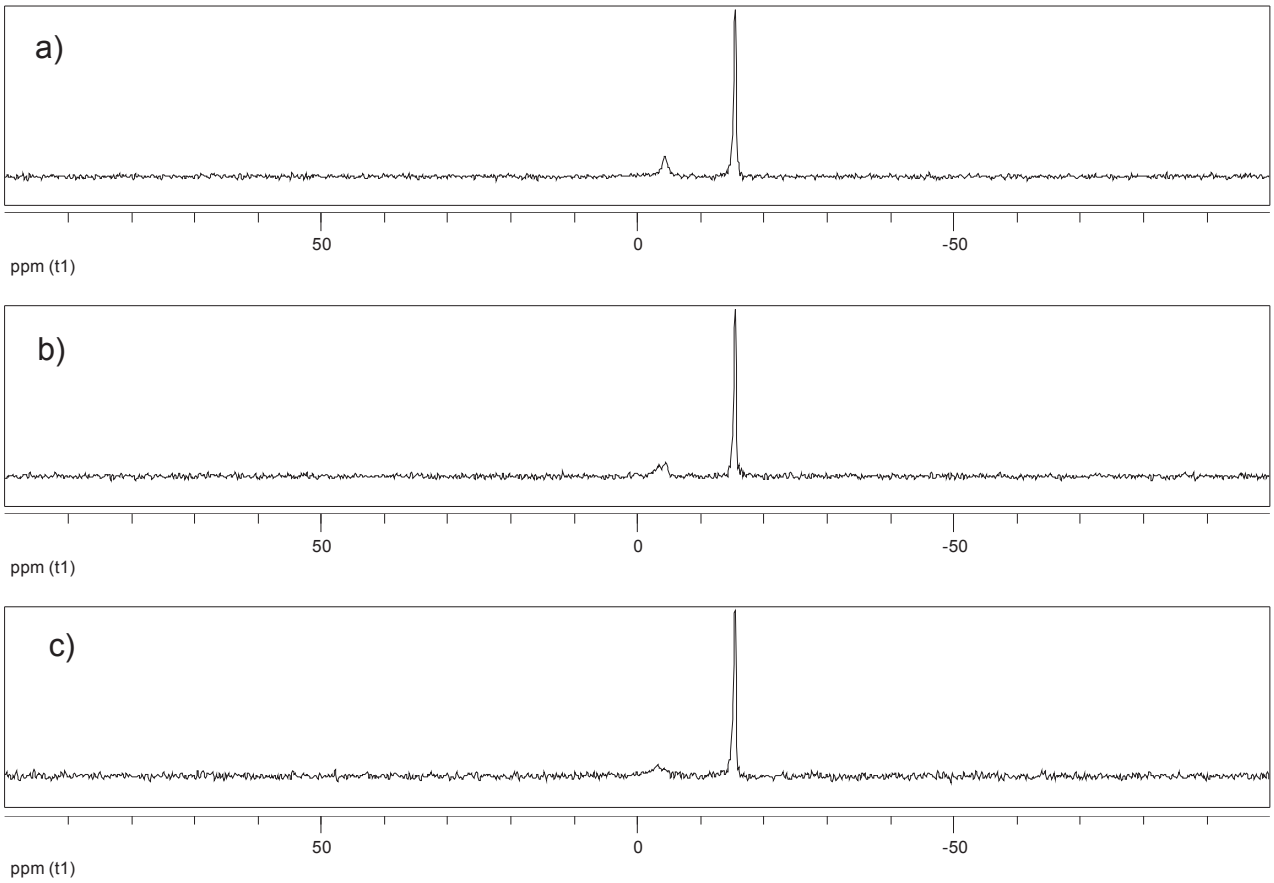

Figure 7. ^{31}P SS NMR spectra of: a) $H_4PVMo_{11}O_{40}/Cs_{2.3}H_{0.7}PW_{12}O_{40}$, b) $H_5PV_2Mo_{10}O_{40}/Cs_{2.3}H_{0.7}PW_{12}O_{40}$ and c) $H_6PV_3Mo_9O_{40}/Cs_{2.3}H_{0.7}PW_{12}O_{40}$.

Spectra of the impregnated materials differ only slightly from the spectra of their parent compounds. The main new feature is appearance of a peak at around -5 ppm, coming from the introduction of vanadomolybdic clusters. At a closer inspection, the aforementioned peak turns out to be well-defined only in the case of $H_4PVMo_{11}O_{40}$, whereas for the other two polyoxometalates it resembles a not particularly well-resolved bump (see Fig. 8).

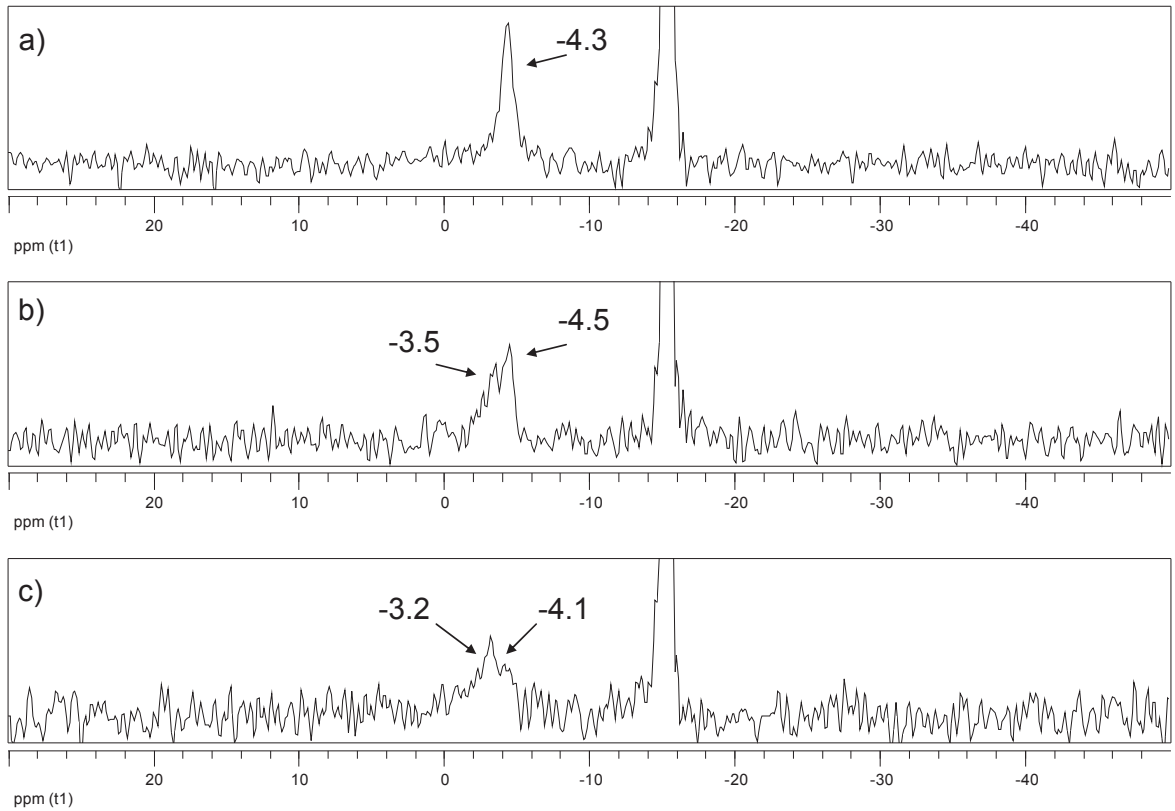

Figure 8. ^{31}P SS NMR spectra of: a) $H_4PVMo_{11}O_{40}/Cs_{2.3}H_{0.7}PW_{12}O_{40}$, b) $H_5PV_2Mo_{10}O_{40}/Cs_{2.3}H_{0.7}PW_{12}O_{40}$ and c) $H_6PV_3Mo_9O_{40}/Cs_{2.3}H_{0.7}PW_{12}O_{40}$.

This in agreement with the commonly accepted view on the structure of vanadomolybdic POMs. While $H_4PVMo_{11}O_{40}$ is a discreet entity, resulting from a replacement of one molybdic octahedron of a Kegggin unit with one vanadic one, $H_5PV_2Mo_{10}O_{40}$ and $H_6PV_3Mo_9O_{40}$ comprise of multiple positional isomers, denominated as they are for the reasons of simplicity [27-28].

Vanadomolybdic POMs were thus introduced successfully on the surface of cesium salts of phosphotungstic and phosphomolybdic acids. Although surface area values of composite materials are lower than for the parent compounds, no vanadomolybdic clusters decomposition was observed upon deposition and the most importantly – uniform distribution of the dopants over whole material was achieved.

3.A.3.3 Deposition of inorganic salts of late-transition metals. Another way leading to potentially interesting catalytic materials is by impregnation of the carrier POMs with inorganic salts of late transition metals. Such composite materials have been known for some time now and evidenced to possess interesting chemical properties [29-31]. Compounds of four most comprehensively studied elements have been chosen, namely: $RuCl_3$, $RhCl_3$, K_2PdCl_4 and K_2PtCl_6. Metal loadings were adjusted to 3% wt. (see Table VIII). This time however, $Cs_{1.7}H_{1.3}PW_{12}O_{40}$ material instead of $Cs_{2.3}H_{0.7}PW_{12}O_{40}$ was chosen as a tungstic support, because it shows higher surface acidity (number of protons per unit of surface). This was done in order to enhance the interactions of metal species with the support.

Table VIII. Elemental composition of the samples.

sample code	**nominal composition**	**calculated %M**	**experimental %M**
16	$RuCl_3$ / $Cs_{1.7}H_{1.3}PW_{12}O_{40}$	3.00	2.18
17	$RuCl_3$ / $Cs_{2.4}H_{0.6}PMo_{12}O_{40}$	3.00	2.27
18	$RhCl_3$ / $Cs_{1.7}H_{1.3}PW_{12}O_{40}$	3.00	2.03
19	$RhCl_3$ / $Cs_{2.4}H_{0.6}PMo_{12}O_{40}$	3.00	2.16
20	K_2PdCl_4 / $Cs_{1.7}H_{1.3}PW_{12}O_{40}$	3.00	2.22
21	K_2PdCl_4 / $Cs_{2.4}H_{0.6}PMo_{12}O_{40}$	3.00	1.75
22	K_2PtCl_6 / $Cs_{1.7}H_{1.3}PW_{12}O_{40}$	3.00	2.41
23	K_2PtCl_6 / $Cs_{2.4}H_{0.6}PMo_{12}O_{40}$	3.00	2.30

Metal loadings established experimentally and shown in Table VIII again differ from the expected values. Since the catalysts were prepared without any washing the observed discrepancies most probably stem from the hydration state of compounds used for the impregnation.

Results of analysis of N_2 adsorption-desorption isotherms of prepared samples were compiled in Table IX. Surface area values obtained from BET method are lower than for parent compounds (decrease of around 20% for tungstic and 30 % for molybdic salts of polyoxometalates) and accounts mostly for the diminishing of the surface area of the micropores as they are being filled with transition metal salts.

Table IX. Surface area of the samples with contribution from the (ultra)micropores.

sample	established composition	total surface area [m^2/g]	micropores (< 20Å) [m^2/g]
2	$Cs_{1.7}H_{1.3}PW_{12}O_{40}$	97	72
5	$Cs_{2.4}H_{0.6}PMo_{12}O_{40}$	140	77
16	$RuCl_3$ / $Cs_{1.7}H_{1.3}PW_{12}O_{40}$	78	42
17	$RuCl_3$ / $Cs_{2.4}H_{0.6}PMo_{12}O_{40}$	92	54
18	$RhCl_3$ / $Cs_{1.7}H_{1.3}PW_{12}O_{40}$	79	51
19	$RhCl_3$ / $Cs_{2.4}H_{0.6}PMo_{12}O_{40}$	102	58
20	K_2PdCl_4 / $Cs_{1.7}H_{1.3}PW_{12}O_{40}$	79	36
21	K_2PdCl_4 / $Cs_{2.4}H_{0.6}PMo_{12}O_{40}$	97	53
22	K_2PtCl_6 / $Cs_{1.7}H_{1.3}PW_{12}O_{40}$	79	56
23	K_2PtCl_6 / $Cs_{2.4}H_{0.6}PMo_{12}O_{40}$	81	47

Two types of powder diffraction patterns have been observed upon characterization of the samples. In the case of Ru and Rh salts, their even distribution on the surface of the carriers is noted. On the other hand, K_2PtCl_6 (and also K_2PdCl_4) behave in a strikingly different way. As shown in Fig. 9, there are clearly visible sharp lines of platinum salt's phase among broad lines of the carrier. Their appearance signifies creation of well-developed crystallites of K_2PtCl_6 over the surface of the support. Apparently, in the case of Ru and Rh compounds simple cation exchange ($Ru^{3+}/Rh^{3+} \leftrightarrow H^+$) is taking place over whole surface of the support followed by HCl release, whereas Pt and Pd, which remain in the form of anionic species and because of the repulsive interactions with polyanionic clusters, prefer to aggregate apart.

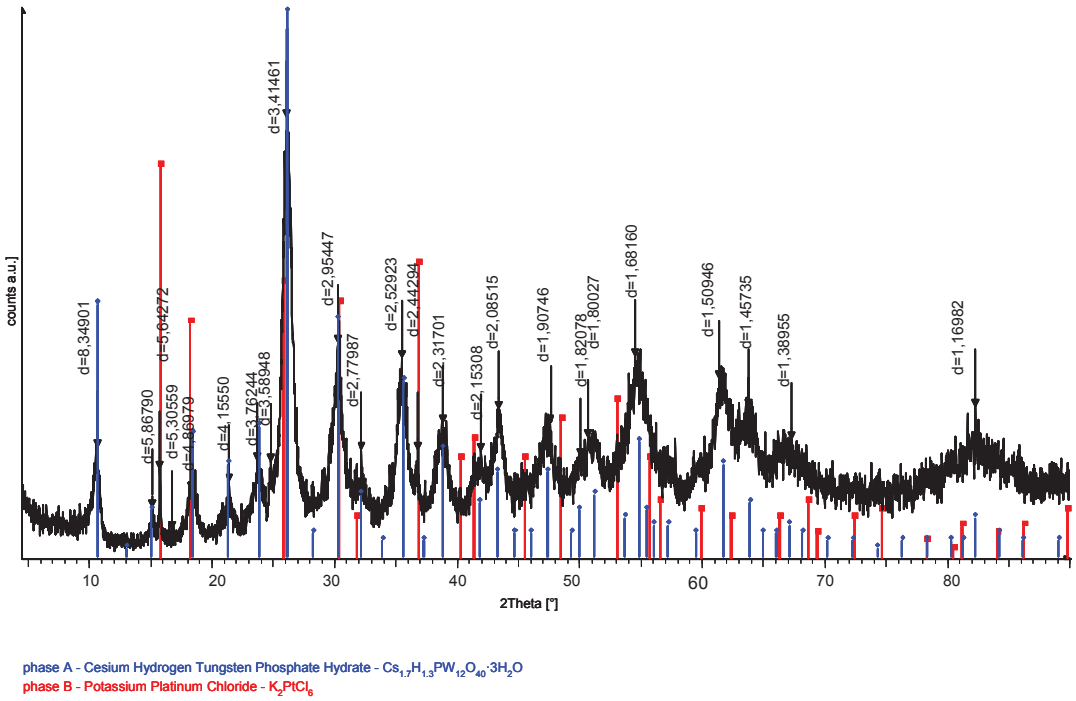

Figure 9. Powder diffraction pattern of $K_2PtCl_6/Cs_{1.7}H_{1.3}PW_{12}O_{40}$ sample, showing fingerprint diffraction lines of both phases together with their calculated interplanar distances values.

Related with this phenomenon must be a change in ^{31}P SS NMR spectrum of $K_2PtCl_6/Cs_{1.7}H_{1.3}PW_{12}O_{40}$ sample (presented in Fig. 10), where a new peak at -17.1 ppm is detected in addition to one at -15.7 ppm.

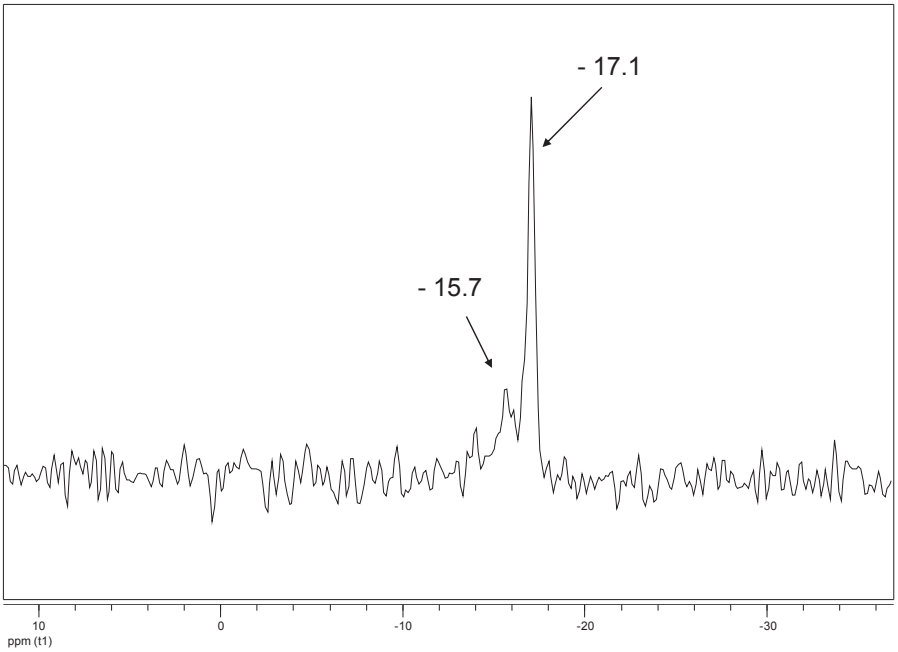

Figure 10. ^{31}P SS NMR spectrum of $K_2PtCl_6/Cs_{1.7}H_{1.3}PW_{12}O_{40}$.

Pt incorporation into the structure of the polyoxometalate is another possibility, though reports describing such phenomena are scarce and presented experimental data are still being debated upon [32]. In any case, they deal with lacunary Keggin clusters, much more prone to structural modifications [33]. Finally, formation of mixed Cs^+/K^+ salt of POMs could be the reason of a second peak appearance.

Mode of dispersion of metal species over the support's surface changes with a type of precursor used for the impregnation. Accordingly, local environment of cesium cations should change as well and find its expression in chemical shifts of ^{133}Cs in the NMR spectra. Indeed, as clearly visible in Fig. 11, peaks position are slightly modified, although no general tendency can be established.

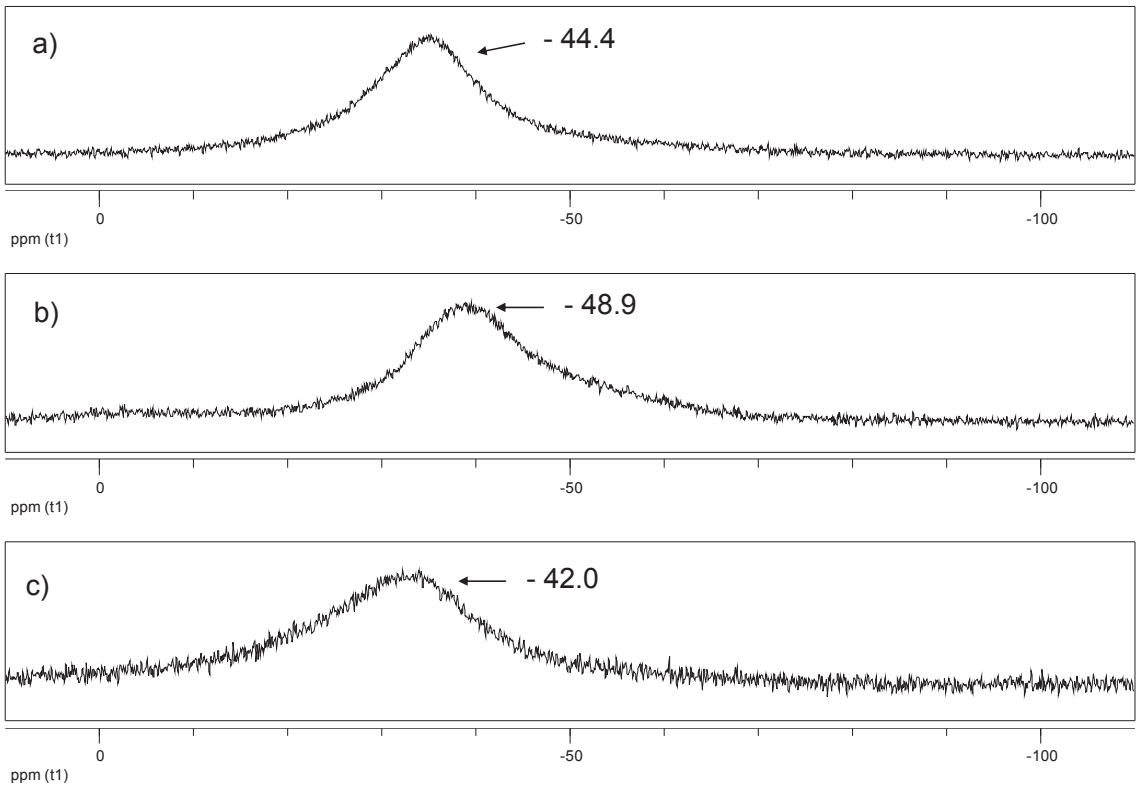

Figure 11. ^{133}Cs SS NMR spectra of: a) $Cs_{1.7}H_{1.3}PW_{12}O_{40}$, b) $RuCl_3/Cs_{1.7}H_{1.3}PW_{12}O_{40}$ and c) $K_2PtCl_6/Cs_{1.7}H_{1.3}PW_{12}O_{40}$.

Another class of composite materials has thus been prepared and characterized on a preliminary basis. Nevertheless, in view of their potential catalytic applications some adjustments of the proposed synthetic procedures come to mind at once. Firstly, washing of the catalysts after impregnation could help eliminate excess of a doping compound. New Pt

and Pd compounds should also be considered as a replacement for the ones that have been used here to prevent creation of multiple phases in the solids. All this concerns are in line with a "single-site" approach to catalysts design.

So-obtained composite materials can be used as prepared or modified even further by treatment, e.g. under hydrogen flow to generate the nanoparticles of respective noble metals on the surface of POMs or calcined under oxygen flow at elevated temperatures to cause polyoxometalates decomposition and formation of various mixed metal oxides. Their main advantage lies therefore in their versatility.

3.A.3.4 Deposition of organometallic complexes of late-transition metal atoms. Surface organometallic chemistry (SOMC) is a way of obtaining well-defined single-site metal catalysts by controlled deposition (grafting) of their organometallic complexes on the surface of various supports [34-35]. Creation of chemical bonds between a support and a metal centre is accompanied by protonation of complex ligand(s) (either neutral or negatively charged) and their release into the solution/gas phase. If the released species are stable enough, based on their quantification (doublechecked with the results of complementary physicochemical characterization techniques) a quantitative-qualitative model of surface-deposited entity or entities can be proposed. This methodology facilitates therefore consecutive studies of reaction mechanisms and allows insights into structure and reactivity of catalytically active species which in turn can lead to catalysts engineering towards better performance.

In this work it will be shown for the first time that SOMC can be also realized on high-surface inorganic salts of POMs, serving as another type of carrier for organometallic species. The concept itself (deposition of metal complexes on POMs in order to create homo- or heterogenous catalysts) has already been studied, although either on dicreet POMs [32] or ones that were previously dispersed on SiO_2 [36-37]. Also, data on the nature of interaction of metal complexes with POMs in such systems are scarce [38]. The obvious advantage of using self-supported POMs is the elimination of a possibility of transfer of organometallic moieties from polyoxometalate clusters to silica (or other support), a trend that has already been observed [39] and which by definition contradicts the "single-site" approach.

Following organometallic complexes: $Ru(Meallyl)_2COD$ (soluble in *n*-pentane), $Pd_2(Meallyl)_2Cl_2$ and $PtMe_2COD$ (both soluble in CH_2Cl_2); and supports: $Cs_{1.7}H_{1.3}PW_{12}O_{40}$ and $Cs_{2.4}H_{0.6}PMo_{12}O_{40}$; were selected for this study and typical deposition procedure is described in the Experimental part.

In the case of grafting of $Ru(Meallyl)_2COD$ and $Pd_2(Meallyl)_2Cl_2$ complexes monitored by GC, no gas release was detected, even after 24-hour reaction period. There are three tentative explanations to this fact:

- neither of two complexes was actually deposited on the carriers, and they were removed from the system upon washing of the solids
- the complexes were deposited on the carriers in their intact chemical forms
- grafting of the complexes (i.e. some type of reaction with surface protons leading to creation of new chemical bonds) did take place yet was undetectable by means of GC

Concerning the third option, it must be noted here that in both cases interactions with protons of POMs leading to isobutene (coming from methallyl protonation) release were quietly assumed. Now, isobutene polymerization is known to take place on the surface of alumina, much less acidic support than POMs, even at room temperature [40-41], so it definitely should be taken into consideration when explaining the lack of gas release. Another possibility is the reaction of protons with Cl^- ligands or COD protonation (for Pd and Ru complexes, respectively). Unfortunately, no analytical test for the presence of HCl (like reaction with an aqueous solution of $AgNO_3$) was made.

Results of elemental analyses presented in Table X enable to dismiss the first hypothesis – some fraction of metal species introduced to the systems actually remained there, bound to the surface of the supports even after consecutive washings (column 6).

Table X. Elemental composition of the samples.

sample code	**nominal composition**	**n H^+ [mol]**	**n M^{2+} used [mol]**	**calculated %M**	**experimental %M**	**n M^{2+} deposited [mol]**
24	$Ru(Meallyl)_2COD$ / $Cs_{1.7}H_{1.3}PW_{12}O_{40}$	4.19 x10^{-4}	3.13 x10^{-4}	2.87	1.07	1.17 x10^{-4}
25	$Ru(Meallyl)_2COD$ / $Cs_{2.4}H_{0.6}PMo_{12}O_{40}$	2.80 x10^{-4}	4.69 x10^{-4}	3.58	1.31	1.72 x10^{-4}
26	$Pd_2(Meallyl)_2Cl_2$ / $Cs_{1.7}H_{1.3}PW_{12}O_{40}$	4.19 x10^{-4}	5.08 x10^{-4}	4.90	3.02	3.13 x10^{-4}

Number of deposited metal species are lower than the number of available protons. Some of them may be "hidden" in the micropores of the supports and thus never come in contact with organometallic compounds, too bulky to penetrate inside. Nevertheless, even if the reactions occur, nothing is known about their stoechiometries, so all assumptions must be made with caution.

^{13}C SS NMR experiments were then carried out to obtain more information about the structure of deposited metal species (see Fig. 12 and 14).

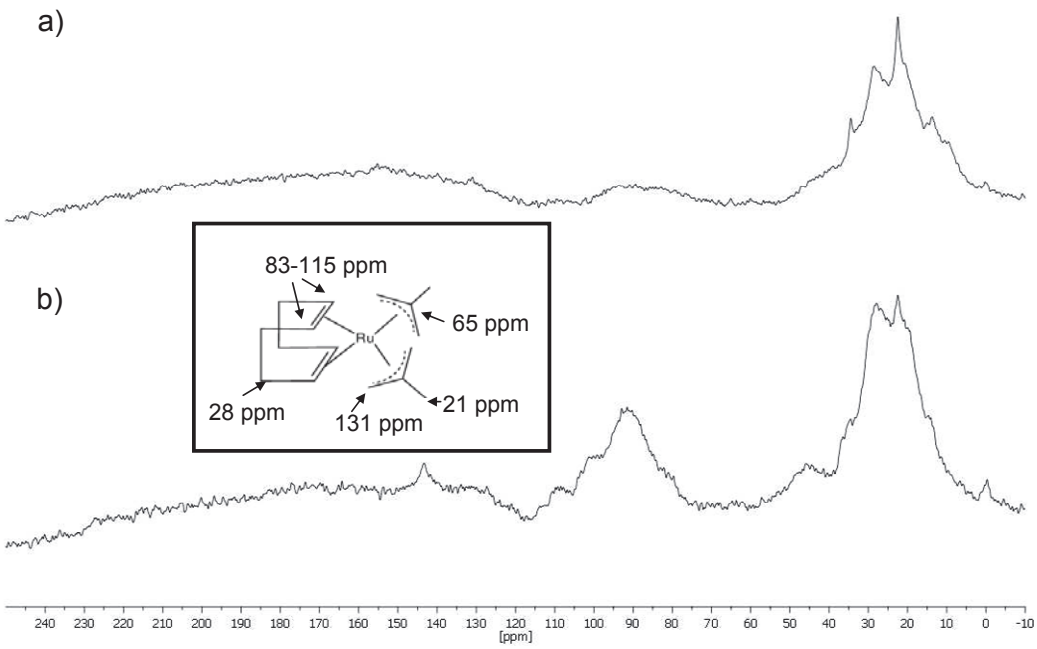

Figure 12. ^{13}C SS NMR spectra of: a) $Ru(Meallyl)_2COD/Cs_{1.7}H_{1.3}PW_{12}O_{40}$ and b) $Ru(Meallyl)_2COD/Cs_{2.4}H_{0.6}PMo_{12}O_{40}$. Chemical shifts of carbon atoms of the parent compound are given in the inset.

Both spectra in Figure 12 exhibit a large band between 10 - 40 ppm with multiple shoulders. Another band – at around 90 ppm, corresponding to olefinic carbons of coordinated COD, is more pronounced in the case of the molybdic polyoxometalate support (Fig. 12 b). Minor peaks at around 140 ppm are also visible. The chemical shifts of the carbon atoms of the parent compound correspond well with the observed bands. The large band between 10-40 ppm is most probably a superposition of peaks of the methyl group of methallyl ligand and carbons of the solvent used for grafting - *n*-pentane. In addition, according to polyisobutene

spectrum [42-43] and its signals attribution taken from the literature [44] and given in Table XI, polymer peaks could contribute as well to the large band. Small features at around 140 ppm could be polymer-related as well. Still, any interpretation of the spectra is far from being conclusive.

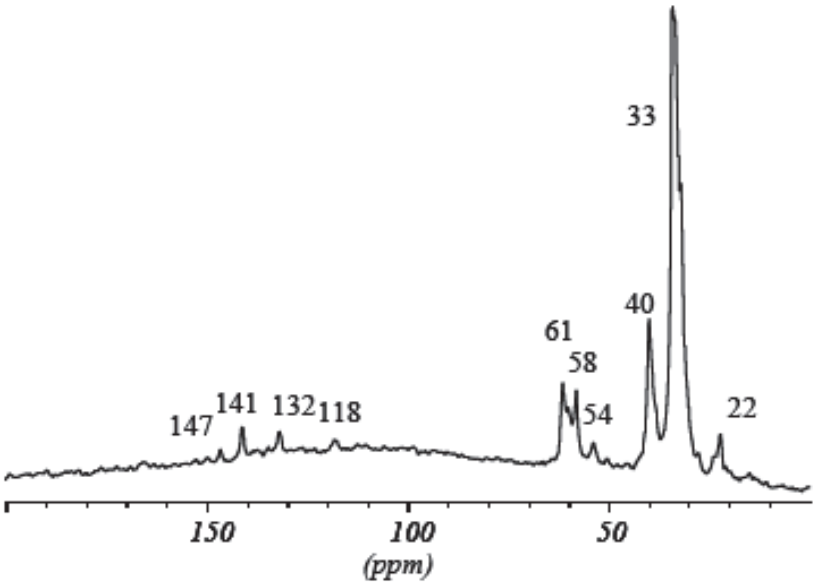

Figure 13. ^{13}C SS NMR spectrum of polyisobutene. Reproduced with permission after [42].

Table XI. Polyisobutene ^{13}C NMR signals (after [44]).

type of carbon atom	peak position [ppm]				
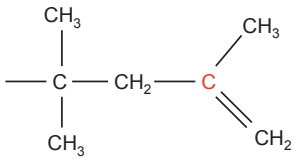	141, 147	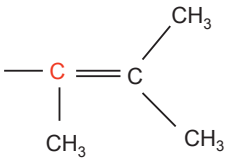	132	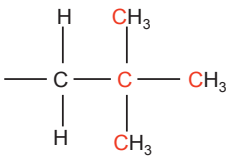	33
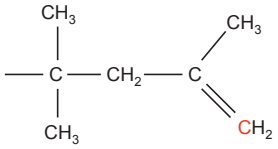	118	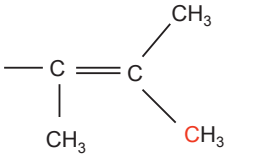	22	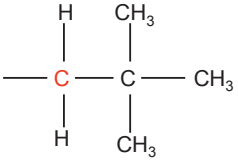	54, 58, 61
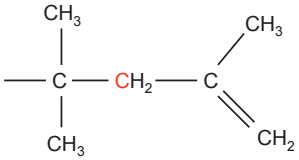	40				

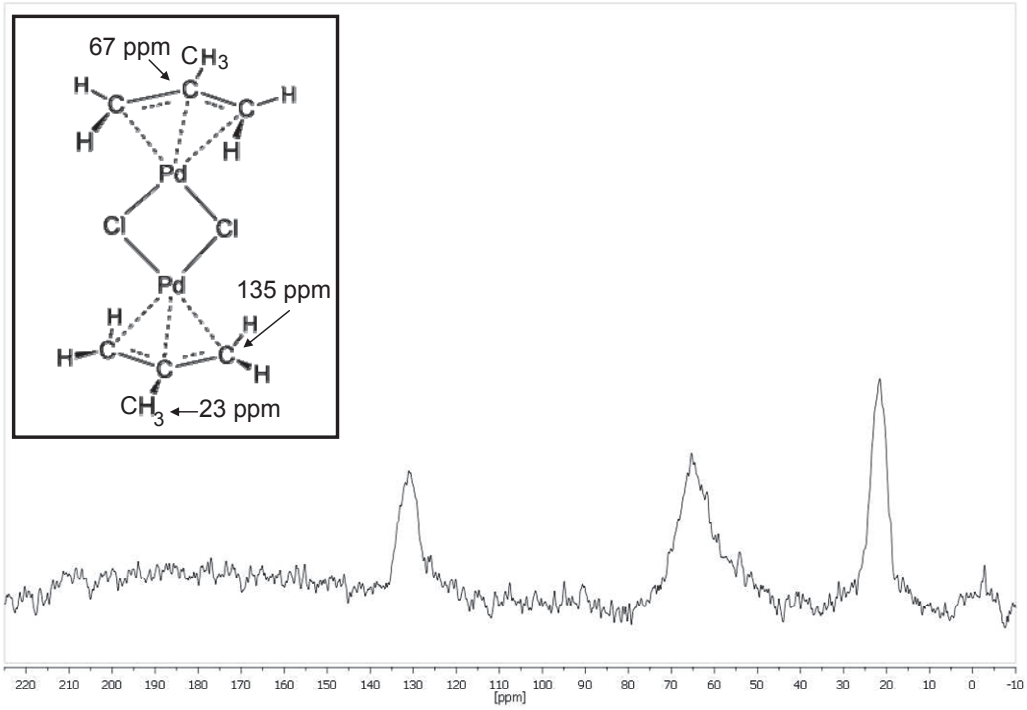

Figure 14. ^{13}C SS NMR spectrum of $Pd_2(Meallyl)_2Cl_2/Cs_{1.7}H_{1.3}PW_{12}O_{40}$. Chemical shifts of carbon atoms of the parent compound are given in the inset.

Interpretation of a spectrum of $Pd_2(Meallyl)_2Cl_2/Cs_{1.7}H_{1.3}PW_{12}O_{40}$ in Fig. 13 seems more straightforward - positions of all the observed peaks correspond exactly with the positions of peaks in the starting compound and no new bands were detected. At least part of the dimeric palladium(II) compound must have been therefore deposited on the support in its intact form. The question remains whether some proton-driven decomposition occurred as well, followed by isobutene release and polymerization or HCl release.

In short, the SOMC methodology can furnish extremely useful information on the surface-metal species interactions, provided that the metal precursors have been properly chosen. The cases of both Pd and Ru complexes presented in this part turned out to give more questions than answers, due to various possible reaction paths that could occur upon their grafting. The presented characterization of surface entities is of course far from completion and use of other physicochemical techniques (like e.g. EXAFS for the determination of their local environments or XANES for oxidation degrees) can be envisaged. Some idea about processes taking place on the surface of the support may also be gathered from performing the reactions of given organometallic compounds with bulk polyoxometalates in the liquid phase. The

striking difference the precursors makes will be made clear by comparison with the extremely interesting results obtained for the grafting of platinum dialkyl complex $PtMe_2COD$ on exactly the same cesium salts of polyoxometalates, which are addressed apart (see Part B of this Chapter).

3.A.4 Conclusions

Three ways of derivatization of inorganic salts of polyoxometalates have been explored in order to obtain novel heterogenous catalysts: by impregnation with other polyoxometalates, with inorganic salts of late transition metal atoms or by grafting of organometallic complexes (SOMC methodology). From the general point of view, high degree of hydration of bulk polyoxometalates causes problems with controlling the supports stoechiometry, especially the quantity of preserved surface protons. To overcome this difficulty either a more methodical approach is needed (preliminary complete dehydration of POMs and their consecutive dissolution in water and precipitation) either some refinements of trail and error method should be made. The attempts of SOMC functionalization of this kind of supports, presented here for the first time, turned out to be somewhat tricky as well. Proper choice of organometallic complexes for grafting was evidenced to be a key factor to allow unequivocal characterization of species obtained on the surface and to comply with the requirements of the "single-site" approach.

3.A.5 References

(1) Yang, Z. L.; Lu, Y. F.; Yang, Z. Z. *Chem. Commun.* **2009**, 2270.

(2) White, R. J.; Budarin, V.; Luque, R.; Clark, J. H.; Macquarrie, D. J. *Chem. Soc. Rev.* **2009**, *38*, 3401.

(3) Schatz, A.; Reiser, O.; Stark, W. J. *Chem.-Eur. J.* **2010**, *16*, 8950.

(4) Mehdi, A.; Reye, C.; Corriu, R. *Chem. Soc. Rev.* **2011**, *40*, 563.

(5) Kanatzidis, M. G. *Adv. Mater.* **2007**, *19*, 1165.

(6) Mizuno, N.; Misono, M. *Chem. Rev.* **1998**, *98*, 199.

(7) Zhang, J.; Ohnishi, R.; Kamiya, Y.; Okuhara, T. *J. Catal.* **2008**, *254*, 263.

(8) Atia, H.; Armbruster, U.; Martin, A. *J. Catal.* **2008**, *258*, 71.

(9) Dupont, P.; Lefebvre, F. *J. Mol. Catal. A-Chem.* **1996**, *114*, 299.

(10) Cuentas-Gallegos, A. K.; Frausto, C.; Ortiz-Frade, L. A.; Orozco, G. *Vib. Spectrosc.* **2011**, *57*, 49.

(11) Cuentas-Gallegos, A. K.; Zamudio-Flores, A.; Casas-Cabanas, M. *J. Nano Res.* **2011**, *14*, 11.

(12) Okuhara, T.; Yamada, T.; Seki, K.; Johkan, K.; Nakato, T. *Micropor. Mesopor. Mat.* **1998**, *21*, 637.

(13) Yamada, T.; Johkan, K.; Okuhara, T. *Micropor. Mesopor. Mat.* **1998**, *26*, 109.

(14) Okuhara, T.; Watanabe, H.; Nishimura, T.; Inumaru, K.; Misono, M. *Chem. Mat.* **2000**, *12*, 2230.

(15) Yamada, T.; Okuhara, T. *Langmuir* **2000**, *16*, 2321.

(16) Yoshimune, M.; Yoshinaga, Y.; Okuhara, T. *Micropor. Mesopor. Mat.* **2002**, *51*, 165.

(17) Berndt, S.; Herein, D.; Zemlin, F.; Beckmann, E.; Weinberg, G.; Schütze, J.; Mestl, G.; Schlögl, R. *Ber. Bunsen. Phys. Chem.* **1998**, *102*, 763.

(18) Misono, M.; Okuhara, T. *Chemtech* **1993**, *23*, 23.

(19) Micek-Ilnicka, A. *J. Mol. Catal. A-Chem.* **2009**, *308*, 1.

(20) Mays, T. J. *Studies in Surface Science and Catalysis* **2007**, *160*, 57.

(21) Barrett, E. P.; Joyner, L. G.; Halenda, P. P. *J. Am. Chem. Soc.* **1951**, *73*, 373.

(22) Gregg, S. J.; Sing, K. S. W. *Adsorption, Surface area and Porosity*; 2nd ed. ed.; Academic Press: London, 1982.

(23) Bajuk-Bogdanovic, D.; Holclajtner-Antunovic, I.; Todorovic, M.; Mioc, U. B.; Zakrzewska, J. *J. Serb. Chem. Soc.* **2008**, *73*, 197.

(24) Lindman, B.; Forsen, S.; Harris, R. K., Mann, B. E., Eds.; Academic Press: London, 1978, p 129.

(25) Langford, J. I.; Wilson, A. J. C. *J. Appl. Crystallogr.* **1978**, *11*, 102.

(26) Mizuno, N.; Kamata, K. *Coord. Chem. Rev.* **2011**, *255*, 2358.

(27) Poppl, A.; Manikandan, P.; Kohler, K.; Maas, P.; Strauch, P.; Bottcher, R.; Goldfarb, D. *J. Am. Chem. Soc.* **2001**, *123*, 4577.

(28) Pettersson, L.; Andersson, I.; Selling, A.; Grate, J. H. *Inorg. Chem.* **1994**, *33*, 982.

(29) Luzgin, M. V.; Kazantsev, M. S.; Volkova, G. G.; Wang, W.; Stepanov, A. G. *J. Catal.* **2011**, *277*, 72.

(30) Mizuno, N.; Ishige, H.; Seki, Y.; Misono, M.; Suh, D. J.; Han, W.; Kudo, T. *Chem. Commun.* **1997**, 1295.

(31) Min, J. S.; Ishige, H.; Misono, M.; Mizuno, N. *J. Catal.* **2001**, *198*, 116.

(32) Putaj, P.; Lefebvre, F. *Coord. Chem. Rev.* **2011**, *255*, 1642.

(33) Kato, M.; Kato, C. N. *Inorg. Chem. Comm.* **2011**, *14*, 982.

(34) Coperet, C.; Chabanas, M.; Saint-Arroman, R. P.; Basset, J. M. *Angew. Chem.-Int. Edit.* **2003**, *42*, 156.

(35) Coperet, C. *Chem. Rev.* **2010**, *110*, 656.

(36) Augustine, R. L.; Tanielyan, S. K.; Mahata, N.; Gao, Y.; Zsigmond, A.; Yang, H. *Appl. Catal. A-Gen.* **2003**, *256*, 69.

(37) Augustine, R. L.; Goel, P.; Mahata, N.; Reyes, C.; Tanielyan, S. K. *J. Mol. Catal. A-Chem.* **2004**, *216*, 189.

(38) Legagneux, N.; Jeanneau, E.; Thomas, A.; Taoufik, M.; Baudouin, A.; de Mallmann, A.; Basset, J. M.; Lefebvre, F. *Organometallics* **2011**, *30*, 1783.

(39) Legagneux, N.; de Mallmann, A.; Grinenval, E.; Basset, J. M.; Lefebvre, F. *Inorg. Chem.* **2009**, *48*, 8718.

(40) Cai, T. X.; Qu, J. P.; Wong, S. Q.; Song, Z. Y.; Min, H. *Appl. Catal. A-Gen.* **1993**, *97*, 113.

(41) Lavrenov, A. V.; Duplyakin, V. K. *Kinet. Catal.* **2009**, *50*, 235.

(42) Tosin, G., Universite Claude Bernard - Lyon I, 2006.

(43) Tosin, G.; Santini, C. C.; Basset, J. M. *Top. Catal.* **2009**, *52*, 1203.

(44) Toman, L.; Spevacek, J.; Vlcek, P.; Holler, P. *J. Polym. Sci. Pol. Chem.* **2000**, *38*, 1568.

Chapter 3

Part B

Polyoxometalate-induced M-C bond cleavage in an alkyl Pt(II) complex

* This part will be submitted as a research article and is reproduced here accordingly.

POLYOXOMETALATE-INDUCED M-C BOND CLEAVAGE IN AN ALKYL Pt(II) COMPLEX

Piotr PUTAJ, Anne BAUDOUIN, Frédéric LEFEBVRE*

Université de Lyon ICL, C2P2 UMR 5265 (CNRS – CPE – Université Lyon 1) LCOMS – CPE Lyon, 43 Boulevard du 11 Novembre 1918 F-69616, Villeurbanne, France
E-mail : lefebvre@cpe.fr

Abstract

Grafting of the dimethyl platinum(II) cyclooctadiene complex on the surface of self-supported polyoxometalates results in methane and ethane release. The overall quantities of the evolved gases depend greatly on the solvent used for the reaction while the methane to ethane ratio depends on the polyoxometalate. A mechanism of oxidative addition/reductive elimination with competition between C-H and C-C coupling on the metal centre is proposed to explain the observed phenomena.

Keywords

polyoxometalates, alkyl-platinum(II) complex, reductive elimination, mechanism

3.B.1 Introduction

The direct transformation of alkanes to alcohols, with the Holy Grail of chemistry - methane to methanol partial oxidation, still remains a challenge [1]. Not surprisingly, the remarkably selective catalytic systems based on Pt(II)/Pt(IV) species proposed by Shilov [2] and later on by Periana [3] attracted a considerable interest of the scientists. Undertaken studies shed some light on a multiple-step mechanism [4-6]. The crucial first stage is the C-H activation, when

the alkane reacts with the Pt(II) centre to yield an alkylplatinum(II) intermediate [7-8]. Insights about this step are however more easily obtained by studying the reverse process of cleavage of M-C σ-bond of alkylplatinum(II) complexes in presence of electrophiles. Two main reaction pathways yielding the same products have been considered: either direct attack of an electrophile on a Pt-C bond according to the classical S_E2 mechanism or an oxidative addition to the metal centre and concomitant reductive elimination of the alkane. Contradictory evidence to support both hypotheses has been put forward, mostly based on indirect methods of investigation of the problem, e.g. while kinetic studies on $[PtR_2(PR_3)_2]$ suggested the S_E2 way [9], studies on selectivity of cleavage of alkyl and arylphosphine Pt(II) complexes supported rather the oxidative addition/reductive elimination process [10]. Later on alkylhydridoplatinum(IV) intermediates were detected and characterized in solution by means of low temperature ^1H NMR: in the reactions of $[PtMe_2(N\text{-}N)]$ with HX, where N-N = bpy, phen and X = Cl, Br, I [11] and in the reactions of $[PtCl(CH_2Ph)(tmeda)]$ with HCl, where tmeda = tetramethylethylenediamine [12]. These octahedral species in *trans* stereochemistry of H and X groups towards metal centre were claimed to be created in a rapid and reversible oxidative addition step. As they are unstable at room temperature, they decompose readily through release of CH_4. In both cases preliminary Pt-X bond dissociation yielding a five-coordinate cationic intermediate was proposed to precede the reductive elimination. Molecular models of such cationic penta-coordinated compounds, resistant to decomposition in solutions at room temperature for a couple of hours, were consecutively obtained [13-14]. Recent calculations tend however to revise some of these notions [15]. First of all, the mechanism is greatly influenced by both ligands and solvent properties (nucleophilicity, steric hindrance) and any a priori issued conclusions about reaction pathways are risky. Moreover, six coordinate platinum hydride intermediates are shown to result also from a hydride migration to the metal center from σ-complex methane molecule in addition to concerted proton attack on metal centre. Their detection cannot be perceived then as a definite proof of the oxidative addition/reductive elimination route.

From a more general point of view, numerous transition metal alkyl-alkyl, alkyl-hydrido, hydrido-hydrido or alkyl-halo complexes undergo reductive elimination, e.g. upon pyrolysis, giving products of coupling of the mentioned groups, often in a competitive manner [16-19]. The final stage involves a decrease of the metal oxidation state and so the presence of oxidizers will enhance the coupling. In a classical example the rhodium complex $(Cp^*)RhMe_2(DMSO)$ decomposes in acid medium to give mostly methane with a small

amount of ethane (1–5 %). The introduction into the system of oxidizers, such as $AgBF_4$ or iodine, increases drastically the percentage of the ethane [20].

The methane oxidation system described some years ago by Neumann et al. [21] spurred our research interest towards combining the chemistry of polyoxometalates [22] and organometallic platinum compounds. Our previous work showed methane evolution during platinum complexes grafting on silica-supported polyoxometalates [23] and formation of cationic alkyl-platinum(II) species weakly bound to polyanions via electrostatic interactions. As such they can be perceived as models for methane oxidation intermediates on Pt centers. In this study we report the first examples of polyoxometalates-induced cleavage of alkyl-Pt(II) complexes leading to a competitive creation of new C-H and C-C bonds. The oxidative addition/reductive elimination sequence of events is presented and factors influencing the overall efficiency of the observed processes are discussed in detail.

3.B.2 Experimental part

All manipulations were performed under vacuum or Ar atmosphere using standard Schlenk techniques.

Materials. Phosphomolybdic acid $H_3PMo_{12}O_{40}.xH_2O$ (99+%, Aldrich), phosphotungstic acid $H_3PW_{12}O_{40}.xH_2O$ (99+%, Aldrich), cesium carbonate Cs_2CO_3 (99%, Aldrich) and $PtMe_2COD$ (99%, Strem) were used as received.
$H_6PV_3Mo_9O_{40}$ was synthesized from MoO_3 (99%, Acros), V_2O_5 (99.6%, Acros) and phosphoric acid H_3PO_4 (85%, Aldrich) according to Berndt et al. [24].
All solvents, distilled and kept on dehydrated molecular sieves, were degassed prior to use.

Preparation of self-supported polyoxometalates. Cesium salts of polyoxometalates showing high specific surface areas [25] and with the general formula $Cs_xH_{3-x}PZ_{12}O_{40}$, where Z = W or Mo, were prepared as follows: A stoechiometric amount of Cs_2CO_3 was added under vigorous stirring to an aqueous solution of the desired polyacid ($H_3PW_{12}O_{40}$, $H_3PMo_{12}O_{40}$), resulting in effervescence and immediate precipitation of a microcrystalline solid. Stirring was continued until complete evaporation of the solvent at room temperature. The powder was then collected without washing and ground in the mortar.
The saturated salt $Cs_3PMo_{12}O_{40}$ was synthesized by a similar manner but after precipitation

and aging for a couple of hours, the solution was centrifuged and the mother liquor decanted and replaced with a fresh portion of an aqueous solution of Cs_2CO_3. The centrifugation was repeated and the mother liquor replaced with distilled water. The centrifugation-decantation cycle was repeated 3 more times and then the solid was collected, dried and ground in the mortar.

The composite material with the formula $H_6PV_3Mo_9O_{40}/Cs_3PMo_{12}O_{40}$ was synthesized as follows: In a first step the precipitation of $Cs_3PMo_{12}O_{40}$ was performed as described above but after half an hour of stirring at room temperature, the appropriate amount of $H_6PV_3Mo_9O_{40}$ was added to the reaction mixture. The resulting powder was gathered after the evaporation of the solvent, without any washing. The quantity of vanadomolybdic acid was calculated so as to create a monolayer on the surface of $Cs_3PMo_{12}O_{40}$.

All these supports were treated under high vacuum (10^{-5} Torr) for 2 hours at 200 °C to dehydrate polyoxometalates and afterwards heated for another 2 hours at 200 °C under dry O_2 to reoxidize the clusters that might have been reduced upon the previous manipulations.

Finally, the samples were fully characterized by means of elemental analyses, BET and DRX techniques to establish their specific surface values, surface proton density and degree of dispersion of the acidic clusters on the microcrystals of the salts.

Grafting reaction of Pt complex on the aforementioned supports. In a typical procedure 0.25 g of a support and a stirring bar were introduced in a Schlenk with a septum. The Schlenk was evacuated at room temperature until a high vacuum (10^{-5} Torr) was reached. A known quantity of reference gas (2 ml of C_3H_8) was then added through the septum. 0.05 g of Pt complex was dissolved in 5 ml of solvent (CH_2Cl_2 or *n*-pentane) under Ar. The resulting solution was transferred into the reaction vessel with a syringe, again via the septum. After 24 hours of stirring at room temperature all volatile compounds were condensed in another vessel of known volume and allowed to equilibrate overnight. The gas phase was then analyzed on a Hewlett-Packard 5890 series II gas chromatograph equipped with a flame ionization detector and a KCl/Al_2O_3 on fused silica column (50 m x 0.32 mm).

The solids were washed three times with small portions (10 ml) of an appropriate solvent, dried under vacuum and transferred in the glovebox. They were then fully characterized by various physico-chemical methods.

Kinetic study of the grafting reaction. The protocol used for kinetic studies was similar to that described above. However, a real time gas phase evolution was carried out. Direct

sampling from the reaction vessel was preceded by short periods (~3 min.) of equilibration when stirring was turned off. Three injections were taken at each time point. The gas phase was analyzed by means of a GC with FID detector. The detector response was compared with calibration curves prepared previously, thus leading to quantification of the amount of released gases and tracing of the kinetic curves.

For preparation of the calibration curves, the same Schlenk vessel with septum and stirring bar were used. 0.25 g of the support was added to the vessel and put under high vacuum (10^{-5} Torr). Then 2 ml of C_3H_8 and 5 ml of the desired solvent were introduced in the Schlenk. Small portions (~400 µl) of the two target gases (CH_4 or C_2H_6) were added successively with a syringe, followed by 10 min. periods of stirring and 3 min. periods of equilibration with stirring turned off. Finally, the gas phase was analyzed by GC.

Reaction of the platinum complex with bulk polyoxometalates. Bulk, purely acidic polyoxometalates $H_3PW_{12}O_{40}$ and $H_3PMo_{12}O_{40}$ were treated under high vacuum at 200 °C for 2 hours and reoxidized in dry O_2 atmosphere at 200 °C for another 2 hours. Stoechiometric quantities of a given polyacid and of the platinum complex were then introduced into a Young tube and dry DMSO-d_6 was added. Progress of the reaction was followed by multinuclear (^1H, ^{13}C, ^{31}P, ^{195}Pt) solution NMR.

Physico-chemical characterization techniques. All compounds were sealed in glass tubes under vacuum and sent to CNRS Central Analysis Department of Solaize in order to establish their elemental compositions.

The surface area of the samples was measured by BET method with an N_2 adsorption system (Micromeritics ASAP-2000) after pretreatment under vacuum at 473 K for 2 h.

X-ray diffraction patterns were recorded with an X-ray Bruker D8 Advance diffractometer using CuKα radiation.

The solution NMR spectra were recorded on a AM-400 Bruker spectrometer. All chemical shifts were measured relative to the residual ^1H or ^{13}C resonance in deuterated DMSO used as solvent (2.50 ppm for ^1H and 39.5 ppm for ^{13}C). The ^{31}P chemical shifts were measured relative to 85% H_3PO_4. The ^{195}Pt chemical shifts were measured relative to $PtMe_2COD$ in DMSO.

3.B.3 Results and discussion

3.B.3.1 Grafting of alkyl Pt(II) complex on polyoxometalate supports. As previously reported in [23], the reaction of alkylPt(II) complexes with silica-supported tungstic polyoxometalates e.g. $H_4SiW_{12}O_{40}/SiO_2$, results in an evolution of methane. In this study we enlarged the scope of the investigated polyoxometalates turning our attention also to molybdic and vanadomolybdic clusters, well known for combining both acidic and redox properties.

For this particular study we decided to work with self-supported polyoxometalates under the form of their partially saturated cesium salts instead of silica-supported clusters. By doing so we were able to take advantage from their increased specific surface areas (~100-150 m^2/g) as well as from the presence of surface protons [25] able to react with Pt complexes, and at the same time to eliminate any possibility of transfer of organometallic moieties from the polyoxometalates to the silica surface, a phenomenon that had already been observed upon grafting of organotin compounds on silica-supported polyanionic clusters [26]. Unfortunately, salts of vanadomolybdic clusters are exceptional in the first respect, exhibiting significantly lower specific surface values. To overcome this technical difficulty we deposited them in form of a monolayer on fully saturated salts of phosphomolybdic acid, thus making composite materials like e.g. $H_6PV_3Mo_9O_{40}/Cs_3PMo_{12}O_{40}$ mimicking the desired systems as much as possible. Powder diffraction images of these so-prepared materials confirmed even distribution of vanadomolybdic clusters over the phosphomolybdic supports.

$PtMe_2COD$ was chosen for the grafting experiments as a typical example of alkylPt(II) complexes. All the gathered data about gas evolution during reactions of polyoxometalates with $PtMe_2COD$ in various solvents are listed in Table I.

Table I. Gas release upon reactions of various self-supported polyoxometalates with $PtMe_2COD$ in CH_2Cl_2 or *n*-pentane.

entry	support	solvent	V CH_4 [ml]	V C_2H_6 [ml]	CH_4/C_2H_6 [mol/mol]	n H^+ [mol]	% H^+ reacted	n Pt(II) [mol]	% Pt(II) reacted
1	$Cs_{1.7}H_{1.3}PW_{12}O_{40}$	CH_2Cl_2	1.86	-	-	1.05 x10^{-4}	71	1.50 x10^{-4}	50
2		*n*-pentane	0.95	-	-		37		26
3	$Cs_{2.35}H_{0.65}PMo_{12}O_{40}$	CH_2Cl_2	0.90	0.30	75/25	0.76 x10^{-4}	63		32
4		*n*-pentane	0.45	0.10	82/18		29		15
5	$Cs_3PMo_{12}O_{40}$	CH_2Cl_2	0.10	0.05	66/33	-	-		4
6	$H_6PV_3Mo_9O_{40}$/ $Cs_3PMo_{12}O_{40}$	CH_2Cl_2	0.50	0.49	50/50	0.98 x10^{-4}	41		27
7		*n*-pentane	0.37	0.27	58/42		22		17

As in the case of silica-supported polyoxometalates, the grafting reaction of $PtMe_2COD$ on the cesium salts of polyoxometalates is accompanied by a gas release. For $Cs_{1.7}H_{1.3}PW_{12}O_{40}$ gas phase analysis shows only presence of methane (entries 1 & 2). However, when $Cs_{2.35}H_{0.65}PMo_{12}O_{40}$ was used a considerable proportion of ethane is also detected (entries 3 & 4). The polyoxometalates are well-known to combine acidic and redox properties, to a various extent. The tungstic compounds are more acidic while the molybdic ones exhibit better redox affinities. Upon introduction of the solution of $PtMe_2COD$ to the reaction vessel containing $Cs_{2.35}H_{0.65}PMo_{12}O_{40}$ an instantaneous colour change from yellow to deep green is observed, which is the outcome of reduction of yellow Mo(VI) to deep blue Mo(V). In contrast, no colour change was observed during the reaction with the corresponding tungstic compound. Thus the major difference in behaviour of $PtMe_2COD$ when exposed to the two types of polyoxometalates is related to their different redox (and acidic, see later on) properties. If so, the grafting reaction of $PtMe_2COD$ on the composite support $H_6PV_3Mo_9O_{40}/Cs_3PMo_{12}O_{40}$ should further shift the ratio of evolved gases towards ethane as replacing molybdenum atoms with vanadium in the polyoxometalate structure makes them more redox active. The entries 6 & 7 in Table I confirm this reasoning.

There is however another trend which is clearly visible when comparing series of entries 1, 3 & 6 with 2, 4 & 7 in Table I. When the acidic strength of the polyoxometalates decreases which is not directly related with the number of surface protons, see [27]) when passing from

tungstic via molybdic to vanadomolybdic clusters, the overall quantity of evolved gases tends to drop as well, although the number of available protons is not a limiting factor in this case (see columns 7 & 8 of Table I). Even for $Cs_{1.7}H_{1.3}PW_{12}O_{40}$, which is the strongest acid of the series, the reaction does not proceed with 100% yield. It has been established however that upon thermal treatment of this kind of materials protons and cesium cations migrate through the solid to create an uniform solid state solution [25]. Some of the protons "hidden" in the microcavities of the support would be therefore inaccessible to the platinum complex.

Finally, a comparison of the grafting reactions of $PtMe_2COD$ on the same supports in CH_2Cl_2 and *n*-pentane allows to distinguish a so to say "solvent factor". The polyoxometalates were recently shown to activate simple alkanes even at room temperature [28]. An alkane solvent like *n*-pentane is therefore expected to compete with the organometallic complex and to hinder reactions and the consecutive gas release. Indeed, in each case, when the grafting reaction is performed in *n*-pentane, a drastic decrease of the amount of evolved gases was observed when compared to dichloromethane.

Generally speaking, upon reaction of $PtMe_2COD$ with the polyoxometalate the C-H and C-C bond formation processes occur, in a competitive manner and are controlled to some extent by the redox properties of the clusters. To the best of our knowledge this is the first time that such a behaviour of an organometallic complex towards polyoxometalates is observed.
In order to better understand how methane and ethane are formed, we studied the kinetics of their release. For this purpose the grafting reaction of $PtMe_2COD$ on $Cs_{2.35}H_{0.65}PMo_{12}O_{40}$ in CH_2Cl_2 was monitored directly by GC as a function of time. The results are shown in Figure1.

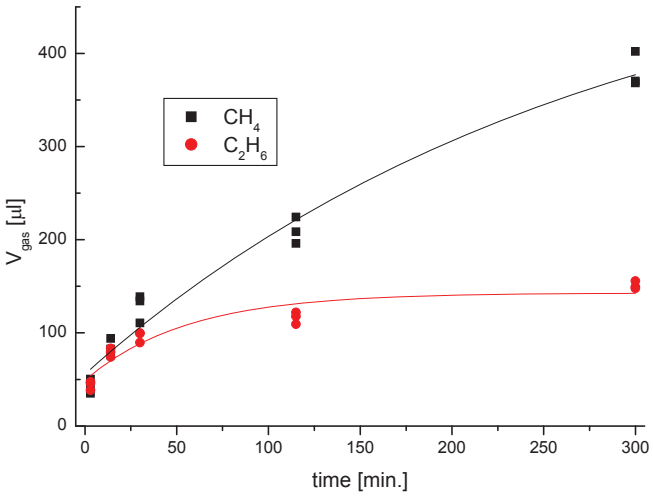

Figure 1. Gas phase evolution as a function of time during the reaction of $PtMe_2COD$ with $Cs_{2.35}H_{0.65}PMo_{12}O_{40}$ in CH_2Cl_2. Black squares = methane. Red circles = ethane. Three injections were taken at each time point.

Clearly the two competing processes, i.e. methane and ethane formation, take place at different time scales. As already mentioned, the reduction of Mo(VI) to Mo(V) related with a distinct color change proceeds very rapidly after introduction of the platinum complex. Accordingly, the ethane evolution is almost finished already after 30 minutes of stirring. It must be noted that the Mo(VI) species consumption is never complete, as upon grafting the support stays green and never turns blue (which is typical for completely reduced Mo(V) species). The methane formation, on the other hand, is a relatively slow process which is completed only after more than 24 hours.

3.B.3.2 ^{195}Pt NMR experiments. To get some insights about the observed processes mechanisms and the nature of the obtained products multinuclear solution NMR experiments were carried out. For this purpose, the reaction between $PtMe_2COD$ and bulk dehydrated polyoxometalates was performed in deuterated DMSO as solvent. The cesium salts of polyoxometalates are insoluble in DMSO. What is one of their main advantages when they are used as supports for the deposition of organometallic complexes and other chemical moieties turns out to be the greatest hindrance for studies of consecutive stages of observed phenomena which are confined to the closest proximity of the surface. In order to obtain a reaction milieu as uniform as possible for solution NMR studies reactions of their bulk precursors need to be investigated. The hydrated polyoxometalates are known to dissolve

readily in a wide range of polar solvents. On the other hand, their thermal treatment, yielding them anhydrous, greatly narrows down the range of efficient solvents – virtually to DMSO alone. An unexpected difficulty of this approach was nevertheless encountered as $PtMe_2COD$, which is soluble in DMSO, undergoes a slow decomposition in this solvent by COD-DMSO ligand exchange, yielding $PtMe_2(DMSO)_2$, as shown by ^{195}Pt NMR (see Figure 2).

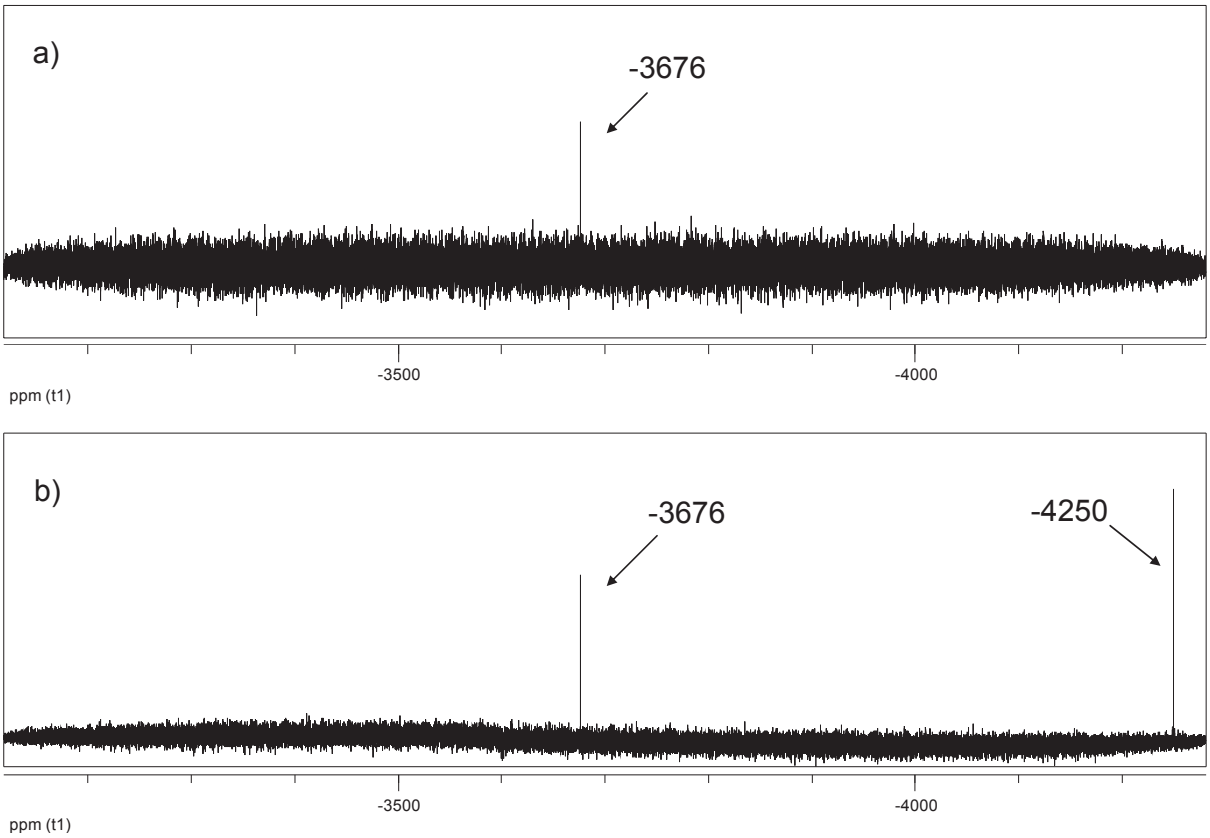

Figure 2. ^{195}Pt NMR spectra of $PtMe_2COD$ in DMSO: a) right after dissolution and b) after a couple of days of standing at room temperature.

The ^{195}Pt NMR spectrum of the freshly prepared solution of $PtMe_2COD$ in DMSO shows only one peak at -3676 ppm. After prolonged standing, however, a second peak at -4250 ppm appears and increases with time. The formation of this species is accompanied by the evolution of the free COD as detected in ^{1}H and ^{13}C NMR. As both compounds: $PtMe_2COD$ and $PtMe_2(DMSO)_2$ were reported to react with tungstic polyoxometalates with methane release, yielding quite similar products [23] two starting complexes reacting along two parallel routes must be taken into account when analyzing the NMR results.

^{195}Pt NMR spectrum of the reaction mixture of $PtMe_2COD$ with $H_3PW_{12}O_{40}$ does not

show any trace of the starting organometallic compound but two new peaks are detected at: -3967 and -4250 ppm (see Figure 3a). Recently we were able to identify and isolate the reaction product of $PtMe_2COD$ with $H_4SiW_{12}O_{40}$ in DMSO [23]. Its partially resolved crystal structure showed the presence of four organometallic cations counterbalancing the negative charge of a $[SiW_{12}O_{40}]^{4-}$ polyanion. In the cation Pt(II) is tetra-coordinated by one methyl group, one doubly-bound COD and a DMSO molecule filling the empty space in the coordination sphere of the metal. A similar structure was suggested for the reaction product of $PtMe_2(DMSO)_2$ with $H_4SiW_{12}O_{40}$ in the same solvent. Peaks corresponding to these two species were identified in the ^{1}H, ^{13}C and ^{195}Pt NMR spectra. As no major differences in reactivity are expected when $H_3PW_{12}O_{40}$ is used instead of $H_4SiW_{12}O_{40}$, we can tentatively assume that there is formation of a congener species $[PtMeCOD(DMSO)]^{+}$ and attribute the ^{195}Pt peak at -3967 ppm to it. The second peak at -4250 ppm comes from $PtMe_2(DMSO)_2$. The ^{31}P spectrum consists of a single peak at -14.4 ppm and demonstrates clearly that no polyanion decomposition takes place upon reaction with Pt complexes and that there is no direct bonding between the organometallic moiety and the polyoxometalates, as also observed in the case of $[PtMeCOD(DMSO)]_4SiW_{12}O_{40}$.

In the case of the reaction of $PtMe_2COD$ with $H_3PMo_{12}O_{40}$ five distinct ^{195}Pt resonances are observed at -3676 ppm, -3967 ppm, -4250 ppm, -4389 ppm and -4444 ppm (see Figure 3b). Two of these peaks at -3676 ppm and -4250 ppm are due to $PtMe_2COD$ and its reaction product with DMSO; $PtMe_2(DMSO)_2$, respectively. As the gas release studies showed methane formation upon grafting of $PtMe_2COD$ on $Cs_{2.35}H_{0.65}PMo_{12}O_{40}$, one of the products formed in presence of the molybdic polyoxometalates should be analogous (if not the same from the point of view of the organometallic moiety) to the one observed for the tungstic compounds. Indeed, peak at -3967 ppm fulfills these requirements. Out of two remaining signals (at -4389 ppm and -4444 ppm) one should in principle come from the moiety that is left after ethane release from the metal center. The other is possibly related to further decomposition of [PtMeCOD(DMSO)] fragment, through COD replacement with DMSO. So far, all the attempts to isolate and convincingly characterize the aforementioned specieshavefailed.

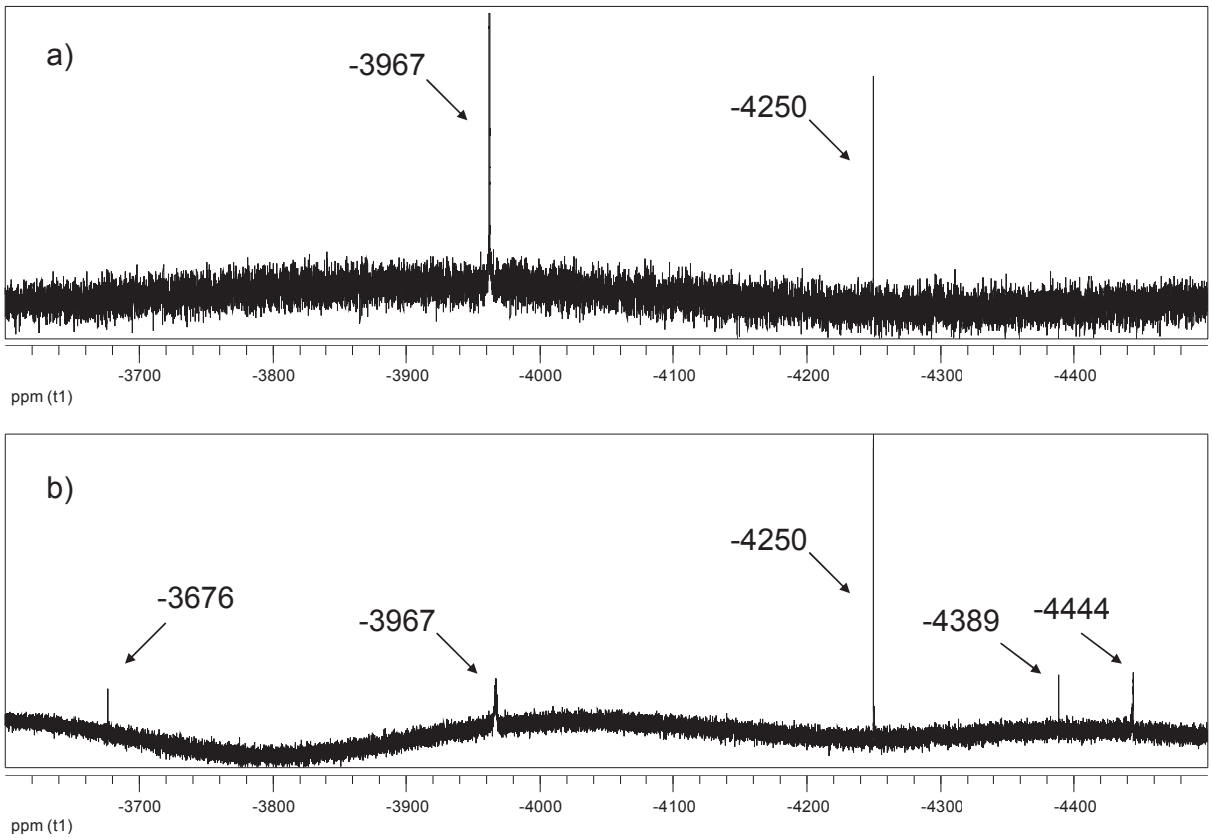

Figure 3. ^{195}Pt NMR spectra of the reaction products of $PtMe_2COD$ with: a) $H_3PW_{12}O_{40}$ and b) $H_3PMo_{12}O_{40}$ in DMSO.

3.B.3.3 Mechanistic aspects. A tentative mechanism of reactions of alkylPt(II) complex with tungstic and molybdic polyoxometalates could be envisaged based on all gathered experimental data. At the beginning an acidic proton of a polyoxometalate (tungstic or molybdic as both exhibit Brönsted acidity) attacks the Pt complex. If so, then no reaction and concomitant gas release should be observed in case of salts which are completely saturated with alkaline metal cations like e.g. $Cs_3PMo_{12}O_{40}$. Preparation of such compounds is a tricky matter though. These materials exhibit inherent microporosity and some acidic clusters could be "hidden" in the pores and effectively preserved from cation exchange. On the other hand, prolonged washing with highly concentrated solutions of alkaline salts can increase pH of mother liquor and lead to a partial decomposition of Keggin-type polyoxometalates yielding lacunary species. Precipitation followed by one washing with Cs_2CO_3 solution and three washings with distilled water seemed to us a reasonable compromise. Gas analysis of the grafting reaction of $PtMe_2COD$ on $Cs_3PMo_{12}O_{40}$ shows (entry 5 in Table I) some gas release anyhow. Compared with the results for the $Cs_{2.35}H_{0.65}PMo_{12}O_{40}$ sample it is a scanty amount though, and in our opinion originates from the presence of unsaturated acidic clusters in the

material. In addition, no visible colour change of POM salt was observed during the reaction, as expected from Mo(VI) reduction.

Two main routes proposed for a protonation step involve either direct attack of an electrophile on a Pt-C bond according to classical S_E2 mechanism or a proton-directed electron transfer from the metal, followed by an oxidation degree change form Pt(II) to Pt(IV) (see Scheme 1).

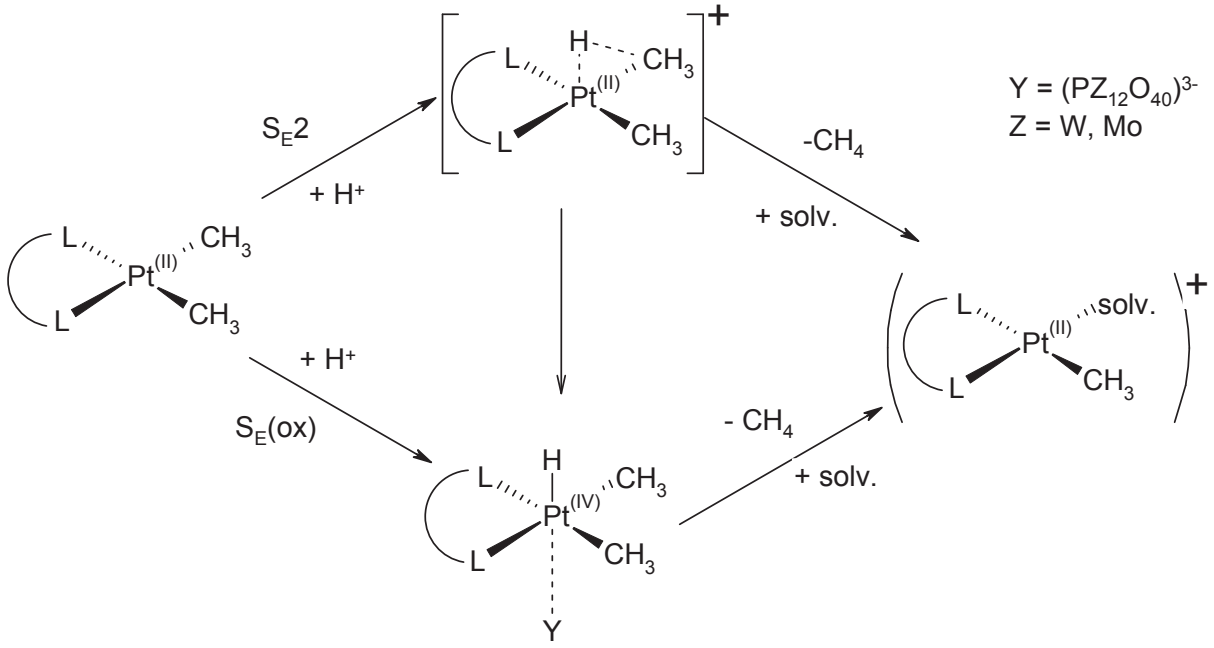

Scheme 1. Tentative mechanism of methane release from $PtMe_2COD$ in the presence of the polyoxometalates.

Although generally a detection of hexa-coordinated platinum(IV)-hydride intermediates was believed to be an indication of the latter pathway, recent calculations shown that they can be formed in both processes [15]. In addition, observation of these intermediates poses difficulties because of their instability and facile decomposition. Low temperature solution NMR experiments aiming at stabilization of reaction intermediates are impossible to be performed in DMSO because of its low freezing point. Other, more suitable solvents do not dissolve anhydrous polyoxometalates. When grafting reaction of $PtMe_2COD$ was performed on $Cs_{2.35}H_{0.65}PMo_{12}O_{40}$ in CD_2Cl_2 at -50 °C no hydride species were evidenced. At this point however, we cannot definitely exclude their formation and presence during the reaction.

In a concomitant reductive elimination process, regardless of the type of polyoxometalate present, C-H bond formation is followed by methane release and one solvent molecule fills the empty coordination site of the metal centre.

After the initial protonation step, pronounced redox properties of molybdic and

vanadomolybdic polyanions were evidenced to give rise to another reaction pathway, namely C-C coupling of two methyl groups resulting in ethane formation. Mechanistically speaking, two possibilities have to be taken into consideration: reaction occurring on one metal centre or dimerization (see Scheme 2).

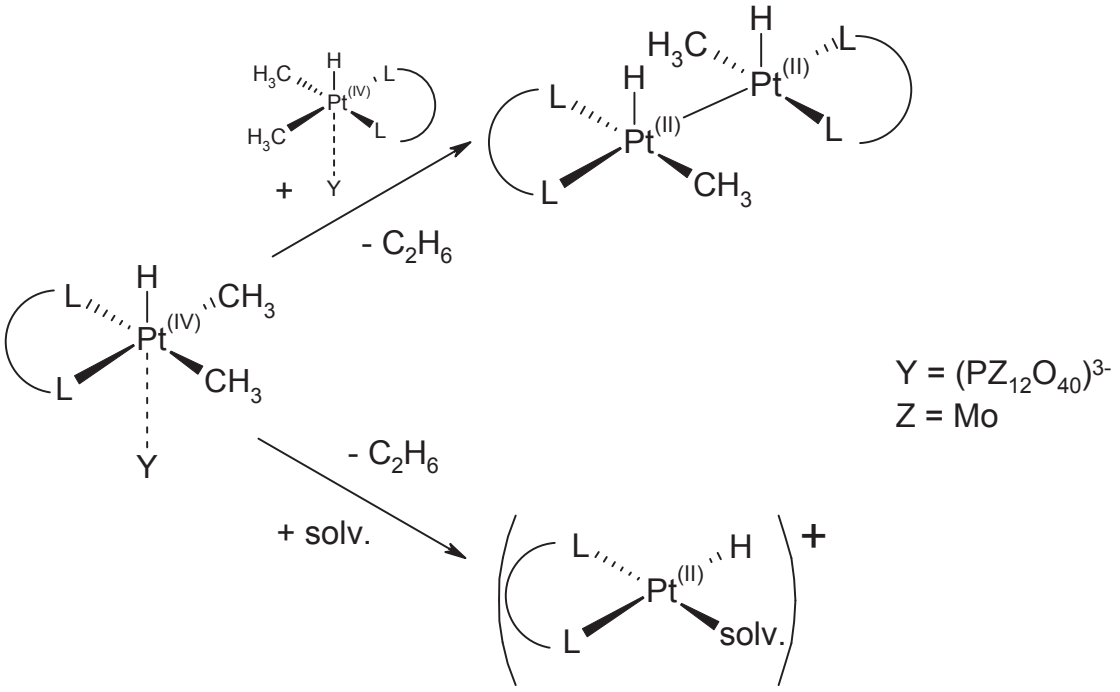

Scheme 2. Possible ways leading to C-C coupling and ethane release from $PtMe_2COD$ in the presence of polyoxometalates.

3.B.4 Conclusions

Novel hybrid compounds based on organometallic complexes of platinum and cesium salts of polyoxometalates were prepared. Upon grafting reactions, C-H and C-C bond formation processes on Pt(II) centers were shown to take place. They were induced by the acidic properties of polyoxometalates and tuned by the redox ones.

These new materials are expected to exhibit interesting catalytic properties towards oxidation of simple alkanes as they are directly related to the system proposed by Neumann some years ago, which in turn is a modification of the systems of Periana and Shilov.

Understanding the chemistry behind the phenomena reported above is therefore of extreme importance and our concomitant studies in this respect, especially by means of theoretical calculations, will be reported in due course.

Acknowledgments

Financial support for presented work was provided by the 7th European framework research program FP7/2007-2013, subvention no. 215193.

3.B.5 References

(1) Alvarez-Galvan, M. C.; Mota, N.; Ojeda, M.; Rojas, S.; Navarro, R. M.; Fierro, J. L. G. *Catal. Today* **2011**, *171*, 15.

(2) Kushch, L. A.; Lavrushko, V. V.; Misharin, Y. S.; Moravsky, A. P.; Shilov, A. E. *New J. Chem.* **1983**, *7*, 729.

(3) Periana, R. A.; Taube, D. J.; Gamble, S.; Taube, H.; Satoh, T.; Fujii, H. *Science* **1998**, *280*, 560.

(4) Luinstra, G. A.; Wang, L.; Stahl, S. S.; Labinger, J. A.; Bercaw, J. E. *Organometallics* **1994**, *13*, 755.

(5) Luinstra, G. A.; Wang, L.; Stahl, S. S.; Labinger, J. A.; Bercaw, J. E. *J. Organomet. Chem.* **1995**, *504*, 75.

(6) Canty, A. J.; Vankoten, G. *Acc. Chem. Res.* **1995**, *28*, 406.

(7) Sen, A.; Lin, M. R.; Kao, L. C.; Hutson, A. C. *J. Am. Chem. Soc.* **1992**, *114*, 6385.

(8) Holtcamp, M. W.; Labinger, J. A.; Bercaw, J. E. *J. Am. Chem. Soc.* **1997**, *119*, 848.

(9) Alibrandi, G.; Minniti, D.; Romeo, R.; Uguagliati, P.; Calligaro, L.; Belluco, U.; Crociani, B. *Inorg. Chim. Acta* **1985**, *100*, 107.

(10) Jawad, J. K.; Puddephatt, R. J.; Stalteri, M. A. *Inorg. Chem.* **1982**, *21*, 332.

(11) Hill, G. S.; Rendina, L. M.; Puddephatt, R. J. *Organometallics* **1995**, *14*, 4966.

(12) Stahl, S. S.; Labinger, J. A.; Bercaw, J. E. *J. Am. Chem. Soc.* **1995**, *117*, 9371.

(13) Jenkins, H. A.; Yap, G. P. A.; Puddephatt, R. J. *Organometallics* **1997**, *16*, 1946.

(14) Jenkins, H. A.; Klempner, M. J.; Prokopchuk, E. M.; Puddephatt, R. J. *Inorg. Chim. Acta* **2003**, *352*, 72.

(15) Mazzone, G.; Russo, N.; Sicilia, E. *Inorg. Chem.* **2011**.

(16) Brown, M. P.; Puddepha.Rj; Upton, C. E. E.; Lavingto.Sw *J. Chem. Soc.*-

Dalton Trans. **1974**, 1613.

(17) Ozawa, F.; Ito, T.; Yamamoto, A. *J. Am. Chem. Soc.* **1980**, *102*, 6457.

(18) Aizenberg, M.; Milstein, D. *Angew. Chem.-Int. Edit. Engl.* **1994**, *33*, 317.

(19) Leatherman, M. D.; Svejda, S. A.; Johnson, L. K.; Brookhart, M. *J. Am. Chem. Soc.* **2003**, *125*, 3068.

(20) Gomez, M.; Yarrow, P. I. W.; Demiguel, A. V.; Maitlis, P. M. *J. Organomet. Chem.* **1983**, *259*, 237.

(21) Bar-Nahum, I.; Khenkin, A. M.; Neumann, R. *J. Am. Chem. Soc.* **2004**, *126*, 10236.

(22) Hill, C. L.; (ed.) *Chem. Rev.* **1998**, *98*, 1.

(23) Legagneux, N.; Jeanneau, E.; Thomas, A.; Taoufik, M.; Baudouin, A.; de Mallmann, A.; Basset, J. M.; Lefebvre, F. *Organometallics* **2011**, *30*, 1783.

(24) Berndt, S.; Herein, D.; Zemlin, F.; Beckmann, E.; Weinberg, G.; Schütze, J.; Mestl, G.; Schlögl, R. *Ber. Bunsen-Ges.Phys.Chem.* **1998**, *102*, 763.

(25) Okuhara, T.; Watanabe, H.; Nishimura, T.; Inumaru, K.; Misono, M. *Chem. Mat.* **2000**, *12*, 2230.

(26) Legagneux, N.; de Mallmann, A.; Grinenval, E.; Basset, J. M.; Lefebvre, F. *Inorg. Chem.* **2009**, *48*, 8718.

(27) Drago, R. S.; Dias, J. A.; Maier, T. O. *J. Am. Chem. Soc.* **1997**, *119*, 7702.

(28) Putaj, P.; Grinenval, E.; Lefebvre, F. *J. Catal.*, *submitted*.

Chapter 4
Skeletal isomerisation of *n*-butane on salts of polyoxometalates

* This part will be submitted as a research article and is reproduced here accordingly.

ALKANE TRANSFORMATION ON POLYOXOMETALATES: PART 3. *n*-BUTANE ISOMERIZATION CATALYZED BY AMMONIUM AND CESIUM SALTS OF POLYOXOMETALATES

Piotr PUTAJ, Sébastien NORSIC, Kai C. SZETO, Frédéric LEFEBVRE*

Université de Lyon ICL, C2P2 UMR 5265 (CNRS – CPE – Université Lyon 1) LCOMS – CPE Lyon, 43 Boulevard du 11 Novembre 1918 F-69616, Villeurbanne, France
E-mail : lefebvre@cpe.fr

Abstract

Various catalysts based on cesium or ammonium salts of Keggin-type polyoxometalates with different degrees of saturation have been prepared and tested in the skeletal isomerization of *n*-butane to isobutane at moderate temperatures (mainly 498 K). High conversions and selectivities were observed, accompanied nevertheless by deactivation of catalysts by coking. Presence of hydrogen in the gas flow and addition of Pt greatly enhanced the catalysts lifetime as well as their selectivity, due to the suppression of the bimolecular pathway of isomerization. The most promising series of catalysts consists of platinum-doped ammonium salts of phosphotungstic acid $H_3PW_{12}O_{40}$, which show catalytic performance comparable to that of Pt-$Cs_{2.5}H_{0.5}PW_{12}O_{40}$, proposed already some time ago as an alternative for currently employed industrial catalysts.

Keywords

polyoxometalates, Keggin, *n*-butane, isobutane, skeletal isomerization

4.1 Introduction

Skeletal isomerization of low carbon *n*-paraffins to *iso*-paraffins is of great importance for the petroleum industry as it allows preparation of fuel mixtures of improved performance, low-octane-number compounds being replaced by high-octane-number ones. As a consequence, the use of lead-containing fuel additives could have been suppressed almost completely, resulting in economical and environmental benefits. In particular, *n*-butane can be transformed in this facile and straightforward way to isobutane, which in turn is used in the synthesis of MTBE (methyl-*tert*butyl ether, another fuel boosting additive) or in the alkylation of butenes.

Various alternatives have been tested so far in order to replace the currently employed commercial systems Pt/Cl-Al_2O_3 (which among other inconveniences is water-sensitive and requires constant addition of a small quantity of organic chloride precursor to the feed gas) or Pt/mordenite (less active than the former but resistant to poisoning). Accordingly, the sulfated zirconia SO_4^{2-}/ZrO_2 was reported to catalyze butane – isobutane isomerization already at room temperature [1]. Although it deactivated rapidly yet still its activity was higher than those of zeolites, like mordenite [2-3]. The presence of H_2 in the feed gas was shown to increase and stabilize the stationary activity of isomerization even in the absence of a noble metal co-catalyst and was ascribed to suppression of the agglomeration of polymeric cracking products on the surface of the catalyst. Nevertheless, when the concentration of hydrogen was too high its inhibiting effect was noted [2]. Some other proposed systems for this reaction were based on sulfated titania SO_4^{2-}/TiO_2 [4] or tungstated zirconia WO_3/ZrO_2 [5].

Polyoxometalates can be perceived as discreet analogues of metal oxide surfaces [6]. Particularly, the Keggin family members are widely used in homogenous catalysis, because of their pronounced and tunable acidic and redox properties. There are however only scarce examples of applications of pure solid heteropolyoxometalates in heterogenous catalysis, due to their very low specific surface area (only a few m^2/g). In order to overcome this issue they can be e.g. deposited by impregnation on various carriers such as silica, alumina or carbon. Investigations showed, nevertheless, that supporting of POMs leads to weakening of the purely Brönsted acid sites [7-8]. On the other hand, precipitation of partially saturated Cs^+, K^+, $(NH_4)^+$ or Rb^+ salts of polyoxometalates results in materials with very high surface areas (typically more than 100 m^2/g) with unreacted acidic clusters deposited on their surface and

stabilized by interactions with the cations [9].

The first report of the use of polyoxometalates in alkane isomerization was published by Ono et al. [10]. Pd-promoted phosphotungstic acid $H_3PW_{12}O_{40}$ deposited on silica was shown to be active in pentane and hexane isomerization in presence of H_2. Later Na et al. [11-12] reported high activity and selectivity of Pt-doped cesium salts of $PW_{12}O_{40}^{3-}$ in butane-isobutane reaction performed in presence of H_2. When the catalyst was studied in absence of H_2 and without doping with noble metal, the activity of isomerization reaction was shown to decrease over time, mainly due to acid-catalyzed cracking, until a stationary state was reached (in contrast to sulfated zirconia, which deactivated completely) [13]. At the same time the selectivity to isobutane changed only slightly. For a series of salts with different Cs contents the catalytic activity was correlated with the surface acidity (i.e. number of protons per unit of mass). An overall performance of the best catalyst in the series, $Cs_{2.5}H_{0.5}PW_{12}O_{40}$ at 573K, was higher than that of sulfated zirconia (in terms of conversion), zeolites (in terms of selectivity to isobutane) or even silica-supported $H_3PW_{12}O_{40}$ (in both). From a mechanistic point of view the reaction was evidenced to proceed via two competing pathways, mono- and bimolecular (see Schemes 1 and 2) and their respective contributions were found to be strongly dependent on the temperature [14-15].

Pt-doping of $Cs_{2.5}H_{0.5}PW_{12}O_{40}$ and performing the reaction in presence of hydrogen greatly enhance both the stationary state activity and selectivity of isomerization [16-17]. This is due to the almost complete suppression of the bimolecular pathway of isomerization. At the same time platinum changes the monomolecular mechanism (see Scheme 3) [18-19].

Although Pt-$Cs_{2.5}H_{0.5}PW_{12}O_{40}$ system seems to be an interesting industrial alternative, there is still plenty of room for its improvements [20-21]. The possibility of developing a novel, better still catalyst cannot be excluded neither. We report herein the promising results of our investigations on the skeletal isomerization of *n*-butane performed on various catalysts from the polyoxometalates family.

4.2 Experimental part

Materials. Silicotungstic acid $H_4SiW_{12}O_{40}.xH_2O$ (99.9+ %, Aldrich), phosphotungstic acid $H_3PW_{12}O_{40}.xH_2O$ (99+ %, Aldrich), cesium carbonate Cs_2CO_3 (99%, Aldrich) and ammonium carbonate $(NH_4)_2CO_3$ (99%, Aldrich) were used as received.

Sample preparation. Three series of catalysts were prepared:

- cesium salts of silicotungstic acid with the general formula $Cs_xH_{4-x}SiW_{12}O_{40}$ – To an aqueous solution of a polyoxometalate ($H_4SiW_{12}O_{40}$) a stoechiometric amount of Cs_2CO_3 was added under vigorous stirring, resulting in effervescence and immediate precipitation of a microcrystalline solid. Stirring was continued until complete evaporation of the solvent at room temperature. The powder was then collected without washing and ground in a mortar.
- ammonium salts of phosphotungstic acid with the general formula: $(NH_4)_xH_{3-x}PW_{12}O_{40}$ – These samples were prepared following the procedure described above, with $(NH_4)_2CO_3$ as a source of ammonium cations.
- composite catalysts given with the formula: $H_4SiW_{12}O_{40}/Cs_{2.6}H_{0.4}PW_{12}O_{40}$, with different contents of silicotungstic acid (from 1.7 wt. % to 13 wt. %) - In a first step precipitation of $Cs_{2.6}H_{0.4}PW_{12}O_{40}$ was performed as described above and after half an hour of stirring at room temperature, an appropriate amount of $H_4SiW_{12}O_{40}$ was added to the reaction mixture. The resulting powder was gathered after the evaporation of the solvent, without any washing. The quantity of silicotungstic acid was calculated so as to create a monolayer on the surface of the cesium salt of phosphotungstic acid. To this purpose specific surface area of $Cs_{2.6}H_{0.4}PW_{12}O_{40}$ was taken from nitrogen adsorption experiment (without the contribution from the micropores) and each Keggin unit was assumed to have a surface of 1.9 nm^2 [22]. So-obtained number (which corresponds to 13 wt. %) was successively decreased for other samples in this series.
- $Cs_{2.6}H_{0.4}PW_{12}O_{40}$ synthesized from $H_3PW_{12}O_{40}$ and Cs_2CO_3 was used as a reference compound.

All samples were fully characterized by means of elemental analyses and BET techniques to establish their compositon, specific surface values, surface proton density and degree of dispersity of acidic clusters on salts microcrystals.

n-butane isomerization. All *n*-butane isomerization reactions were performed in a continuous flow reactor at atmospheric pressure. The temperature ranged from 423 K to 548 K. Gas flow rates were varied between 0.5-2.0 mL/min. and 0-4.0 mL/min. for *n*-butane and hydrogen, respectively. 200 mg of each polyoxometalate catalyst was used, with or without addition of 100 mg of a Pt/SiO_2 co-catalyst (1% wt. of metal). A mechanical mixture of both components was prepared by prolonged grinding in the mortar. All powders were put in the reactor and first pre-treated in Ar flow (10 mL/min) at 498 K for 2 hours. The temperature was then adjusted to the desired value and the reaction carried out. The composition of the evolved gases was determined online by gaseous chromatography.

Physicochemical characterization techniques. All compounds were sealed in glass tubes under vacuum and sent to CNRS Central Analysis Department of Solaize in order to establish their elemental compositions.

The surface area of the samples was measured by BET method with an N_2 adsorption system (Micromeritics ASAP-2000) after pretreatment under vacuum at 498 K for 2 h.

4.3 Results and discussion

4.3.1 Catalyst preparation and characterization. Keggin type polyoxometalates seem particularly predisposed to serve as catalysts in skeletal isomerization of alkanes because they combine tunable acidic properties and robustness against thermal decomposition. The low specific surface area of purely acidic POMs no longer constitutes a major obstacle to their applications as it can be significantly increased either by supporting the clusters on e.g. silica or other carriers or by exchanging some of their protons with alkaline metal cations, creating partially saturated salts. Indeed, such a compound, the unsaturated cesium salt of phosphotungstic acid $Cs_{2.5}H_{0.5}PW_{12}O_{40}$, has been suggested by Na et al. [13] already some time ago to be a promising system for the *n*-butane-isobutane reaction, showing high activity and selectivity at moderate temperatures. Nevertheless, the research continues and further developments in this field are regularly reported, e.g. resulting from investigations of support effects on catalytic activity of polyoxometalates [23-24] and/or the influence of supercritical reaction conditions [25]. Modifications of the synthetic strategies of salts of polyoxometalates is yet another approach which has not been explored thoroughly so far. If one considers the already mentioned cesium salt of phosphotungstic acid as a 'parent' species, by varying its components (cations or anions or both) or by simply doping it, so to say 'offspring' compounds can be proposed and expected to show improved catalytic activity or other advantages. On one hand, there exists another strongly acidic polyoxometalate from the Keggin family, the silicotungstic acid $H_4SiW_{12}O_{40}$, which in its pure form contains a higher number of protons than its phosphotungstic counterpart (namely 4 versus 3). In principle its cesium salts should then exhibit higher surface acidity values, that had been directly correlated with catalytic activity in alkane isomerization [13]. Alternatively, cesium cations could be exchanged for other alkaline metals (K^+, Rb^+ etc.) [26] or preferentially - ammonium ones, yielding much less expensive though still temperature resistant, high surface materials. As for doping, it has already been shown that mechanical addition of $H_3PW_{12}O_{40}$ to the

$Cs_{2.5}H_{0.5}PW_{12}O_{40}$ enhances its activity [20]. As a result of all these considerations three series of novel catalysts based on polyoxometalates were obtained and characterized using standard techniques.

Figure 1 presents examples of N_2 adsorption-desorption isotherms obtained for some of the synthesized compounds.

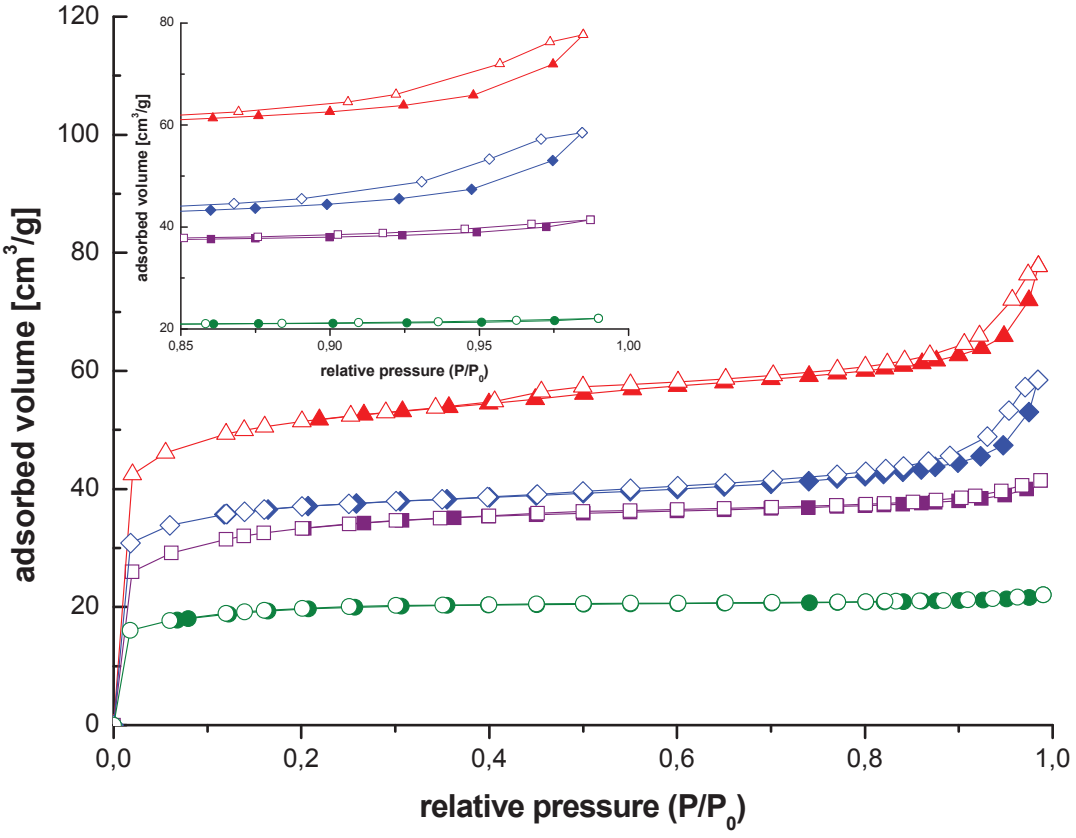

Figure 1. Adsorption-desorption isotherms of N_2 at 77 K for: $Cs_{2.6}H_{0.4}PW_{12}O_{40}$ (■, □); $Cs_4SiW_{12}O_{40}$ (▲, Δ); $(NH_4)_{1.2}H_{1.8}PW_{12}O_{40}$ (♦, ◊) and $H_4SiW_{12}O_{40}/Cs_{2.6}H_{0.4}PW_{12}O_{40}$ (3.4% wt.) (●, ○). Open symbols, adsorption branch, solid symbols, desorption branch. Hysteresis loops magnified in the inset.

$Cs_4SiW_{12}O_{40}$ and $(NH_4)_{1.2}H_{1.8}PW_{12}O_{40}$ exhibit isotherms of Type IV, with a hysteresis loop, typical for mesoporous materials, but with a steep increase of the adsorption at low-pressure ($P/P_0 < 0.1$), suggesting also the presence of micropores. On the other hand, the reference compound $Cs_{2.6}H_{0.4}PW_{12}O_{40}$ and the composite material $H_4SiW_{12}O_{40}/Cs_{2.6}H_{0.4}PW_{12}O_{40}$ (3.4% wt.) show curves of type I, characteristic of purely microporous materials [27]. These results are quite similar to those of Okuhara et al. [28] who reported isotherms of Type I for

$Cs_{2.1}H_{0.9}PW_{12}O_{40}$ and $Cs_{2.2}H_{0.8}PW_{12}O_{40}$ compounds, but Type IV for $Cs_{2.5}H_{0.5}PW_{12}O_{40}$. Indeed, it is now well admitted that the cesium salt is in the form of very small particles leading to an intergranular microporosity. The mesoporosity observed by Okuhara for $Cs_{2.5}H_{0.5}PW_{12}O_{40}$ is probably related to the preparation method. We used a different synthetic procedure, being somewhat harsher (rapid addition of solid Cs_2CO_3 in one portion to the solution of polyanion versus prolonged dripping of the aqueous solution of Cs_2CO_3 to the solution of polyoxometalate) and therefore favorable to the formation of finer crystallites [9].

Nevertheless, the pore size distribution curves derived from the desorption branches by BJH method [29] show presence of some mesopores with widths of about 35 Å also in the reference compound $Cs_{2.6}H_{0.4}PW_{12}O_{40}$ (see Figure 2).

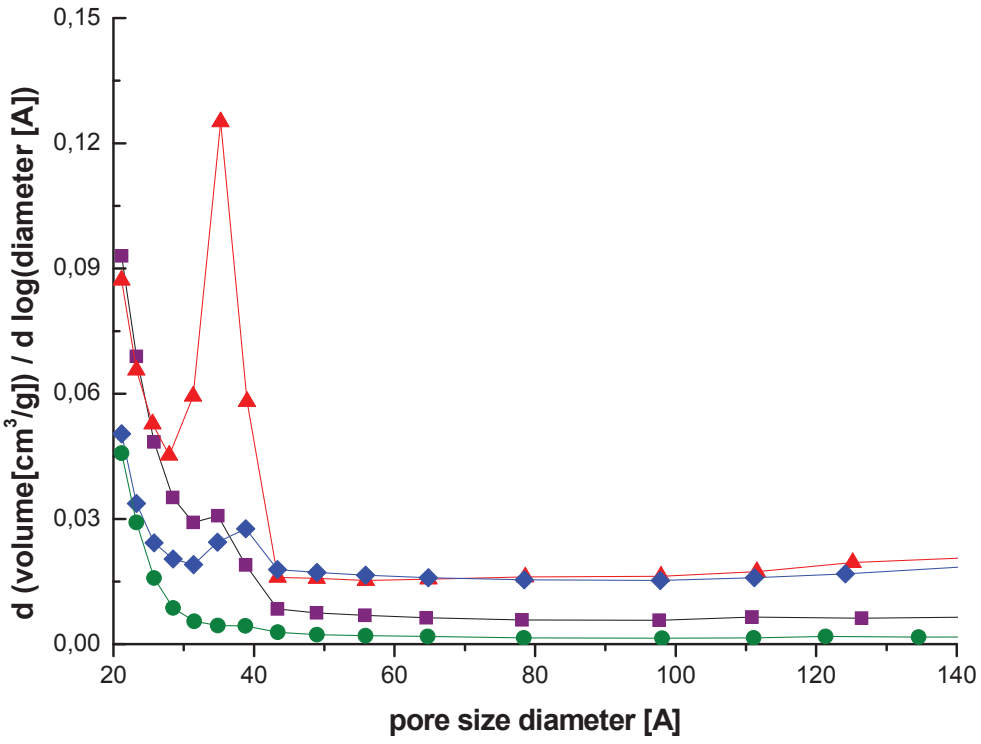

Figure 2. Pore size distribution curves derived from BJH method for: $Cs_{2.6}H_{0.4}PW_{12}O_{40}$ (■); $Cs_4SiW_{12}O_{40}$ (▲); $(NH_4)_{1.2}H_{1.8}PW_{12}O_{40}$ (♦) and $H_4SiW_{12}O_{40}/Cs_{2.6}H_{0.4}PW_{12}O_{40}$ (3.4% wt.) (●).

Nitrogen adsorption experiments results are given in Table I. It is clearly visible that micro- (7-20 Å) and ultramicropores (less than 7 Å) [30] constitute the major part of the surface of all obtained samples. The surface acidity (the number of protons located on the surface per unit of mass) was calculated based on chemical formulae and specific surface area values, assuming that each Keggin unit has a surface area of 1.9 nm^2 [22]. The quantity of protons in

the micropores is also given, according to a model which states that protons spread evenly over whole volume of the solid upon thermal treatment [9].

Table I. Surface area and surface acidity of the samples.

Sample	BET surface area		surface acidity	
	total [m^2/g]	(ultra)micropores (< 20Å) [m^2/g]	total [µmol/g]	(ultra)micropores (< 20Å) [µmol/g]
$Cs_{2.6}H_{0.4}PW_{12}O_{40}$	96	80	34	28
$Cs_{2.15}H_{1.85}SiW_{12}O_{40}$	9*	-	15	-
$Cs_{2.65}H_{1.35}SiW_{12}O_{40}$	41	35.5	48	40.3
$Cs_{3.1}H_{0.9}SiW_{12}O_{40}$	88	78	69	61.4
$Cs_4SiW_{12}O_{40}$	145	113	0	0
$(NH_4)_{0.8}H_{2.2}PW_{12}O_{40}$	23*	-	44	-
$(NH_4)_1H_2PW_{12}O_{40}$	75	51	131	88
$(NH_4)_{1.2}H_{1.8}PW_{12}O_{40}$	114	95	177	147
$H_4SiW_{12}O_{40}/Cs_{2.6}H_{0.4}PW_{12}O_{40}$ (13.0% wt.)	14*	-	49	-
$H_4SiW_{12}O_{40}/Cs_{2.6}H_{0.4}PW_{12}O_{40}$ (6.7% wt.)	52	46	100	88.5
$H_4SiW_{12}O_{40}/Cs_{2.6}H_{0.4}PW_{12}O_{40}$ (3.4% wt.)	64	52	73	60
$H_4SiW_{12}O_{40}/Cs_{2.6}H_{0.4}PW_{12}O_{40}$ (1.7% wt.)	68	55	51	41.3

* - single point surface area value

Provided that the degree of ultramicroporosity of the so-obtained materials (which has not been established) is not excessively high, the molecular sizes (MS) of *n*-butane: 4.3 Å and isobutane: 5 Å, according to [31], should allow both substrate and product molecules to penetrate the solids and undergo reactions on their surface.

4.3.2 Catalysis of isomerization. Mechanistic studies have shown that isomerization of alkanes on polyoxometalates may follow either mono- or bimolecular pattern (see Schemes 1 and 2). Monomolecular way starts with a hydride abstraction accompanied by hydrogen release and creation of a secondary C_4 carbocation. In an intermolecular rearrangement step more stable tertiary cation is obtained. Hydride transfer from another butane molecule perpetuates the reaction. If isomerization happened to proceed exclusively via this way, theoretically selectivity to isobutane could reach 100%. It is worth noticing, though, that the efficiency of the monomolecular process is limited itself by thermodynamics. In the equilibrium conditions, the conversion to isobutane could reach up to 65% for the reaction performed at 500 K [32]. However, some butane molecules undergo dehydrogenation to butenes as well. In a highly acidic environment the resulting olefins can get protonated and yield additional carbocations, but they are also able to couple with already existing ones. As a result, various C_8 intermediate species are created and their concomitant rearrangements and scissions lead to the presence of wide range of low carbon compounds (mainly C_3-C_5 but C_1, C_2, C_6 etc. are observed as well). Even though formation of isobutane via this route is also possible, the selectivity of the overall process suffers significant decrease. Moreover, formation of carbonaceous deposits on the catalysts surface (coking) causes its deactivation over time. Contribution of both routes is strongly temperature-dependent as has been evidenced in mechanistic studies using ^{13}C-labeled *n*-butane [14-15]. Between 353-373 K the monomolecular route prevails but as the temperature rises to 393-493 K the bimolecular mechanism becomes predominant. Further temperature increase again favors monomolecular way.

Scheme 1. *n*-butane isomerization via monomolecular way in an acidic environment.

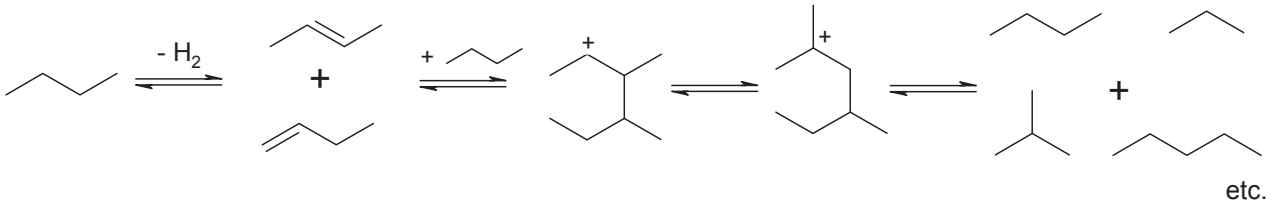

Scheme 2. Bi-molecular way of *n*-butane isomerization.

In view of these considerations, performance of all samples was evaluated in the *n*-butane to isobutane isomerization at 498 K and the results are presented in Table II.

Table II. Activity and selectivity for skeletal isomerization of *n*-butane at 498 K.

Catalyst	Conv.[a] (%)	Conv.[b] (%)	Conv.[c] (%)	Selectivity (%)[b]					
				iC_4	$C_{4=}$	C_1	C_2	C_3	C_{5+}
$Cs_{2.6}H_{0.4}PW_{12}O_{40}$	37.2	18.2	15.2	85.1	1.1	0.1	0.2	11.2	2.3
$Cs_{2.15}H_{1.85}SiW_{12}O_{40}$	9.3	1.0	0.4	71.7	1.6	0.9	1.9	23.9	0
$Cs_{2.65}H_{1.35}SiW_{12}O_{40}$	16.8	7.9	5.2	73.8	1.9	0.4	0.8	20.9	2.2
$Cs_{3.1}H_{0.9}SiW_{12}O_{40}$	7.2	3.3	2.4	87.5	0.9	0.2	0.4	8.9	2.1
$Cs_4SiW_{12}O_{40}$	0.2	0.1	0.1	82.5	0.6	3.3	5.2	8.4	0
$(NH_4)_{0.8}H_{2.2}PW_{12}O_{40}$	27.5	13.3	10.3	68.7	1.6	0.5	0.5	25.4	3.3
$(NH_4)_1H_2PW_{12}O_{40}$	33.0	9.8	5.6	80.8	1.0	0.5	0.3	14.0	3.4
$(NH_4)_{1.2}H_{1.8}PW_{12}O_{40}$	18.9	14.7	12.6	75.2	2.0	0.3	0.4	20.4	1.7
$H_4SiW_{12}O_{40}/Cs_{2.6}H_{0.4}PW_{12}O_{40}$ (13.0% wt.)	17.4	1.5	0.4	44.9	1.5	2.1	2.4	43.6	5.5
$H_4SiW_{12}O_{40}/Cs_{2.6}H_{0.4}PW_{12}O_{40}$ (6.7% wt.)	40.6	6.0	2.1	63.9	1.4	1.8	0.6	28.0	4.3
$H_4SiW_{12}O_{40}/Cs_{2.6}H_{0.4}PW_{12}O_{40}$ (3.4% wt.)	32.8	6.8	1.6	73.4	1.1	0.4	0.4	21.2	3.5
$H_4SiW_{12}O_{40}/Cs_{2.6}H_{0.4}PW_{12}O_{40}$ (1.7% wt.)	35.9	11.0	6.2	85.4	0.8	0.2	0.2	11.0	2.4

Conditions: T = 498 K, gas flow: 1mL/min. *n*-C_4, 0.2 g of each catalyst was used. Pre-treatment for 2 h in 10mL/min. of Ar flow at T = 498 K.

Conversion: a) max. value, after 20-30 minutes on stream, b) after five hours and c) after ten hours on stream. Selectivity: C_1 = methane, C_2 = ethane and ethene, C_3 = propane and propene, iC_4 = isobutane, $C_{4=}$ = isobutenes and C_{5+} = pentanes, pentenes and higher homologues.

Pre-treatment in the Ar flow at 498 K yields anhydrous polyoxometalates. This is a crucial step as presence of water was shown to weaken the strength of acid sites of polyanionic clusters, thus lowering their activity in alkanes isomerization [33]. Temperature of the thermal treatment cannot be too high though (preferentially not more than 573 K) as decomposition of

the clusters occurs (however reversible [34]) and catalytic activity is gradually lost [13].

For a majority of samples from Table II initial activities reach high values. In the course of the isomerization reaction, however, all catalysts undergo deactivation, being more rapid during first couple of hours on stream (data in columns 2 and 3) and slowing down further on (column 4). Some compounds are nevertheless able to maintain significant activity even after 10 hours on stream. Deactivation is due to the coke formation on the surface of solids, being fast in case of the bimolecular mechanism and much slower for monomolecular one (see Figure 3, it is important to realize that both pathways contribute to isobutane formation, especially at the initial stages of the reaction, so presented isomerisation profile is a superposition of two curves). Figure 4 shows how elimination of active sites responsible for the bimolecular pathway leads to the improvement of overall selectivities of isomerisation. In most cases, after 5 h on stream a steady state is reached, with high selectivities to isobutane, ranging from 72-88%.

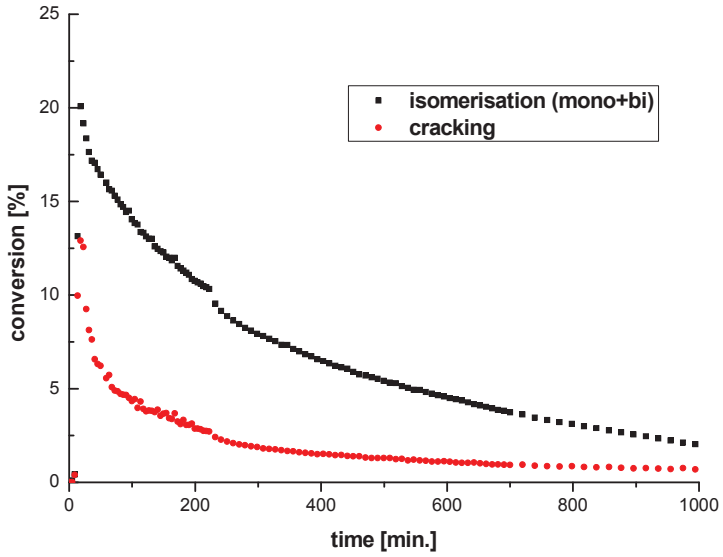

Figure 3. Time profile of conversion of *n*-butane to isomerisation species (isobutane, in black) and all products of cracking jointly (in red) over the surface of $(NH_4)_1H_2PW_{12}O_{40}$ at 498 K.

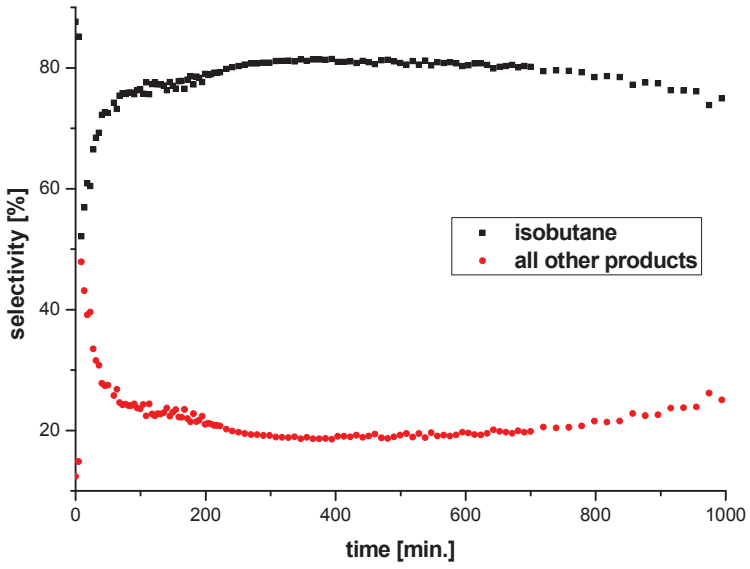

Figure 4. Time profile of selectivity of n-butane transformations over the surface of $(NH_4)_1H_2PW_{12}O_{40}$ at 498 K.

Compared to their phosphotungstic congener, cesium salts of silicotungstic acid show astonishingly poor performance in all considered categories. This is even more surprising when taking into account the surface acidity values of samples in this series (see Table I and Figure 5), two of them being clearly higher than for $Cs_{2.6}H_{0.4}PW_{12}O_{40}$. Surface acidity was directly correlated with catalyst performance in isomerization [13] but in view of all our results this approach seems an oversimplification. Doping cesium salts of phosphotungstic acid with silicotungstic acid yields very active catalysts that in most cases get poisoned almost completely during the process. Another effect of the doping is the drastic decrease of selectivity, leading to the formation of propane(+ propene) and isobutane in almost 1:1 ratio for the sample with the highest loading of $H_4SiW_{12}O_{40}$. These high-cracking compounds will be addressed in detail in the next section.

Even at this initial stage of investigation, ammonium salts of phosphotungstic acid turned out to be the best among all new tested catalysts in terms of activity, durability and selectivity and comparable with a reference compound. Because of their affordability they can be perceived as an attractive alternative for $Cs_{2.5}H_{0.5}PW_{12}O_{40}$-based system [16] and currently employed industrial catalysts. Further studies were therefore focused on one of the samples of this series.

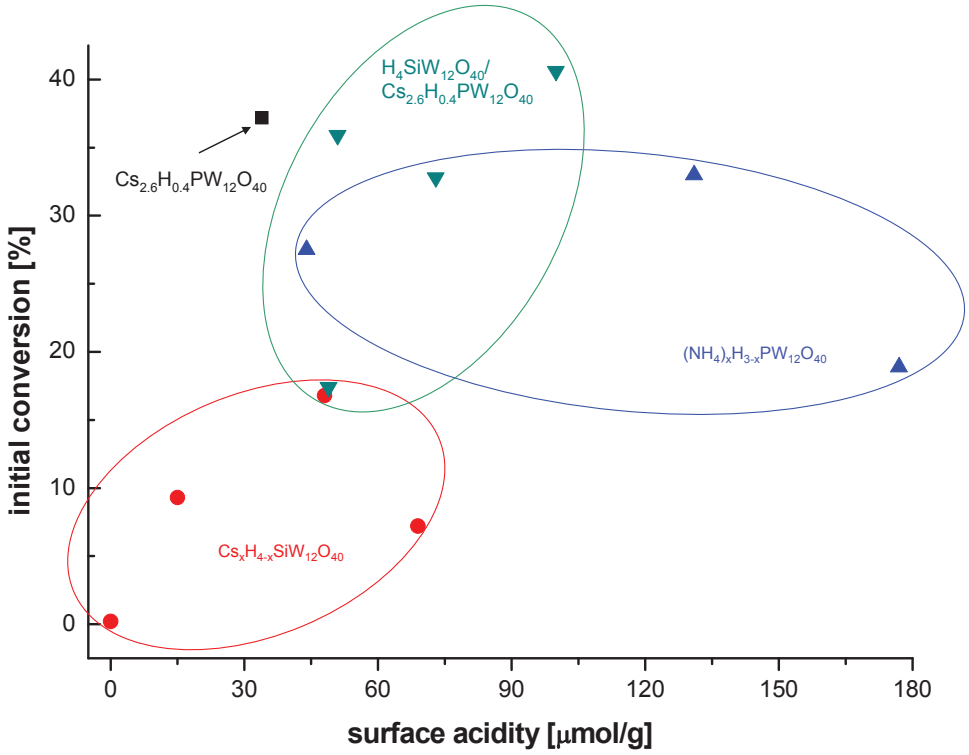

Figure 5. Effect of surface acidity on *n*-butane conversion at 498 K.

First of all, the influence of the contact time of *n*-butane molecules with catalysts surface was studied, by means of varying *n*-butane flow velocity and the results are given in Table III.

Table III. Activity and selectivity of isomerization with variable *n*-butane flow at 498 K.

Catalyst	*n*-C_4 flow [mL/min.]	Conv.[a] (%)	Conv.[b] (%)	Conv.[c] (%)	Selectivity (%)[b]					
					iC_4	$C_{4=}$	C_1	C_2	C_3	C_{5+}
$(NH_4)_1H_2PW_{12}O_{40}$	0.5	50.3	14.1	10.3	75.7	1.6	0.4	0.4	19.5	2.4
	1.0	33.0	9.8	5.6	80.8	1.0	0.5	0.3	14.0	3.4
	2.0	25.1	8.9	5.9	82.6	1.4	0.3	0.4	12.9	2.4

[a], [b], [c] – see Footnote to Table II. 0.2 g of catalyst was used. Pre-treatment for 2 h in 10mL/min. of Ar flow at T = 498 K.

While diminishing the *n*-butane flow rate (i.e. increasing the contact time) enhances markedly initial and steady state conversions, at the same time it results in lowering of the selectivity to isobutane. This is understandable, considering that bimolecular reaction pathway is more time-dependent that monomolecular one. When molecules spend more time over the surface of the catalyst, they have higher chances of coupling and yielding undesired products. This

effect is typically observed for this type of reactions [35].

The positive effect of the presence of small quantity of hydrogen in the gas flow on catalytic performance of sulfated zirconia has been observed [2] and explained to arise from a suppression of formation of butenes (hence – the bimolecular mechanism) and thus reducing the rate of deactivation and improving the reaction's selectivity. However, at higher concentrations its inhibiting role has been shown and explained by shifting the equilibrium of the first stage of the process (i.e. dehydrogenation). Performance of polyoxometalate catalyst in similar conditions was studied and results are presented in Table IV and Figure 6.

Table IV. Influence of hydrogen on activity and selectivity of *n*-butane isomerization. *n*-butane flow = 1mL/min.

Catalyst	H_2 flow [mL/min.]	Conv.[a] (%)	Conv.[b] (%)	Conv.[c] (%)	Selectivity (%)[b]					
					iC_4	$C_{4=}$	C_1	C_2	C_3	C_{5+}
$(NH_4)_1H_2PW_{12}O_{40}$	0	33.0	9.8	5.6	80.8	1.0	0.5	0.3	14.0	3.4
	1.0	27.6	9.2	6.8	86.2	0.9	0.2	0.3	9.8	2.6
	2.0	23.8	6.1	3.2	78.0	1.4	0.4	0.6	16.8	2.8
	4.0	22.4	5.6	4.7	84.3	1.0	0.6	1.3	12.8	0.0

[a], [b], [c] – see Footnote to Table II. 0.2 g of catalyst was used. Pre-treatment for 2 h in 10mL/min. of Ar flow at T = 498 K.

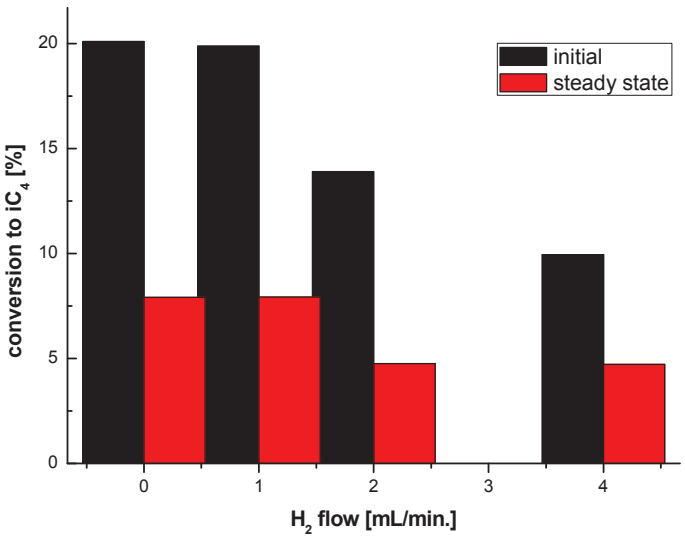

Figure 6. Influence of hydrogen concentration in the gas flow on initial (in black) and steady state (in red) conversion to isobutane over the surface of $(NH_4)_1H_2PW_{12}O_{40}$ at 498 K.

In the case of $(NH_4)_1H_2PW_{12}O_{40}$ sample, presence of hydrogen in the system affects negatively both initial and stationary overall conversions of *n*-butane. Nevertheless, the overall deactivation seems to proceed at a slower pace then in its absence. Also selectivity to isobutane reaches maximum value when small quantity of hydrogen is present in the feed. Two first sets of columns seen in Fig. 6 show that positive and negative effects of hydrogen eventually neutralize each other. Possibly, even lower concentrations of H_2 lead to improvement of catalysts performance. These have not been tested yet, though.

Introduction of a noble-metal into the system results in profound changes of its chemistry. The isomerization reaction can still proceed via mono- or bi-molecular mechanism. This time however, monomolecular way is clearly distinct (see Scheme 3).

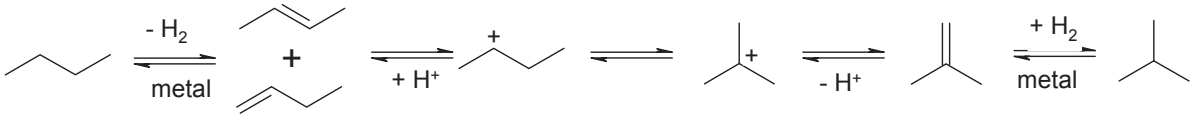

Scheme 3. Monomolecular pathway of *n*-butane isomerization in presence of a noble metal.

Isomerization via monomolecular way is bifunctional. On metal sites dehydrogenation of butane to butenes takes place. Butenes isomerize to isobutylene on acid sites and back on metal sites undergo rehydrogenation to isobutane. This has an ambivalent effect, since higher concentration of butenes leads to increased production of isobutane on one hand, but also of C_8 coupling products, hence coking, on the other. Bi-functional catalysts performance can be improved by addition of hydrogen to the gas flow – resulting in suppression of deactivation through hydrogenation of coke deposits [16]. However, too high hydrogen concentration would shift the equilibrium of dehydrogenation process thus affecting negatively the conversion. Another role of the metal has been pointed out – that of creation of "active" hydrogen atoms on the catalysts surface from the gas phase. As such, they can hydrogenate coke deposits preventing desactivation but also contribute to creation of new acid sites on the catalysts surface. This last assumption was put forward in the case of sulfated zirconia catalyst [36] but later dismissed for polyoxometalates [16].

Polyoxometalate catalyst was therefore combined with a noble metal co-catalyst (Pt/SiO_2, 1% wt. of Pt) by mechanical mixing to yield such a bifunctional system and its performance was evaluated in absence and presence of H_2. The results were gathered in Table V.

Table V. Influence of hydrogen on performance of bifunctional catalyst. *n*-butane flow = 1 mL/min. Reaction temperature 498 K.

Catalyst	H_2 flow [mL/min.]	Conv.[a] (%)	Conv.[b] (%)	Conv.[c] (%)	Selectivity (%)[b]					
					iC_4	$C_{4=}$	C_1	C_2	C_3	C_{5+}
$(NH_4)_1H_2PW_{12}O_{40}$	0	33.0	9.8	5.6	80.8	1.0	0.5	0.3	14.0	3.4
Pt/SiO_2-$(NH_4)_1H_2PW_{12}O_{40}$	0	84.5	1.0	0.4	64.8	1.3	1.9	2.8	28.0	1.2
	0.5	9.9	8.4	6.8	87.0	0.7	0.7	1.0	9.0	1.6
	1.0	8.5	7.0	*	92.6	0.4	0.6	0.9	4.4	1.2

[a],[b],[c] – see Footnote to Table II. 0.3 g of bifunctional catalyst was used (0.2g of POM + 0.1 of Pt/SiO_2). Pre-treatment for 2 h in 10mL/min. of Ar flow at T = 498 K. * - stopped before 10h.

Addition of platinum to $(NH_4)_1H_2PW_{12}O_{40}$ sample leads to a dramatic increase of the initial conversion (84.5 %, with selectivity to isobutane being only 6% – not shown in the table). This means that although dehydrogenation and butenes formation on noble metal are extremely efficient, olefins preferentially undergo coupling than isomerisation. As a result, much faster deactivation occurs and selectivity to isobutane increases with time, according to expectations. Introduction of even small quantity of hydrogen contributes to a restitution of steady state activity of a bifunctional catalyst to the level shown by purely POM sample, with additional gain in iC_4 selectivity. At 1 mL/min. flow of hydrogen selectivity to isobutane can reach ~93%. As seen in Fig. 7, overall conversion to isobutane on bifunctional catalyst in presence of H_2 practically does not change during 5 h on stream – due to suppression of deactivation.

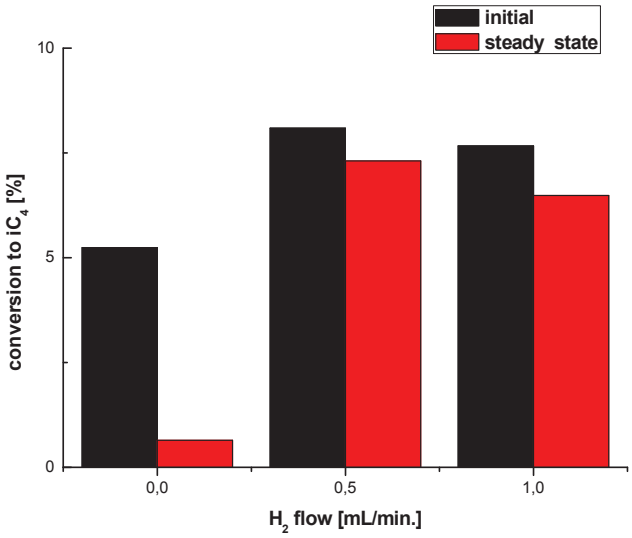

Figure 7. Influence of hydrogen concentration in the gas flow on initial (in black) and steady state (in red) conversion to isobutane over Pt/SiO_2-$(NH_4)_1H_2PW_{12}O_{40}$ at 498 K.

The most important observation comes from analysis of data from Tables IV and V and Fig. 6 and 7. In terms of isobutane yield and catalyst lifetime on stream there is not much difference between the purely polyoxometalate catalyst working under 1 mL/min. H_2 flow (Table IV, row 2) and Pt-doped catalyst under 0.5 ml/min. H_2 flow (Table V, row 3). Albeit stemming from different chemistries of both materials, these comparable net results are of high economical importance if one considers industrial applications. Depending on price and availability of hydrogen and platinum, the inherent system's flexibility makes it possible to adjust working conditions to the circumstances.

Finally, the interrupted flow experiment shows in a spectacular manner the effect of hydrogen presence on the course of the reaction (see Fig. 8).

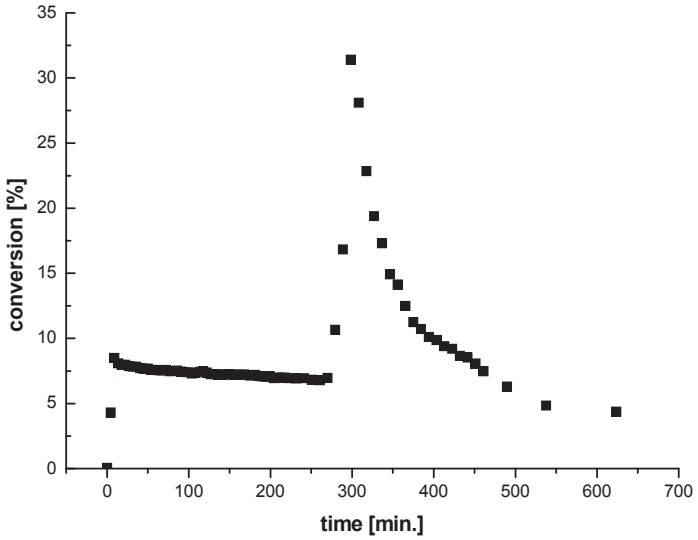

Figure 8. Time profile of *n*-butane isomerisation over the Pt/SiO_2-$(NH_4)_1H_2PW_{12}O_{40}$ at 498 K. 1 mL/min. of H_2 flow was cut off at t=300 min.

Reaction under hydrogen proceeds at a steady rate showing only minor signs of deactivation of the catalyst. At the moment when hydrogen flow is cut off, the conversion curve literally explodes (increase of 300%), due to unsuppressed butenes formation. Their increased concentration, however, leads to pronounced coking phenomena and fast (~100 min.) deactivation of the catalyst.

To sum up this part, among all prepared compounds, ammonium salts of phosphotungstic acid were found to be a high performance *n*-butane isomerisation catalysts at mild conditions. Obtained values of activity and selectivity combined with their durability and low price may qualify them on a preliminary basis as a replacement for currently employed industrial catalysts. Still, further research on these systems is needed, especially tests reproducing proper industrial conditions.

4.3.3. Special case of high-cracking solids. As has already been mentioned, silicotungstic acid was dispersed over the surface of a cesium salt of phosphotungstic acid in an attempt to increase the overall surface acidity of the catalyst and thus – its activity. Accordingly, as clearly visible in Table I and Fig. 5, surface acidity values for composite materials are much higher than for the parent compound. This is accompanied, however, by a pronounced decrease of specific surface area values of all samples, dependent on the loading of the $H_4SiW_{12}O_{40}$. Understandably, as $Cs_{2.6}H_{0.4}PW_{12}O_{40}$ is mostly microporous, additional polyanionic clusters at its surface may effectively block the pores entrances, especially in the case of a monolayer coverage for $H_4SiW_{12}O_{40}/Cs_{2.6}H_{0.4}PW_{12}O_{40}$ (13% wt.). The overall influence of two contradictory tendencies on catalytic performance of these solids is presented in Table II. First of all, increase in activity of doped catalysts is almost negligible, while $H_4SiW_{12}O_{40}/Cs_{2.6}H_{0.4}PW_{12}O_{40}$ (13% wt.) is actually less active than the undoped salt. Clearly higher surface acidity cannot compensate for the diminishing of specific surface. Catalysts are also deactivated much more rapidly – mean loss of 80 % after 5 h and 93 % after 10 h versus 50 % after 5 h and 60 % after 10 h for $Cs_{2.6}H_{0.4}PW_{12}O_{40}$. The most astonishing, however, is the drastic drop of selectivity to isobutane, accompanied by corresponding sharp rise of contribution from propane and propene (and to a lesser degree all C_{5+} products). These results remind more the ones obtained for the zeolites than polyoxometalate catalysts [13]. Here again, the dopants concentration plays a crucial role – the less the silicotungstic acid on the surface, the more the catalysts resembles with its properties the starting compound. This could be explained phenomenologically by considering two directions of the methyl shift on the surface of catalysts heavy- and sparsely-loaded with $H_4SiW_{12}O_{40}$ (see Fig. 9 and 10).

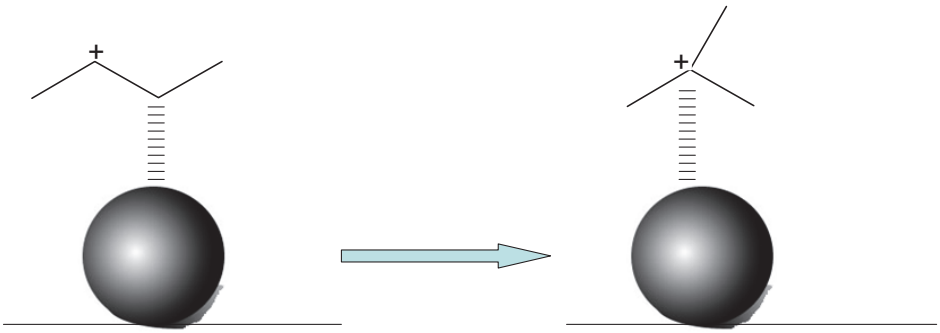

Figure 9. Isomerisation of *sec*-butyl carbocation on an isolated polyoxometalate on the catalyst surface.

On isolated clusters isomerisation prevails whereas presence of additional carbocations in vicinity results in preferential homologation activity.

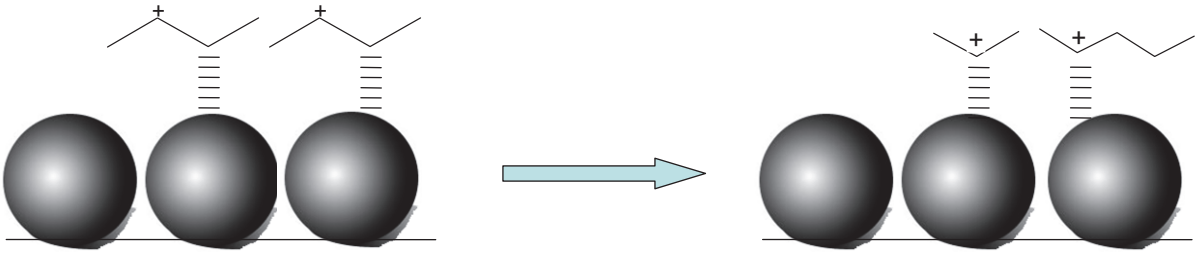

Figure 10. Homologation of *sec*-butyl carbocations on high-polyoxometalate-loaded catalyst surface.

Our setup did not allow us to distinguish between propane/propene nor pentanes/pentenes/higher homologues so the exact numbers are unavailable. Nevertheless, the amount of detected C_{5+} products in comparison to C_3 species is curiously low. A tentative explanation could be put forward - pentane, being more reactive than propane and butane, is probably undergoing further rapid isomerisations, couplings and so on to less and less volatile compounds. Still, proper mechanistic studies with ^{13}C-labelled butane would be of interest to clarify the mechanisms of observed processes.

In order to get some further insights about the reaction mechanism the effect of the temperature on the activity and selectivity of one of the catalysts from this series was tested and the results are shown in Table VI.

Table VI. Activity and selectivity of isomerization as a function of temperature. *n*-butane flow = 1mL/min.

Catalyst	T [K]	Conv.[a] (%)	Conv.[b] (%)	Conv.[c] (%)	Selectivity (%)[b]					
					iC_4	$C_{4=}$	C_1	C_2	C_3	C_{5+}
$H_4SiW_{12}O_{40}/Cs_{2.6}H_{0.4}PW_{12}O_{40}$ (6.7% wt.)	423	4.0	3.2	2.5	83.3	1.7	0.1	0.5	14.2	0.2
	498	40.6	6.0	2.1	63.9	1.4	1.8	0.6	28.0	4.3
	548	39.5	0.3	0.1	50.2	1.3	4.7	3.0	40.8	0.0

[a],[b],[c] – see Footnote to Table II. 0.2 g of catalyst was used. Pre-treatment for 2 h in 10mL/min. of Ar flow at T = 498 K.

It was observed that the reaction temperature had critical effect on the reactant conversion and product selectivity in the studied range. At 423 K the initial conversion value is extremely low (only 4%) but tends to increase rapidly (by a factor of ten) as temperature is raised to 498 K. Further increase to 548 K results only in a slight decrease of conversion to 39.5%. Whereas initial and stationary conversions at 423 K hardly differ, after 5 hours on stream at 548 K catalyst is already practically inactive. Selectivity to iC_4 reaches the highest value of 83% when the reaction is performed at the lowest temperature and drops with its increase, while propane formation tendency follows quite the opposite direction. This suggests that whereas at low temperatures a monomolecular pathway of isomerization prevails, bimolecular one is gradually "switched on" as the reaction is performed at higher temperatures. The sequence of events is therefore reversed than for undoped $Cs_{2.5}H_{0.5}PW_{12}O_{40}$ catalyst, according to the results obtained by Suzuki et al. [[18]].

The influence of the contact time of *n*-butane molecules with catalysts surface was studied by means of varying n-butane flow velocity and the results are given in Table VII.

Table VII. Activity and selectivity of isomerization with variable *n*-butane flow at 498 K.

Catalyst	*n*-C_4 flow [mL/min.]	Conv.[a] (%)	Conv.[b] (%)	Conv.[c] (%)	Selectivity (%)[b]					
					iC_4	$C_{4=}$	C_1	C_2	C_3	C_{5+}
$H_4SiW_{12}O_{40}$/	0.5	64.6	9.9	2.8	58.0	1.7	0.8	0.7	34.4	4.4
$Cs_{2.6}H_{0.4}PW_{12}O_{40}$	1.0	40.6	6.0	2.1	63.9	1.4	1.8	0.6	28.0	4.3
(6.7% wt.)	2.0	35.6	2.5	0.8	61.6	2.2	0.4	0.6	29.2	6.0

[a],[b],[c] – see Footnote to Table II. 0.2 g of catalyst was used. Pre-treatment for 2 h in 10mL/min. of Ar flow at T = 498 K.

Just like for $(NH_4)_1H_2PW_{12}O_{40}$, the conversion values for $H_4SiW_{12}O_{40}/Cs_{2.6}H_{0.4}PW_{12}O_{40}$ (6.7% wt.) sample decrease with lowering of the contact time. Curiously though, the selectivity to isobutane first rises when increasing the butane flow and then tends to drop down. Whether this tendency is related with different rates of inter- and intramolecular rearrangements upon methyl shift, stays an open question.

The effect of the hydrogen on catalytic performance of polyoxometalate catalyst in presence and absence of Pt was verified and results are presented in Table VIII and Fig. 11.

Table VIII. Influence of hydrogen on activity and selectivity of *n*-butane isomerization. *n*-butane flow = 1mL/min.

Catalyst	**H_2 flow [mL/min.]**	**Conv.[a] (%)**	**Conv.[b] (%)**	**Conv.[c] (%)**	**Selectivity (%)[b]**					
					iC_4	$C_{4=}$	C_1	C_2	C_3	C_{5+}
$H_4SiW_{12}O_{40}$/ $Cs_{2.6}H_{0.4}PW_{12}O_{40}$ (6.7% wt.)	0	40.6	6.0	2.1	63.9	1.4	1.8	0.6	28.0	4.3
	1.0	29.3	6.6	4.7	72.9	0.5	0.4	0.5	21.0	3.9
	2.0	31.0	6.6	4.5	72.7	0.8	0.6	0.8	21.9	2.7
	4.0	19.8	4.1	3.3	67.3	1.3	0.8	1.1	24.1	5.4
Pt/SiO_2-	0	40.4	1.2	0.3	70.5	0.6	2.1	2.0	24.6	0.2
$H_4SiW_{12}O_{40}$/ $Cs_{2.6}H_{0.4}PW_{12}O_{40}$ (6.7% wt.)	0.5	18.4	8.4	5.8	76.7	1.1	0.9	1.1	17.3	2.9
	1.0	10.9	6.6	5.3	76.9	1.0	0.9	1.4	16.9	2.9

[a], [b], [c] – see Footnote to Table II. 0.2 g of POM catalyst and 0.3 g of bifunctional catalyst (0.2g of POM + 0.1 of Pt/SiO_2) were used. Pre-treatment for 2 h in 10mL/min. of Ar flow at T = 498 K.

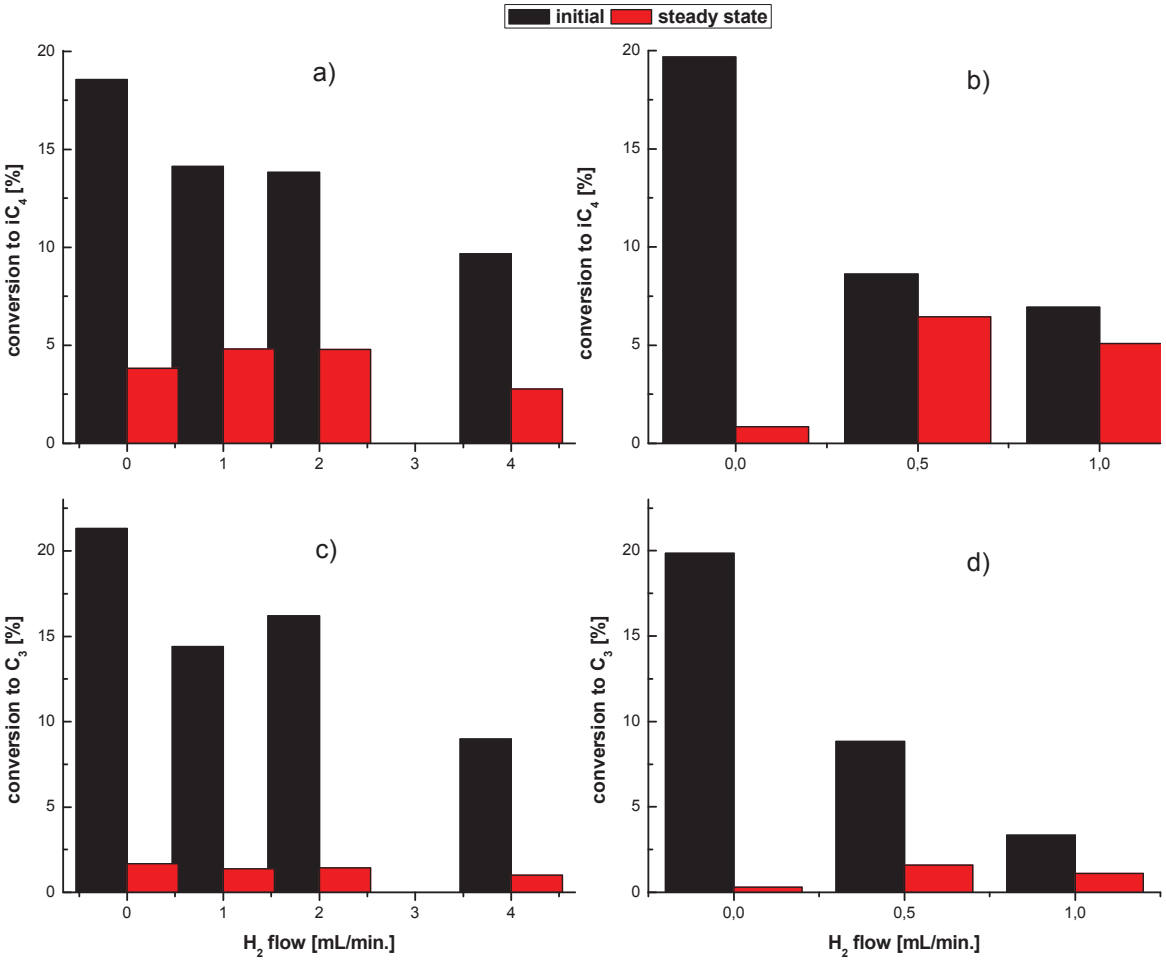

Figure 11. Influence of hydrogen concentration in the gas flow on initial (in black) and steady state (in red) conversion to isobutane (upper row) and C_3 products (lower row) over:
a);c) $H_4SiW_{12}O_{40}/Cs_{2.6}H_{0.4}PW_{12}O_{40}$(6.7% wt.) and
b);d) Pt/SiO_2-$H_4SiW_{12}O_{40}/Cs_{2.6}H_{0.4}PW_{12}O_{40}$(6.7% wt.) at 498 K.

Similar qualitative tendencies can be observed for $H_4SiW_{12}O_{40}/Cs_{2.6}H_{0.4}PW_{12}O_{40}$ (6.7% wt.) that already has been described for $(NH_4)_1H_2PW_{12}O_{40}$ in the previous part. Introduction of hydrogen to the gas flow results in decrease of initial conversion values, regardless of presence or absence of Pt. The rate of deactivation due to coking slows down and gain in selectivity to isobutane is noted. What is astonishing are the absolute numbers, showing that in spite of noble metal doping and hydrogen presence in the gas flow (even in high concentrations) formation of C_3 products never drops below 15 % at a steady state. This could be another supporting evidence that a considerable amount of it comes from the methyl shift

since this process is related to acid sites of the catalyst which are not directly influenced by Pt and H_2.

Summarizing, a new class of solid state catalysts based on $H_4SiW_{12}O_{40}$ dispersed on $Cs_{2.6}H_{0.4}PW_{12}O_{40}$ was shown to catalyze *n*-butane-isobutane isomerisation reaction and at the same time selective cracking of *n*-butane to C_3 products. This could lead to new, interesting applications but deeper understanding of the reaction mechanism (direct evidence for methyl shift and its kinetics) is needed as well as proper quantification and characterization of reaction products (propane vs. propene).

4.4 Conclusions

Various solids based on polyoxometalates were prepared, characterized and tested as catalysts in *n*-butane to isobutane isomerization reaction at mild conditions. The ammonium salts of phosphotungstic acid can be perceived as promising alternatives for current industrial catalysts and as such are object of an on-going research from our part. On the other hand, the unusual properties of another family of solids, cesium salts of phosphotungstic acid doped with silicotungstic acid, showing high efficiency in both isomerisation and selective cracking to C_3 species, make them important from more fundamental point of view, allowing insights into reaction mechanism over solid state acid surfaces.

Acknowledgments

The authors gratefully acknowledge the financial support for presented work that was provided by 7th European framework research program FP7/2007-2013, subvention no. 215193.

4.5 References

(1) Hino, M.; Kobayashi, S.; Arata, K. *J. Am. Chem. Soc.* **1979**, *101*, 6439.

(2) Garin, F.; Andriamasinoro, D.; Abdulsamad, A.; Sommer, J. *J. Catal.* **1991**, *131*, 199.

(3) Chen, F. R.; Coudurier, G.; Joly, J. F.; Vedrine, J. C. *J. Catal.* **1993**, *143*, 616.

(4) Hino, M.; Arata, K. *J. Chem. Soc.-Chem. Commun.* **1979**, 1148.

(5) Hino, M.; Arata, K. *J. Chem. Soc.-Chem. Commun.* **1988**, 1259.

(6) Hill, C. L.; (ed.) *Chem. Rev.* **1998**, *98*, 1.

(7) Lefebvre, F. *J. Chem. Soc.-Chem. Commun.* **1992**, 756.

(8) Grinenval, E.; Rozanska, X.; Baudouin, A.; Berrier, E.; Delbecq, F.; Sautet, P.; Basset, J. M.; Lefebvre, F. *J. Phys. Chem. C* **2010**, *114*, 19024.

(9) Okuhara, T.; Watanabe, H.; Nishimura, T.; Inumaru, K.; Misono, M. *Chem. Mat.* **2000**, *12*, 2230.

(10) Suzuki, S.; Kogai, K.; Ono, Y. *Chem. Lett.* **1984**, 699.

(11) Na, K.; Okuhara, T.; Misono, M. *Chem. Lett.* **1993**, 1141.

(12) Na, K. T.; Okuhara, T.; Misono, M. *J. Chem. Soc.-Chem. Commun.* **1993**, 1422.

(13) Na, K.; Okuhara, T.; Misono, M. *J. Chem. Soc.-Faraday Trans.* **1995**, *91*, 367.

(14) Suzuki, T.; Okuhara, T. *Chem. Lett.* **2000**, 470.

(15) Ma, Z. N.; Hua, W. M.; Ren, Y.; He, H. Y.; Gao, Z. *Appl. Catal. A-Gen.* **2003**, *256*, 243.

(16) Na, K.; Okuhara, T.; Misono, M. *J. Catal.* **1997**, *170*, 96.

(17) Na, K.; Iizaki, T.; Okuhara, T.; Misono, M. *J. Mol. Catal. A-Chem.* **1997**, *115*, 449.

(18) Suzuki, T.; Okuhara, T. *Catal. Lett.* **2001**, *72*, 111.

(19) Miyaji, A.; Echizen, T.; Li, L. S.; Suzuki, T.; Yoshinaga, Y.; Okuhara, T. *Catal. Today* **2002**, *74*, 291.

(20) Gayraud, P. Y.; Essayem, N.; Vedrine, J. C. *Catal. Lett.* **1998**, *56*, 35.

(21) Yang, W.; Billy, J.; Taarit, Y. B.; Vedrine, J. C.; Essayem, N. *Catal. Today* **2002**, *73*, 153.

(22) Misono, M.; Okuhara, T. *Chemtech* **1993**, *23*, 23.

(23) Xu, Y. D.; Zhang, X.; Li, H. L.; Qi, Y. X.; Lu, G. X.; Li, S. B. *Catal. Lett.* **2008**, *125*, 340.

(24) Xu, Y. D.; Zhang, X.; Li, H. L.; Qi, Y. X.; Lu, G. X.; Li, S. B. *Catal. Lett.* **2009**, *129*, 215.

(25) Bogdan, V. I.; Klimenko, T. A.; Kustov, L. M.; Kazansky, V. B. *Appl. Catal. A-Gen.* **2004**, *267*, 175.

(26) Yoshimune, M.; Yoshinaga, Y.; Okuhara, T. *Microporous Mesoporous Mat.* **2002**, *51*, 165.

(27) Gregg, S. J.; Sing, K. S. W. *Adsorption, Surface area and Porosity*; 2nd ed. ed.;

Academic Press: London, 1982.

(28) Okuhara, T.; Yamada, T.; Seki, K.; Johkan, K.; Nakato, T. *Micropor. Mesopor. Mat.* **1998**, *21*, 637.

(29) Barrett, E. P.; Joyner, L. G.; Halenda, P. P. *J. Am. Chem. Soc.* **1951**, *73*, 373.

(30) Mays, T. J. *Studies in Surface Science and Catalysis* **2007**, *160*, 57.

(31) Breck, D. W. *Zeolite Molecular Sieves*; Wiley: New York, 1974.

(32) Chen, S. S.; Wilhoit, R. C.; Zwolinski, B. J. *J. Phys. Chem. Ref. Data* **1975**, *4*, 859.

(33) Essayem, N.; Coudurier, G.; Vedrine, J. C.; Habermacher, D.; Sommer, J. *J. Catal.* **1999**, *183*, 292.

(34) Bardin, B. B.; Davis, R. J. *Appl. Catal. A-Gen.* **2000**, *200*, 219.

(35) Mishra, H. K.; Dalai, A. K.; Parida, K. M.; Bej, S. K. *Appl. Catal. A-Gen.* **2001**, *217*, 263.

(36) Ebitani, K.; Konishi, J.; Hattori, H. *J. Catal.* **1991**, *130*, 257.

Chapter 5
Enantioselective carbene C-H insertions

5.1 Introduction

Metal-catalyzed insertion of carbenes generated from diazo compounds is a well-known method of functionalization of C-H bonds [1]. So far, rhodium catalysts have been shown to be the most efficient in this type of reactions [2]. However, their biggest drawback - high price - spurs continuous efforts of the scientist to come up with new, more economically feasible alternatives. Copper complexes with various types of organic ligands like scorpionates or bisoxazolines, seem particularly predisposed to serve as a replacement for the rhodium-based systems. They were demonstrated to be catalytically active in inter- [3-4] and intramolecular [5] reactions of this type, as well as in asymmetric carbene insertions [6]. Ways of their heterogenization were also investigated and the most successful one proved to be by deposition on laponite, a bidimensional clay, by means of a simple cation exchange [6]. Quite recently purely inorganic copper catalysts deposited on silica or silica-alumina were shown to catalyze the insertion reaction of a carbene from methyl phenyldiazoacetate into C-H bond of THF, thus allowing to simplify the synthetic procedures by avoiding laborious, time-consuming ligand preparation steps [7].

There exist numerous reports in the literature dealing with a combined chemistry of copper and polyoxometalates. Interests of the scientists range from copper-exchanged clusters (where acidic protons are replaced with copper cations) [8] through copper-containing or copper-substituted compounds [9-11] up to complicated multidimensional supramolecular architectures of polyanions and organometallic copper fragments [12-15]. By comparison examples of polyoxometalate-copper (bifunctional) catalytic systems are scarce. Cu-exchanged phosphomolybdic acid $H_3PMo_{12}O_{40}$ was reported to be active in selective dehydration of ethanol [16]. A mixture of copper-substituted polyoxometalates was used as catalyst for the epoxidation of limonene in biphasic (water-organic) reaction media using hydrogen peroxide as the oxygen donor [17]. Copper-substituted cobaltotungstic acid $[CuCoW_{11}O_{39}]^{7-}$ catalyzed oxidation of ascorbic acid by peroxynitrite [18]. Di-copper substituted silicotungstic acid was recently shown to catalyze efficiently oxidative alkyne homocoupling [19-20] and cyclopropanations of olefins with ethyl diazoacetate in the homogenous conditions [21].

Because of their tendency to develop high specific surface areas upon exchange of their acidic protons with alkaline metal cations [22], inorganic salts of polyoxometalates could serve as another type of support for the stereoselective copper catalysts, anchored to their surface via cation-anion electrostatic interactions. Similar heterogenous systems for asymmetric cyclopropanations of olefins with diethyl acetate, consisting of: silica-supported

phosphotungstic acid $H_3PW_{12}O_{40}$ and copper complexes [23] or copper salts of $H_3PW_{12}O_{40}$ [24] have already been described. Moreover, unexpected transformations of metal complexes upon grafting on anhydrous polyanionic clusters were observed to take place (see Chapter 3 Part B) and new interesting chemical phenomena are still to be expected as the domain will expand.
As it will be shown, this work is a pioneering example of the use of self-supported polyoxometalates as carriers for copper and rhodium species, for the asymmetric carbene insertion reactions into non-olefinic C-H bonds.

5.2 Experimental part

Materials. Phosphomolybdic acid $H_3PMo_{12}O_{40}.xH_2O$ (99+%, Aldrich), phosphotungstic acid $H_3PW_{12}O_{40}.xH_2O$ (99+%, Aldrich), cesium carbonate Cs_2CO_3 (99%, Aldrich), copper(II) triflate $Cu(OTf)_2$ (98%, Aldrich) and rhodium(II) acetate dimer $Rh_2(OAc)_4$ (99.99%, Aldrich) were used as received.
$H_5PV_2Mo_{10}O_{40}$ and $H_6PV_3Mo_9O_{40}$ were synthesized from MoO_3 (99%, Acros), V_2O_5 (99.6%, Acros) and phosphoric acid H_3PO_4 (85%, Aldrich) according to Berndt et al. [25].
All solvents were distilled according to published procedures and kept under Ar.

Preparation of the supports. Cesium salts of polyoxometalates showing high specific surface areas [22] and with the general formula $Cs_xH_{3-x}PZ_{12}O_{40}$, where Z = W or Mo, were prepared as follows: A stoechiometric amount of Cs_2CO_3 was added under vigorous stirring to an aqueous solution of the desired polyacid ($H_3PW_{12}O_{40}$, $H_3PMo_{12}O_{40}$), resulting in effervescence and immediate precipitation of a microcrystalline solid. Stirring was continued until complete evaporation of the solvent at room temperature. The powder was then collected without washing and ground in the mortar.
The composite materials: $H_6PV_3Mo_9O_{40}/Cs_3PW_{12}O_{40}$, $H_5PV_2Mo_{10}O_{40}/Cs_3PMo_{12}O_{40}$ and $H_3PW_{12}O_{40}/Cs_3PMo_{12}O_{40}$ were synthesized as follows: in a first step the precipitation of fully saturated salts $Cs_3PZ_{12}O_{40}$, where Z = W or Mo, was performed as described above but after half an hour of stirring at room temperature, the appropriate amount of an acidic form of a given polyoxometalate: $H_6PV_3Mo_9O_{40}$, $H_5PV_2Mo_{10}O_{40}$ or $H_3PW_{12}O_{40}$ was added to the reaction mixture. The resulting powders were gathered after the evaporation of the solvent, without any washing. The quantities of doping acids were calculated so as to create a monolayer on the surface of completely saturated salts of POMs, based on the specific surface

area values of the supports and assuming that each Keggin unit had a surface area of 1.9 nm^2 [26].

All these supports were treated under high vacuum (10^{-5} Torr) for 2 hours at 200°C to dehydrate polyoxometalates and afterwards heated for another 2 hours at 200°C under dry O_2 to reoxidize the clusters that might have been reduced upon the previous manipulations and transferred to the glovebox.

Deposition of metal precursors. Copper(II) triflate $Cu(OTf)_2$ and rhodium(II) acetate dimer $Rh_2(OAc)_4$ were chosen as metal precursors. Appropriate amount of each compound was dissolved in a small quantity (1 mL) of dry acetonitrile under Ar and resulting solution was transferred to a Schlenk vessel containing the prepared support. Suspension was left stirring overnight at RT under Ar and afterwards the solvent was removed under vacuum at 50°C. So-obtained catalysts were gathered and stored in the glovebox. Three catalysts with different metal loading were prepared for each type of the support. The quantities of metal precursors were calculated so as to give H^+:M^{2+} ratios of 1:2, 1:1 and 2:1, where H^+ = surface protons of the support and $M^{2+} = Cu^{2+}$ or Rh^{2+}.

Synthesis of methyl phenyldiazoacetate according to [27] (see Scheme 1). In a round-bottom flask 3.125 g (20 mmol) of methyl 2-phenyl acetate and 6.0 g (25 mmol) of 4-acetamidobenzenesulfonyl azide were dissolved in 60 mL of acetonitrile at room temperature. The solution was put in an ice bath and 3.8 g (25 mmol) of DBU (1,8-diazabicyclo[5.4.0]undec-7-ene) were added dropwise under vigorous stirring at 0°C. The reaction mixture was then left to warm up and stirred for 24 hours at room temperature. Afterwards the solution was extracted with saturated solutions of NH_4Cl (2x60 mL) and NaCl (1x60 mL). The resulting portions of the aqueous phase were extracted with Et_2O (1x180 mL). All four portions of organic phases were then combined and dried by vigorous stirring with anhydrous Mg_2SO_4. The solvents were removed under vacuum and obtained solid extracted with Et_2O/hexane mixture (1:1) until complete discoloration. After filtration the solvents were removed under vacuum. The crude liquid product was purified on the chromatographic column with SiO_2 as a stationary phase and AcOEt/hexane (1:9) mixture as eluent. Typically, 1.6 g (9 mmol) of orange liquid product was obtained (yield = 45%). ^1H NMR (300 MHz, $CDCl_3$): 7.47 (m, 2H), 7.39 (m, 2H), 7.19 (m, 1H), 3.87 (s, 3H); ^{13}C NMR (75 MHz, $CDCl_3$): 165.6, 129.0, 125.9, 125.5, 124.0, 52.0.

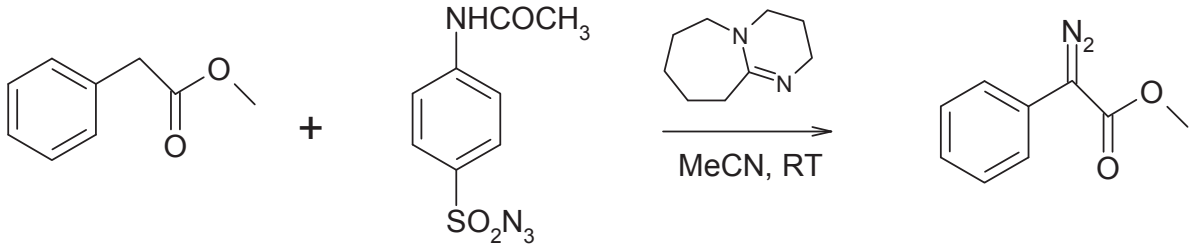

Scheme 1. Synthesis of methyl phenyldiazoacetate.

Heterogenous catalysis. In a typical procedure 50 mg of each catalyst were put in a two-neck round bottom flask with a stirring bar and connected to the reflux condenser under Ar. 100 mg of *n*-decane (used as an internal standard) was dissolved in 6 ml of dry THF/THP and added to the catalyst. In the case of the reaction with cyclohexane, *n*-decane was added after the completion of the reaction. The suspension was stirred and refluxed for 15 min. and then 150 mg of methyl phenyldiazoacetate dissolved in 9 mL of dry THF was slowly added to the vessel over the period of 2h via syringe pump. Stirring under reflux continued for one hour once the addition has been completed. Afterwards, reaction mixture was cooled down to room temperature and the catalyst separated by means of centrifugation. Liquid phase was analysed by means of GC with FID detector. The detector response was compared with calibration curves prepared previously, thus leading to the determination of yield and diastereoselectivity. Column: 30 m, phenylsilicone. Pressure: 20 psi. Oven temperature program: 120ºC (3 min) – 3ºC/min. – 200ºC (5 min). Retention times: *n*-decane 1.4 min, methyl phenyldiazoacetate 6.0 min, *syn* and *anti* products ~15.0 min.

5.3 Results and discussion

In the first instance the most rudimentary technique of metal deposition was used to prepare heterogenous catalysts – solubilization of the precursor in an organic solvent, stirring with the support overnight and removal of the solvent under vacuum. Acetonitrile was chosen as a solvent because it is able to solubilize both copper and rhodium precursors and to some extent also anhydrous acidic polyoxometalates [[28]]. Upon impregnation, various colour changes of the supernatant solutions were noted from light blue to green and yellow (see Figure 1). As no physico-chemical catalysts characterization was performed, these phenomena may only speculatively be attributed to either changes of oxidation degree of copper or copper reactions with polyoxometalates other than cation exchange. Indeed, reports about copper incorporation into the structure of the polyanionic clusters preceded by their partial decomposition and

reorganization or self-assembly of sandwich polyoxometalates around copper-oxo cores etc. are widely encountered in the literature [29-30].

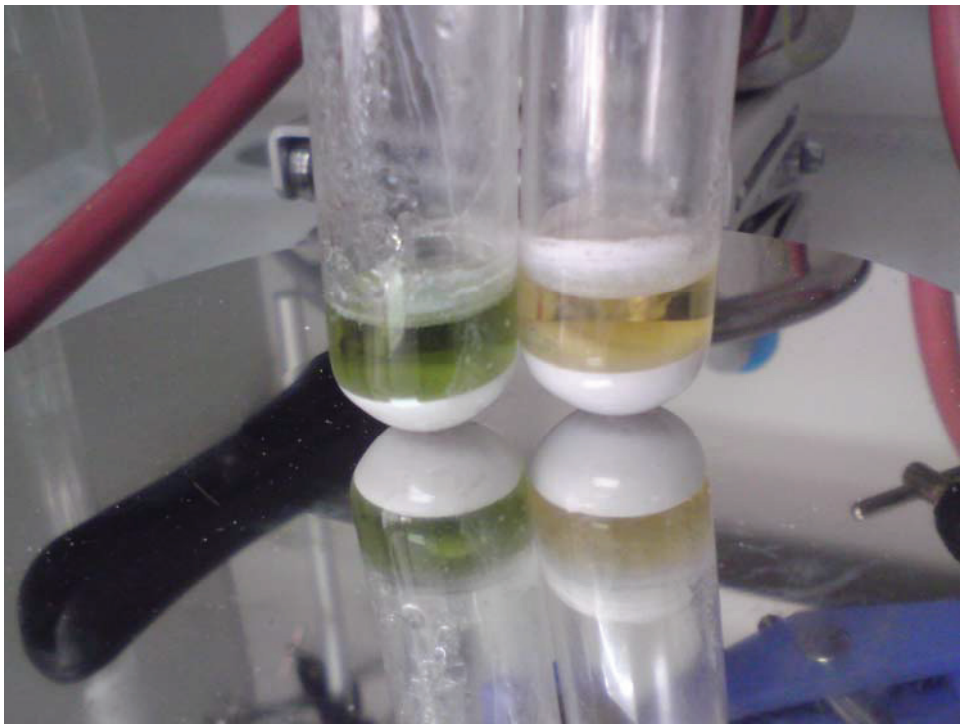

Figure 1. Suspensions of copper triflate in acetonitrile over $Cs_{1.7}H_{1.3}PW_{12}O_{40}$ after 1 night of stirring at RT. H^+:Cu^{2+} ratios of 1:2 (left) and 2:1 (right).

As no washing of so-obtained catalysts has been performed, a possibility that some copper precursor was only physisorbed on the surface of the support cannot be excluded either and must be taken into account when interpreting the catalytic results.

5.3.1 Carbene insertion into C-H bonds of tetrahydrofuran (THF)

A reaction of insertion of the carbene generated from methyl phenyldiazoacetate into C-H bonds of tetrahydrofuran was chosen to be the first test of the performance of so-prepared catalysts (see Scheme 2).

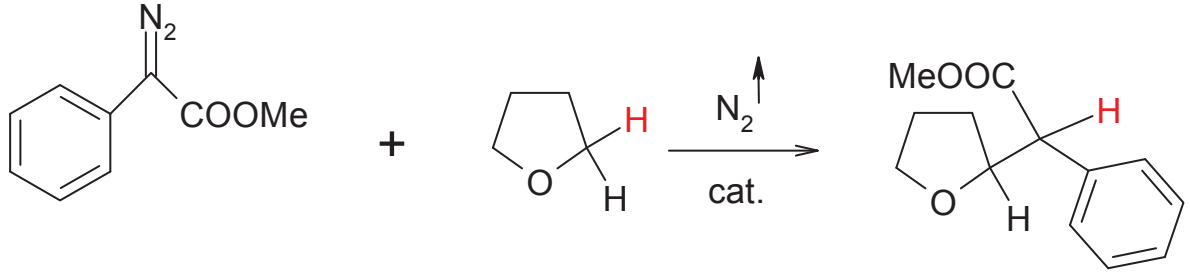

Scheme 2. Catalytic carbene insertion of methyl phenyldiazoacetate into THF.

The products are two diastereoisomers in *syn* and *anti* configurations, each existing in two enantiomeric forms (see Scheme 3). The stereochemical course of the insertion of carbene with copper catalysts cannot be outlined, as the reaction mechanism is still poorly understood. What is known, though, is that the reaction itself is catalyzed by Cu(I) species generated *in situ* by diazo compounds.

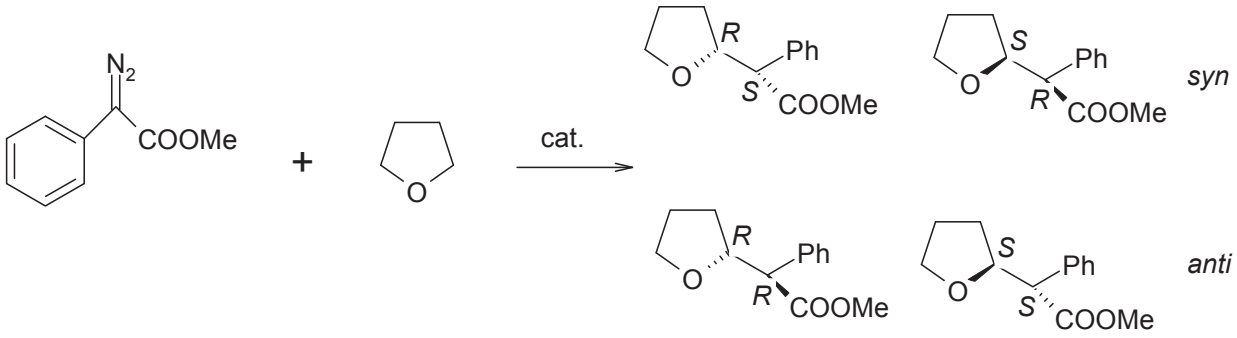

Scheme 3. Stereoselectivity of the carbene insertion from methyl phenyldiazoacetate into THF.

The catalytic results are given in Table I.

Table I. Catalysts performance in carbene insertion to THF.

sample	**support**	**mass catalyst [mg]**	**mass Cu [mg]**	**mass Cu/ mass substrate [%]**	**product yield [%]**	***anti/syn***
$Cu(OTf)_2$ homogenous	-	6.7	1.190	0.73	37.6	23:77
blank A	$Cs_{1.7}H_{1.3}PW_{12}O_{40}$	55.8	0	0	7.3	43:57
blank B	$Cs_{2.5}H_{0.5}PMo_{12}O_{40}$	55.0	0	0	5.2	40:60
CuO_x	SiO_2-Al_2O_3	26.2	2.096	1.40	43.0	34:66
P100	$Cs_{1.7}H_{1.3}PW_{12}O_{40}$	48.5	0.606	0.41	78.0	25:75
P101		48.4	1.129	0.76	97.9	25:75
P101 recycled		25.9	0.604	0.40	63.4	34:66
P102		45.2	1.861	1.21	88.0	24:76
P103	$Cs_{2.5}H_{0.5}PMo_{12}O_{40}$	49.0	0.537	0.36	55.4	24:76
P104		56.0	1.156	0.73	88.0	23:77
P105		48.4	1.787	1.20	94.8	24:76
P106	$H_6PV_3Mo_9O_{40}$/ $Cs_3PW_{12}O_{40}$	54.3	0.787	0.53	73.7	24:76
P107		49.6	1.327	0.90	77.5	24:76
P108		55.6	2.580	1.75	89.8	24:76
P109	$H_5PV_2Mo_{10}O_{40}$/ $Cs_3PMo_{12}O_{40}$	52.4	0.628	0.42	76.4	24:76
P110		47.3	1.082	0.74	86.8	24:76
P112	$H_3PW_{12}O_{40}$/ $Cs_3PMo_{12}O_{40}$	57.2	0.402	0.26	87.1	25:75
P113		46.2	0.781	0.52	86.9	25:75
P114		51.3	1.582	1.05	81.4	24:76

Reaction is routinely performed in dry THF, serving here as a solvent and reagent at the same time and at high temperatures (reflux conditions), in order to overcome carbenes tendency to dimerize, which demands significantly less energy than the insertion reaction. Because of the high reactivity of diazocompounds when in contact with the catalyst, the reaction is almost instantaneous and the whole substrate is consumed in one way or another.

All prepared catalysts show remarkably high activities with product yields being in general greater than 75%. High diastereoselectivites (*anti/syn* ratios 25:75) are also observed. The enantioselectivities, however, were not established. Copper-polyoxometalate systems are much more efficient than copper triflate precursor tested in homogenous conditions as well as purely inorganic heterogenous catalyst - copper oxide deposited on silica-alumina. It has been claimed that this support (i.e. SiO_2-Al_2O_3) can have a stabilizing effect on the Cu(I) species, which are catalytically active in this reaction [[7]]. The same explanation may apply to polyoxometalate supports, especially because yields and stereoselectivities hardly vary with their type, which could suggest no direct involvement of polyanionic clusters in the reaction mechanism. On the other hand, blank tests performed in absence of copper do show some product generation, though almost without any stereopreference at all. Extremely low copper/substrate mass ratios (around 1%) constitute another advantage of these new catalysts. The effect of copper loading on the catalyst performance is plotted in Fig. 2.

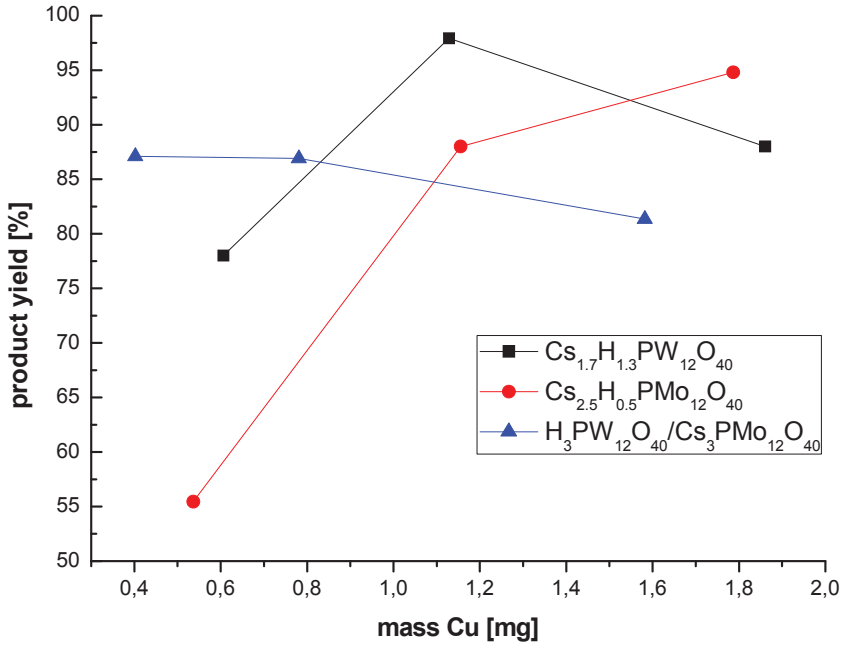

Figure 2. Effect of the copper loading on the product yield for three series of polyoxometalate supports.

For each type of the support: $Cs_{1.7}H_{1.3}PW_{12}O_{40}$, $Cs_{2.5}H_{0.5}PMo_{12}O_{40}$ and $H_3PW_{12}O_{40}/Cs_3PMo_{12}O_{40}$ a different influence of the metal loading on yield of the insertion product is noted. However, the possibility of presence of multiple copper species on the surface of the catalysts calls to treat the curves presented above with caution and precludes any further going assumptions.

Only one recyclability test has been performed and the results show considerable loss of activity of the tested catalyst (decrease of around 30%). Nevertheless, only half of it was gathered and reused. Slight change of diastereoselectivity was also observed between the runs and may be an indication that at least some of the copper species participating in the first reaction got eliminated when the solid catalyst was separated from the supernatant liquid and washed.

.

5.3.2 Carbene insertion into C-H bonds of tetrahydropyran (THP)

Carbene insertion into tetrahydropyran is known to be more difficult to promote by copper catalysts, possibly because of the bulkier ether ring of the substrate causing greater steric hindrance. The reaction stereoselectivity is outlined in Scheme 4.

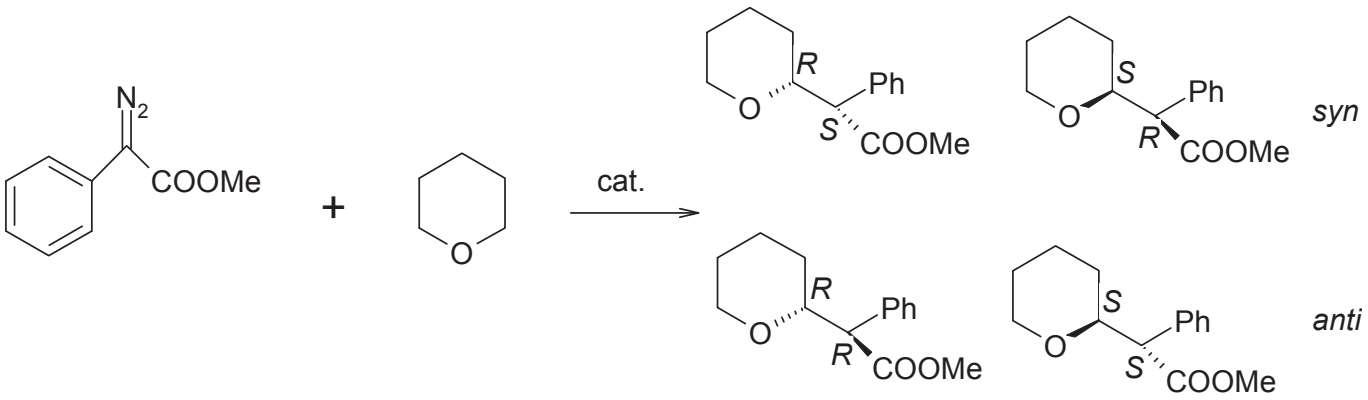

Scheme 4. Stereoselectivity of the carbene insertion from methyl phenyldiazoacetate into THP.

The catalytic results are given in Table II. Product yield values are given only as estimated based on the calibration curves prepared for the reaction with THF and should be therefore used only to evaluate catalysts performance in relation to themselves.

Table II. Catalysts performance in carbene insertion to THP.

sample	support	mass catalyst [mg]	mass Cu [mg]	mass Cu/ mass substrate [%]	product yield* [%]	*anti/syn*
$Cu(OTf)_2$ homogenous	-	4.6	0.817	0.54	13.5	25:75
P101	$Cs_{1.7}H_{1.3}PW_{12}O_{40}$	51.1	1.192	0.77	25.2	25:75
P101 4h addition		97.0	2.263	1.52	26.2	23:77
P102		52.5	2.162	1.43	29.4	25:75
P104	$Cs_{2.5}H_{0.5}PMo_{12}O_{40}$	59.6	1.230	0.85	19.3	25:75
P105		51.9	1.916	1.16	15.0	24:76
P108	$H_6PV_3Mo_9O_{40}$/ $Cs_3PW_{12}O_{40}$	57.3	2.659	1.76	25.6	24:76
P110	$H_5PV_2Mo_{10}O_{40}$/ $Cs_3PMo_{12}O_{40}$	47.0	1.075	0.69	30.6	24:76
P115	$Cs_{1.7}H_{1.3}PW_{12}O_{40}$	54.7	Rh 0.933	0.60	10.6	34:66

* estimated

Performance of all tested catalysts is again significantly similar, in terms of yields as well as stereoselectivities. Heterogenous catalysts are clearly superior than the copper precursor. There was no visible influence on the reaction outcome of the combined increase of catalysts amount and decrease of the speed of substrate addition. This could mean that the inherent limitations of this catalytic system in this particular reaction has been reached. One rhodium catalyst was also prepared and tested in order to compare its behaviour with copper-containing samples but its performance was rather disappointing.

5.3.3 Carbene insertion into C-H bonds of cyclohexane

There are no examples in the literature so far of purely inorganic copper catalysts able to promote efficiently carbene insertions into purely aliphatic C-H bonds (like the ones in e.g. cyclohexane). Because of the substrate's symmetry, the reaction should proceed to only two isomeric products (Scheme 5).

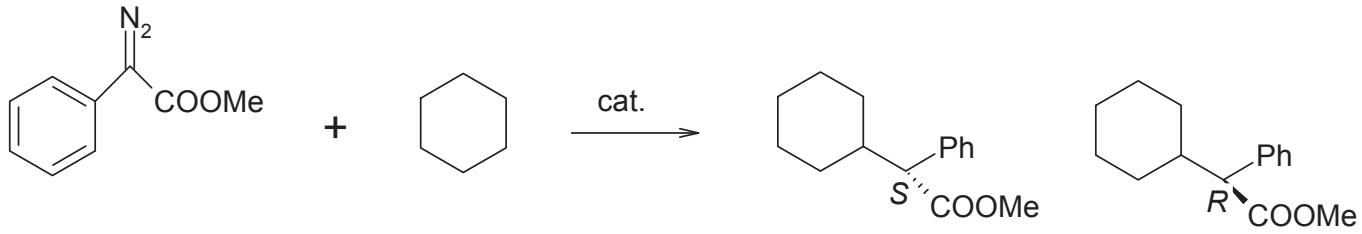

Scheme 5. Stereoselectivity of the carbene insertion from methyl phenyldiazoacetate into cyclohexane.

The catalytic results are given in Table III. Product yield values are given only as estimated based on the calibration curves prepared for the reaction with THF and should be therefore used only to evaluate catalysts performance in relation to themselves.

Table III. Catalysts performance in carbene insertion to cyclohexane.

sample	**support**	**mass catalyst [mg]**	**mass Cu [mg]**	**mass Cu/ mass substrate [%]**	**product yield* [%]**
$Cu(OTf)_2$ homogenous	-	6.7	1.190	0.80	5.8
$Rh_2(OAc)_4$ homogenous	-	7.6	Rh 3.535	2.29	81.5
P102	$Cs_{1.7}H_{1.3}PW_{12}O_{40}$	49.6	2.042	1.41	2.4
P104	$Cs_{2.5}H_{0.5}PMo_{12}O_{40}$	49.0	1.012	0.69	6.3
P105		56.1	2.070	1.36	4.2
P108	$H_6PV_3Mo_9O_{40}$/ $Cs_3PW_{12}O_{40}$	57.3	2.659	1.75	4.9
P110	$H_5PV_2Mo_{10}O_{40}$/ $Cs_3PMo_{12}O_{40}$	54.7	1.251	0.83	9.4
P115	$Cs_{1.7}H_{1.3}PW_{12}O_{40}$	51.3	Rh 0.875	0.57	14.4

* estimated

All the tested catalysts show poor performance in this reaction, regardless of the support type and copper loading. Especially in comparison with a rhodium complex, their behavior looks particularly unimpressive. This time however, rhodium-containing sample works better than copper-containing ones. Optimization of catalyst preparation is therefore needed by proper choice of metal precursor and deposition method.

5.4 Conclusions

The extremely promising preliminary results have been obtained in the carbene insertion reactions into C-H bonds of cyclic ethers (tetrahydrofuran, tetrahydropyran) catalyzed by purely inorganic composite materials made of copper and cesium salts of polyoxometalates. All prepared catalysts proved superior to their homogenous copper counterpart in terms of yield and diastereoselectivity.

In the case of carbene insertion to cyclohexane, copper-polyoxometalate catalysts were practically inactive. Rhodium-containing material proved only slightly better.

Nevertheless, all these heterogenous systems are not yet well-defined nor is their catalytic behaviour understood. In the future four main lines of investigations should be addressed:

- Extensive characterization of the catalysts, especially as the nature of copper-polyoxometalate interactions remains obscure
- The still elusive reaction mechanism
- Proper catalyst recyclability and reusability tests, verification of catalysts resistance to air and humidity
- Introduction of bisoxazoline ligands in order to test their influence on catalysts performance especially in terms of enantioselectivity

Heterogenous catalytic systems for carbene insertions to aliphatic C-H bonds remain a challenge on its own.

5.5 References

(1) Ye, T.; McKervey, M. A. *Chem. Rev.* **1994**, *94*, 1091.

(2) Davies, H. M. L.; Beckwith, R. E. J. *Chem. Rev.* **2003**, *103*, 2861.

(3) Caballero, A.; Diaz-Requejo, M. M.; Belderrain, T. R.; Nicasio, M. C.; Trofimenko, S.; Perez, P. J. *J. Am. Chem. Soc.* **2003**, *125*, 1446.

(4) Diaz-Requejo, M. M.; Belderrain, T. R.; Nicasio, M. C.; Trofimenko, S.; Perez, P. J. *J. Am. Chem. Soc.* **2003**, *125*, 12078.

(5) Doyle, M. P.; Phillips, I. M. *Tetrahedron Lett.* **2001**, *42*, 3155.

(6) Fraile, J. M.; Garcia, J. I.; Mayoral, J. A.; Roldan, M. *Org. Lett.* **2007**, *9*, 731.

(7) Fraile, J. M.; Mayoral, J. A.; Ravasio, N.; Roldan, M.; Sordelli, L.; Zaccheria, F. *J. Catal.* **2011**, *281*, 273.

(8) Zhou, G. D.; Yang, X. M.; Liu, J.; Zhen, K. J.; Wang, H. S.; Cheng, T. X. *J. Phys. Chem. B* **2006**, *110*, 9831.

(9) Yu, F.; Long, Y. X.; Ren, Y. P.; Kong, X. J.; Long, L. S.; Huang, R. B.; Zheng, L. S. *Dalton Trans.* **2010**, *39*, 7588.

(10) Bi, L. H.; Kortz, U. *Inorg. Chem.* **2004**, *43*, 7961.

(11) Mal, S. S.; Bassil, B. S.; Ibrahim, M.; Nellutla, S.; van Tol, J.; Dalal, N. S.; Fernandez, J. A.; Lopez, X.; Poblet, J. M.; Biboum, R. N.; Kelta, B.; Kortz, U. *Inorg. Chem.y* **2009**, *48*, 11636.

(12) Zhang, C. J.; Pang, H. J.; Tang, Q.; Wang, H. Y.; Chen, Y. G. *J. Solid State Chem.* **2010**, *183*, 2945.

(13) Pavani, K.; Singh, M.; Ramanan, A. *Aust. J. Chem.* **2011**, *64*, 68.

(14) Wang, X. L.; Wang, Y. F.; Liu, G. C.; Tian, A. X.; Zhang, J. W.; Lin, H. Y. *Dalton Trans.* **2011**, *40*, 9299.

(15) Zhang, C. H.; Zhang, C. J.; Chen, Y. G.; Liu, S. X. *Inorg. Chem. Comm.* **2011**, *14*, 1465.

(16) Ali, T. T.; Al-Thabaiti, S. A.; Alyoubi, A. O.; Mokhtar, M. *J. Alloy Compd* **2010**, *496*, 553.

(17) Casuscelli, S.; Herrero, E.; Crivello, N.; Perez, C.; Egusquiza, M. G.; Cabello, C. I.; Botto, I. L. *Catal. Today* **2005**, *107-08*, 230.

(18) Geletti, Y. V.; Bailey, A. J.; Boring, E. A.; Hill, C. L. *Chem. Comm.* **2001**, 1484.

(19) Kamata, K.; Yamaguchi, S.; Kotani, M.; Yamaguchi, K.; Mizuno, N. *Ang. Chem.-Int. Ed.* **2008**, *47*, 2407.

(20) Yamaguchi, K.; Kamata, K.; Yamaguchi, S.; Kotani, M.; Mizuno, N. *J. Catal.* **2008**, *258*, 121.

(21) Boldini, I.; Guillemot, G.; Caselli, A.; Proust, A.; Gallo, E. *Adv. Synth. Catal.* **2010**, *352*, 2365.

(22) Okuhara, T.; Watanabe, H.; Nishimura, T.; Inumaru, K.; Misono, M. *Chem. Mat.* **2000**, *12*, 2230.

(23) Torviso, M. R.; Blanco, M. N.; Caceres, C. V.; Fraile, J. M.; Mayoral, J. A. *J. Catal.* **2010**, *275*, 70.

(24) Yadav, J. S.; Reddy, B. V. S.; Purnima, K. V.; Nagaiah, K.; Lingaiah, N. *J. Mol. Catal. A-Chem.* **2008**, *285*, 36.

(25) Berndt, S.; Herein, D.; Zemlin, F.; Beckmann, E.; Weinberg, G.; Schütze, J.; Mestl, G.; Schlögl, R. *Ber. Bunsen Phys. Chem.* **1998**, *102*, 763.

(26) Misono, M.; Okuhara, T. *Chemtech* **1993**, *23*, 23.

(27) Starmans, W. A. J.; Thijs, L.; Zwanenburg, B. *Tetrahedron* **1998**, *54*, 629.

(28) Legagneux, N. PhD, Université Claude Bernard - Lyon 1, 2009.

(29) Limanski, E. M.; Piepenbrink, M.; Droste, E.; Burgemeister, K.; Krebs, B. *J. Clust. Sci.* **2002**, *13*, 369.

(30) Zheng, S.-T.; Yuan, D.-Q.; Zhang, J.; Yang, G.-Y. *Inorg. Chem.* **2007**, *46*, 4569.

Concluding remarks

Perspectives

To conclude, the main goal of this work was to show that because of their unique chemical properties, polyoxometalates can be used as catalysts in a variety of reactions in heterogenous conditions, either in gas-solid or gas-liquid systems. Their main advantages lay in a combination of acidic and redox properties, chemical and thermal stability and commercial availability.

More specifically, mechanistic studies in the area of oxidation catalysis were performed, focusing on methane-to-methanol partial oxidation reaction. On the silica-supported polyoxometalates methane was shown to be readily activated at room temperature and that regardless of a polyoxometalate type, a C-H activation, typically considered as difficult, was never a limiting step for an overall process. The first reaction intermediate: methoxy species $[SiMo_{12}O_{40}(CH_3)]^{3-}$ coming from the ^{13}C-enriched methane adsorption at 200C on the surface of a silica-dispersed silicomolybdic acid, was detected by means of ^{13}C SS NMR technique. Hydrolysis of this species led to methanol formation, evidenced by ^{13}C liquid NMR and thus completing the catalytic cycle. In parallel studies, various surface species were formed on the surface of bulk and silica-supported polyoxometalates upon adsorption of ^{13}C-enriched MeOH and their reactivity followed by ^{13}C SS NMR upon thermal treatment. Presence of two distinct types of methoxy species on the surface of polyoxometalates was shown, located on topologically unequivalent oxygen atoms: terminal (single coordinated) and bridging (double coordinated). Different local environments of oxygen atoms influence the chemical shifts of methyl species attached to them, resulting in the resonances at 58 and 77 ppm, respectively. The evolution of methoxy species can proceed via two ways i.e. by dehydration/coupling leading to dimethyl ether formation or by oxidation to formyl entity (detected at 172 ppm) and further to CO_2. Both pathways coexist although not to the same degree, their respective contributions complying with the predominant polyoxometalate characteristics (acidity for tungstic clusters or redox for molybdic ones).

In the future, the most important issue to address is of course how to apply this model methane-to-methanol catalytic system on a larger scale. As has been shown, reaction in methane-oxygen (or methane-air, for the sake of safety issues) stream leads only to CO_2 production. Introduction of water vapour to the gas flow could work, provided that proper parameters are found so as not to decrease significantly the polyoxometalates acidity by rehydration. The same holds for the temperature range which is seriously limited by high

surface species reactivity and risk of their decomposition. Use of membrane reactor to get rid of the released H_2 is another tempting idea. From the mechanistic point of view, detailed studies on the surface methoxy/formyl species could provide some additional data about factors influencing their stability on various polyoxometalate frameworks (like lacunary species, substituted Keggin-type clusters etc.) and thus contribute to efficiently realize their desorption.

Functionalization of high specific surface area cesium salts of tungstic and molybdic polyoxometalates in order to prepare catalysts with new properties was shown via three different ways: deposition of vanadomolybdic polyanionic clusters, impregnation with salts of late transition and noble metal atoms and surface organometallic chemistry (SOMC). Various physico-chemical techniques were employed for a detailed characterization of obtained solids. Main disadvantages of these approaches are given so that synthetic procedures could be modified in the future. The next step is obviously their application in catalysis in order to evaluate their performance and consecutive studies on reactivity/structure relations. These in turn can lead to rational catalyst design and facilitate reaction mechanism investigations.

A special case of SOMC of platinum (II) dialkyl complex was treated separately. Grafting of $PtMe_2COD$ on the surface of various polyoxometalate supports at room temperature led to methane or combined methane and ethane release. These phenomena were shown to be dependent on predominant polyoxometalate characteristics (acidity for tungstic clusters or redox for molybdic and vanadomolybdic ones), just as the methoxy species reactivity described in the previous chapter. Oxidative addition of a polyoxometalate proton to the Pt(II) center followed by C-H/C-C coupling and reductive elimination led to a gas molecule formation and release. Mechanism of a decomposition of alkyl platinum complexes in acidic media is of outmost importance in modern chemistry as a way to indirectly probe alkane activation and oxidation on Pt(II) centers, according to microscopic reversibility principle. Based on the gathered experimental data, we can assume that a proper combination of platinum(II) and polyoxometalates is therefore likely to give a long-awaited short chain alkanes oxidation system.

First of all, however, further studies are needed to elucidate each reaction step of the grafting process and isolate and characterize the intermediate species. Formation of Pt hydride entity is cited in the literature as a likely intermediate but low-temperature NMR was not successful in

its detection. Employing mass spectrometry seems a reasonable alternative as it is faster, more sensitive and ion separation techniques allow to isolate the interesting species from their environment (other reagents, solvent molecules) thus increasing their life time.

An example of acidic catalysis with polyoxometalates was presented as well. Different types of self-supported polyanionic clusters based on phosphotungstic $H_3PW_{12}O_{40}$ and silicotungstic $H_4SiW_{12}O_{40}$ were synthesized and characterized. They were evidenced to catalyze efficiently *n*-butane to isobutane skeletal isomerisation reaction at mild conditions (225 °C, atmospheric pressure). Platinum co-catalyst and addition of hydrogen to the gas flow were used to prevent deactivation by coking. Contributions of mono- and bimolecular mechanisms of isomerisation to the overall conversion and selectivity were discussed.

Pt in combination with ammonium salts of $H_3PW_{12}O_{40}$ seem an interesting alternative for currently used industrial catalysts but further optimization of these systems is needed, e.g. through testing of other methods of functionalization with Pt. The effect of calcination of the salts in order to remove ammonium cations on their reactivity would be interesting to verify, as well as an introduction of small fraction of water vapour to the gas flow to stimulate coke burning. At last, isomerisation of other short chain alkanes (pentane, hexane) is also expected to give good to excellent results.

Finally, preliminary experimental data were gathered on the performance of copper catalysts dispersed on cesium salts of polyoxometalates in carbene insertions of diazo compounds into non-olefinic C-H bonds of cyclic ethers. Copper precursors were deposited on polyoxometalate supports by means of impregnation and tested in solid-liquid phase reactions, showing unprecedented high yields and stereoselectivities for purely inorganic catalysts in this type of processes.

Research in this area has just started so a lot is still to be done. The most important issue is the catalysts characterization in order to verify: how much of the introduced copper interacts with the polyoxometalates and how much retains the form of the precursor (in other words – how many copper species are there and what is there independent catalytic activity, is washing needed to get rid of the excess of copper precursor and how will it affect the catalysts performance), what is the nature of the interaction with the polyanionic clusters, do they undergo some kind of decomposition to incorporate copper cations, is there a copper

oxidation degree change. A plethora of techniques may be used here e.g. elemental analyses, IR, DRX, SS NMR (mainly of ^{31}P but also ^{133}Cs), although Cu^{2+} species are paramagnetic and may hinder the measurements, EXAFS, XPS and XANES. The next step would be an attempt to introduce some bisoxazoline ligands and verify whether the catalysts performance is improved this way. Finally, larger scope of diazocompounds and ether reagents should be investigated to generalize the observed tendencies and suggest a mechanistic picture explaining the observed phenomena.

RESUME en français
L'objectif de la thèse était la préparation et la caractérisation des catalyseurs hétérogènes à base de polyoxometalates. L'étude mécanistique d'oxydation du méthane jusqu'au méthanol a montré que sur des polyoxometalates supportés sur la silice l'activation C-H a lieu déjà à la température ambiante. L'adsorption du méthane-^{13}C sur $H_4SiMo_{12}O_{40}$ supporté, suivie par RMN solide a mis en évidence la création de l'espèce methoxy $[SiMo_{12}O_{40}(CH_3)]^{3-}$. Le cycle catalytique est complété par l'hydrolyse de cette espèce - méthanol est formé et une molécule de l'eau recrée la structure du départ de polyoxometalate. L'adsorption du méthanol-^{13}C sur des polyoxometalates a montré la création de deux types des espèces methoxy, localisées sur des atomes d'oxygène terminaux ou pontants est caractérisées par deux signaux RMN distincts – à 58 et 77 ppm, respectivement. En greffant un complexe de platine $PtMe_2COD$ sur les sels de césium de polyoxometalates, le dégagement du méthane ou de la mélange du méthane et de l'éthane a été observé et expliqué par la séquence de l'addition oxydative du proton de polyoxometalate au centre métallique, couplage C-H ou C-C et finalement l'élimination réductrice et libération d'une molécule de gaz. Sels d'ammonium de l'acide phosphotungstique $H_3PW_{12}O_{40}$ ont été montrées de catalyser l'isomérisation du *n*-butane a l'isobutane dans des conditions douces (225°C, 1 atm.). Composé du cuivre $Cu(OTf)_2$ sur la surface des sels inorganiques des polyoxometalates donne des catalyseurs très actifs en insertion des carbenes aux liaisons C-H des éthers cycliques.

TITRE en anglais
Applications of polyoxometalates in heterogenous catalysis.

RESUME en anglais
The aim of this work was preparation and characterization of catalysts based on polyoxometalates and their use in various catalytic reactions in heterogenous conditions. Methane C-H activation on silica-supported polyoxometalates was shown already at room temperature. Methoxy species $[SiMo_{12}O_{40}(CH_3)]^{3-}$ from the ^{13}C-enriched methane adsorption at 200°C on the surface of a silica-dispersed silicomolybdic acid was detected by means of ^{13}C SS NMR. Its hydrolysis led to methanol formation, thus completing the catalytic cycle. After ^{13}C-enriched MeOH adsorption presence of two distinct methoxy species on the surface of polyoxometalates was shown, located on terminal (single coordinated) and bridging (double coordinated) oxygen atoms and resulting in the resonances at 58 and 77 ppm in ^{13}C SS NMR. Grafting of $PtMe_2COD$ on the surface of various polyoxometalate supports led to methane or combined methane and ethane release, explained by means of oxidative addition/reductive elimination mechanism on metal centers. Ammonium salts of phosphotungstic acid catalyzed efficiently *n*-butane to isobutane skeletal isomerisation at mild conditions (225 °C, atmospheric pressure). Successful heterogenization of copper catalysts, active in enantioselective C-H carbene insertion reactions, on polyoxometalate supports have been shown.

DISCIPLINE
Chimie

MOTS-CLES
catalyse heterogene, polyoxometalate, Keggin, molybdène, tungstène, cesium, silice, greffage, Chimie Organométallique de Surface, platine, mecanisme, methane, activation, methanol, *n*-butane, isomérisation, carbene, insertion, composes diazo, RMN, infrarouge, DRX, BET

INTITULE ET ADRESSE DE L'U.F.R. OU DU LABORATOIRE :
Laboratoire de Chimie, Catalyse, Polymères et Procédés, UMR 5265 CNRS - ESCPE Lyon
Equipe de Chimie Organométallique de Surface, ESCPE Lyon, Université de Lyon, 43 Bd du 11 Novembre 1918, F-69616 Villeurbanne, France.